

---

Masters Theses

Student Theses and Dissertations

---

Summer 2016

## Influence of mix design parameters on dynamic segregation of self-consolidating concrete and consequences on performance of precast beams

Aida Margarita Ley Hernandez

Follow this and additional works at: [https://scholarsmine.mst.edu/masters\\_theses](https://scholarsmine.mst.edu/masters_theses)



Part of the [Civil Engineering Commons](#)

Department:

---

### Recommended Citation

Ley Hernandez, Aida Margarita, "Influence of mix design parameters on dynamic segregation of self-consolidating concrete and consequences on performance of precast beams" (2016). *Masters Theses*. 7557.

[https://scholarsmine.mst.edu/masters\\_theses/7557](https://scholarsmine.mst.edu/masters_theses/7557)

This thesis is brought to you by Scholars' Mine, a service of the Missouri S&T Library and Learning Resources. This work is protected by U. S. Copyright Law. Unauthorized use including reproduction for redistribution requires the permission of the copyright holder. For more information, please contact [scholarsmine@mst.edu](mailto:scholarsmine@mst.edu).

INFLUENCE OF MIX DESIGN PARAMETERS ON DYNAMIC SEGREGATION OF  
SELF-CONSOLIDATING CONCRETE AND CONSEQUENCES ON  
PERFORMANCE OF PRECAST BEAMS

by

AIDA MARGARITA LEY HERNANDEZ

A THESIS

Presented to the Faculty of the Graduate School of the  
MISSOURI UNIVERSITY OF SCIENCE AND TECHNOLOGY

In Partial Fulfillment of the Requirements for the Degree

MASTER OF SCIENCE IN CIVIL ENGINEERING

2016

Approved by

Dr. Dimitri Feys, Advisor  
Dr. Kamal H. Khayat  
Dr. Joontaek Park



## ABSTRACT

Self-Consolidating Concrete (SCC) is more vulnerable to stability problems as a consequence of its high flowing ability compared to conventional vibrated concrete. Dynamic segregation refers to the tendency of the concrete constituents to separate from the suspended matrix, usually in horizontal direction while being cast into the formwork or due to an impact. Similarly to static segregation, dynamic segregation can affect the homogeneity of SCC. Therefore, it is highly essential to ensure a proper dynamic stability in order to enhance the uniformity of in-situ properties of pre-stressed beams.

In this research project, the effects of SCC mix design parameters are investigated using the T-box test as a method to assess dynamic segregation. Changes in chemical admixture type and content, paste volume, sand-to-total aggregate ratio (S/A), w/cm and the width of the T-box have been evaluated. The results show that dynamic segregation of SCC is dependent on the rheological properties of the concrete, paste volume and S/A.

In a second part, the influence of dynamic segregation on the uniformity of precast, pre-stressed beams is investigated. Six 9 m and three 18 m long beams were produced with SCC. To determine the uniformity of the mixture, a comparative survey across the beam height and along its length was performed. Also, the bond strength of pre-stress strands with SCC was investigated. Results from the UPV and compressive strength demonstrate a variation in the uniformity of the concrete, mainly at the casting point. For the bond strength, with increasing dynamic segregation, the bond between the strand and the concrete at the top 1/3<sup>rd</sup> of the beam height, relative to the bond in the middle 1/3<sup>rd</sup>, decreases.

## ACKNOWLEDGMENTS

First and foremost, I would like to thank my advisor Dr. Dimitri Feys, for giving me the opportunity to participate in a very interesting research project that made me expand my knowledge and experience. Also, I am thankful for his patient guidance, valuable suggestions and consistent encouragement, which made my graduate experience at Missouri S&T more enjoyable.

I would like to thank Coreslab Structures and especially Jim Myers and Tier-1 UTC (RE-CAST) for the financial support of this project.

I would like to thank Jason Cox, John Bullock, Sarah Vanhooser, Hayder Owayez, Saipavan Rallabhandhi, Kristian Krc, Andrew Bryde, Shane Burkdoll, Nikkolas Edgmond, Enrique Nieblas and Raul Florez for their assistance in this project.

I would like to thank the members of my committee Dr. Kamal H. Khayat and Dr. Joontaek Park, for the time spent reviewing and improving my thesis. Also, I would like to thank Dr. Julie Ann Hartell and her research team for helping on this research project.

I would also like to thank my family Hernandez Aguilar and Ley Gonzalez but especially I must express my very profound gratitude to my parents Aida Margarita Hernandez Aguilar and Pedro Rafael Ley Gonzalez for providing me with unfailing support and contiguous encouragement throughout my years of study. This accomplishment would not have been possible without them. Also, to my siblings Pedro and Neibary for the love and encouragement they show me throughout my life.

Last but certainly not least, I would like to thank my fiancé Daniel Galvez Moreno for his love, support and understanding through my undergraduate and graduate studies. Thank you so much for your patience, I love you so much!

Aida Margarita Ley Hernandez

## TABLE OF CONTENTS

	Page
ABSTRACT.....	iii
ACKNOWLEDGMENTS .....	iv
LIST OF ILLUSTRATIONS.....	x
LIST OF TABLES .....	xv
SECTION	
1. INTRODUCTION.....	1
1.1. BACKGROUND .....	1
1.2. SIGNIFICANCE OF DYNAMIC SEGREGATION .....	2
1.3. SCOPE OF WORK.....	2
2. JUSTIFICATION, HYPOTHESIS AND OBJECTIVES.....	4
2.1. JUSTIFICATION .....	4
2.2. HYPOTHESIS.....	5
2.3. OBJECTIVES.....	5
2.3.1. General Objective.....	5
2.3.2. Specific Objectives.....	5
3. BACKGROUND .....	6
3.1. SELF-CONSOLIDATING CONCRETE .....	6
3.2. RHEOLOGY OF CONCRETE.....	9
3.3. SEGREGATION RESISTANCE .....	10
3.4. DYNAMIC SEGREGATION.....	11

3.5. FACTORS INFLUENCING DYNAMIC SEGREGATION .....	12
3.5.1. Effect of Rheology .....	12
3.5.2. Effect of Casting Conditions (Flow Distance and Flow Velocity) .....	13
3.5.3. Effect of Mix Design Parameters .....	13
3.5.3.1. Effect of cementitious materials content (paste volume).....	16
3.5.3.2. Effect of water to cement ratio .....	18
3.5.3.3. Effect of HRWRA and VMA dosages.....	19
3.5.3.4. Effect of coarse/total aggregate ratio (C/A).....	20
3.6. CURRENT METHODS TO ASSESS DYNAMIC SEGREGATION .....	21
3.6.1. Visual Stability Index .....	22
3.6.2. Flow Trough [19].....	22
3.6.3. Penetration Test [21] .....	24
3.6.4. Tilting Box [24].....	26
3.6.5. Modified Penetration Depth Apparatus [10].....	29
3.6.6. Modified L-box Apparatus [25] .....	31
3.6.7. Dynamic Sieve Stability Test (DSST) [26].....	34
3.7. INDIRECT INDICATORS OF DYNAMIC SEGREGATION .....	36
3.8. ASSESSMENT OF UNIFORMITY OF SELF-CONSOLIDATING CONCRETE BY HARDENED CONCRETE TESTING .....	37
3.8.1. Ultrasonic Pulse Velocity Test .....	38
3.8.2. Compressive Strength on Cores .....	39
3.8.3. Pullout Test.....	39
4. MATERIAL .....	42
4.1. MATERIALS CHARACTERIZATION .....	42

4.1.1. Portland Cement .....	42
4.1.2. Fly Ash .....	42
4.1.3. Fine Aggregate .....	42
4.1.4. Coarse Aggregate .....	43
4.1.5. Chemical Admixtures.....	46
5. EXPERIMENTAL WORK.....	47
5.1. INTRODUCTION .....	47
5.2. TASK 1: LABORATORY WORK.....	48
5.2.1. Mix Design.....	48
5.2.2. Variations in Mix Design Parameters .....	49
5.2.3. Mixing Procedure .....	50
5.3. TASK 2: FIELD WORK.....	51
5.3.1. Mix Design.....	51
5.3.2. Induced Variations in the Mix Design .....	54
5.3.3. Mixing Procedure .....	54
5.4. TEST METHODS .....	55
5.4.1. Slump Flow, $T_{50}$ and VSI .....	55
5.4.2. V-funnel Time .....	58
5.4.3. Air Content (Pressure Method) .....	58
5.4.4. Sieve Stability.....	58
5.4.5. Tilting Box Test.....	59
5.4.6. Concrete Rheology .....	61
5.4.6.1. ConTec viscometer .....	61



5.4.6.2. RHM-3000 ICAR rheometer).....	62
5.4.6.3. Data treatment.....	64
5.4.6.4. Plug flow correction .....	65
5.4.7. Compressive Strength.....	66
5.4.8. Ultrasonic Pulse Velocity Test .....	68
5.4.9. Pullout Test.....	71
6. RESULTS AND DISCUSSION .....	72
6.1. PARAMETERS INFLUENCING DYNAMIC SEGREGATION .....	72
6.1.1. Effect of the Rheological Properties .....	74
6.1.2. Effect of Water-to-Cement Ratio .....	76
6.1.3. Effect of SP Content.....	77
6.1.4. Effect of VMA Content.....	79
6.1.5. Effect of Paste Volume.....	80
6.1.6. Effect of Sand-to-Total Aggregate Ratio .....	82
6.1.7. Effect of Formwork Dimensions.....	84
6.2. CONSEQUENCES OF DYNAMIC SEGREGATION ON PERFORMANCE .	85
6.2.1. Effect of Dynamic Segregation on Ultrasonic Pulse Velocity .....	86
6.2.2. Ultrasonic Pulse Velocity Measured on Concrete Cores .....	88
6.2.3. Effect of Dynamic Segregation on Compressive Strength.....	90
6.2.4. Effect of Dynamic Segregation on Bond Strength.....	96
7. CONCLUSIONS, RECOMMENDATIONS AND FUTURE WORK .....	98
7.1. CONCLUSIONS .....	98
7.2. RECOMMENDATIONS .....	100

7.3. FUTURE WORK .....	101
APPENDICES	
A. COMPRESSIVE STRENGTH AND UPV DATA OF CONCRETE CORES...	103
B. PULL-OUT TEST DATA FOR BEAMS .....	111
REFERENCES .....	115
VITA.....	120

## LIST OF ILLUSTRATIONS

	Page
Figure 3.1 Example of volumetric mixture proportions of CVC and SCC [11].	8
Figure 3.2 Bingham model.	10
Figure 3.3 Concrete remains stable during placement.	12
Figure 3.4 Concrete is segregating during placement.	12
Figure 3.5 Relationship between rheological properties and dynamic segregation of SCC [19].	13
Figure 3.6 Effect of cementitious materials content on dynamic segregation (black line) of SCC, w/cm= 0.45 [10].	17
Figure 3.7 Effect of cementitious materials content on dynamic segregation (black line) of SCC, w/cm= 0.40 [10].	18
Figure 3.8 Effect of w/cm on dynamic segregation (black line) of SCC [10].	19
Figure 3.9 Effect of HRWRA on dynamic segregation (black line) of SCC [10].	20
Figure 3.10 Effect of VMA on dynamic segregation (black line) of SCC [10].	20
Figure 3.11 Effect of coarse/total aggregate on dynamic segregation (black line) of SCC [10].	21
Figure 3.12 Flow trough for dynamic segregation [19].	23
Figure 3.13 Penetration Apparatus (PA) [21].	25
Figure 3.14 The L box and cylinder mold (type N) [21].	26
Figure 3.15 Configuration of the T-box [24].	27
Figure 3.16 Surface Penetration technique [24].	28
Figure 3.17 Three compartment hinged cylindrical mold [10].	29
Figure 3.18 Modified Penetration depth apparatus [10].	29

Figure 3.19 Modified L-box apparatus [24].	31
Figure 3.20 General view of the section [24].	32
Figure 3.21 Demonstration of the ratio $V_{gsi}/V_{csi}$ from the L-box [24].	34
Figure 3.22 Configurations of the DSST apparatus [26].	35
Figure 3.23 Internal and external bleeding [28].	41
Figure 3.24 Effect of rebar direction on bond strength [40].	41
Figure 4.1 Gradation curve of fine aggregates from the Missouri and Kansas Rivers.	43
Figure 4.2 Gradation curve of 9.5 to 2.36 mm crushed limestone (CL1).	44
Figure 4.3 Gradation curve of 12.5 to 4.75 mm crushed limestone (CL2).	45
Figure 4.4 Gradation curve for the combination of CL1 and PG (9.5 to 1.18 mm).	45
Figure 4.5 Gradation curve of 9.5 to 1.18 mm crushed limestone (CL3).	46
Figure 5.1 Sequence of executed tasks.	48
Figure 5.2 Induced variations on the mixture.	50
Figure 5.3 Configuration of the rectangular beams.	51
Figure 5.4 Configuration of the “I” beams.	52
Figure 5.5 Left: Reinforcement of the rectangular beams. Right: Casting beam.	52
Figure 5.6 Configurations and strand positions in the 9 m long beams.	53
Figure 5.7 Beam 5 with the three sets of pre-stressed strands. The arrows indicate the direction of casting.	53
Figure 5.8 Induced variations in each beam.	54
Figure 5.9 Testing sequence.	55
Figure 5.10 Slump flow.	56
Figure 5.11 Configuration of the T-box test.	60
Figure 5.12 Contec viscometer 5.	61

Figure 5.13 The applied rotational velocity profile performed in Contec Rheometer.....	62
Figure 5.14 ICAR rheometer. ....	63
Figure 5.15 The applied rotational velocity profile performed in ICAR rheometer.....	63
Figure 5.16 Torque vs rotational velocity diagram.....	64
Figure 5.17 Drilled core in beam. ....	67
Figure 5.18 Extracting cores from a beam.....	67
Figure 5.19 Compressive strength test setup of cores.....	68
Figure 5.20 Extraction points of concrete cores for 9 m long beam. ....	68
Figure 5.21 On-site UPV testing on beam. ....	69
Figure 5.22 Lay-out of UPV measuring points per section. ....	70
Figure 5.23 Ultrasonic pulse velocity testing equipment.....	70
Figure 5.24 Lay-out of pull-out test.....	72
Figure 5.25 Strands being tested using pull-out test. ....	72
Figure 6.1 Relationship between dynamic segregation and plastic viscosity.....	75
Figure 6.2 Relationship between dynamic segregation and yield stress.....	75
Figure 6.3 Relationship between dynamic segregation and shear stress @ $1s^{-1}$ .....	76
Figure 6.4 Influence of water-cement ratio on dynamic segregation in mix design 2.....	77
Figure 6.5 Influence of superplastizicer content on dynamic segregation in mix design 1.....	78
Figure 6.6 Influence of superplastizicer content on dynamic segregation in mix design 2.....	79
Figure 6.7 Influence of superplastizicer content on dynamic segregation in mix design 3.....	79
Figure 6.8 Influence of VMA content on dynamic segregation in mix design 1.....	80
Figure 6.9 Influence of paste volume on dynamic segregation in mix design 2. ....	81

Figure 6.10 Relationship between dynamic segregation and rheological properties @ $1s^{-1}$ . Highlighted points reflect the increase in paste volume.....	82
Figure 6.11 Influence of sand-to-total aggregate ratio on dynamic segregation in mix design 2.....	83
Figure 6.12 Influence of formwork dimensions on dynamic segregation. ....	84
Figure 6.13 UPV results, in % relative to the average value 4130 m/s for beam 1. ....	87
Figure 6.14 UPV results, in % relative to the average value of 4602 m/s for beam 2 for the 9 m closest to the casting point. ....	87
Figure 6.15 UPV results, in % relative to the average value of 4311 m/s for beam 5.....	87
Figure 6.16 Correlation between UPV on beam 1 and UPV on cores.....	88
Figure 6.17 Correlation between UPV on beam 2 and UPV on cores.....	89
Figure 6.18 Correlation between UPV on beam 5 and UPV on cores.....	89
Figure 6.19 Relationship between Average UPV and Average compressive strength of each beam. ....	89
Figure 6.20 Relationship between individual UPV measurements and compressive strength of each core. ....	90
Figure 6.21. Compressive strength results in absolute values for beam 1 (Avg. $f_c = 42.8$ MPa).....	91
Figure 6.22 Compressive strength results in absolute values for beam 2 (Avg. $f_c = 74.2$ MPa).....	92
Figure 6.23 Compressive strength results in absolute values for beam 3 (Avg. $f_c = 72.8$ MPa).....	92
Figure 6.24 Compressive strength results in absolute values for beam 4 (Avg. $f_c = 69.5$ MPa).....	92
Figure 6.25 Compressive strength results in absolute values for beam 5 (Avg. $f_c = 53.3$ MPa).....	93
Figure 6.26 Compressive strength results in absolute values for beam 6 (Avg. $f_c = 50.4$ MPa).....	93
Figure 6.27 Compressive strength results in absolute values for beam 7 (Avg. $f_c = 47.7$ MPa).....	93

Figure 6.28 Compressive strength results in absolute values for beam 8 (Avg. $f_c = 44.5$ MPa).....	94
Figure 6.29 Compressive strength results in absolute values for beam 9 (Avg. $f_c = 56.9$ MPa).....	94
Figure 6.30 Compressive strength results in absolute values for beam 2 (18 m). ....	94
Figure 6.31 Compressive strength results in absolute values for beam 4 (18 m). ....	95
Figure 6.32 Compressive strength results in absolute values for beam 9 (18 m). ....	95
Figure 6.33 Relationship between air content and compressive strength of all beams. ...	96
Figure 6.34 Relationship between dynamic segregation and delta $f_c$ (avg. of bottom – middle) of all beams.....	96
Figure 6.35 Relationship between bond strength and volumetric index of beams. ....	97

## LIST OF TABLES

	Page
Table 3.1 Effects of proportioning and casting variables on segregation of SCC [20]. ...	14
Table 3.2 Visual stability index rating [22] .....	22
Table 4.1 Physical properties of cement. ....	42
Table 4.2 Physical properties of the fine aggregates. ....	43
Table 4.3. Properties of the different coarse aggregates. ....	44
Table 4.4. Properties of different chemical admixtures. ....	46
Table 5.1 Constituents comparison between EFNARC and ACI 237 recommended values with reference mixture. ....	48
Table 5.2 Reference mix design.....	49
Table 5.3 Materials and parameters used for each mix design. ....	49
Table 5.4 Mixing sequence for the SCC tested mixtures.....	50
Table 5.5 Test methods used to characterize the fresh properties of SCC. ....	55
Table 5.6 Visual stability index criteria [48]. ....	57
Table 5.7 Conformity criteria for V-funnel flow time [9]. ....	58
Table 5.8 Conformity criteria for static segregation of SCC [9]. ....	59
Table 6.1 Workability, dynamic segregation, rheological and mechanical properties for the tested mixtures. ....	73
Table 6.2 Workability characteristics, dynamic segregation, rheological and mechanical properties for the SCC tested. ....	85



# 1. INTRODUCTION

## 1.1. BACKGROUND

Concrete is the most widely used building material in the world. In its most basic form, concrete consists of portland cement, water, fine and coarse aggregates. After mixing and placement, concrete hardens and forms a stone-like mass. As the use of concrete becomes more common around the world, the specifications for concrete, such as requirements for durability, quality control, workability and optimization of the mix design of concrete, become more important.

Recently, advanced flowable concretes, such as self-consolidating concrete (SCC), have been developed. SCC has the ability to flow by its own weight, filling any kind of formwork and passing through congested reinforcement bars or narrow gaps without segregation of its constituents. It can also be used for filling sections with limited or no reinforcement to speed up the construction process without compromising the mechanical properties or durability, potentially induced by segregation and bleeding.

Due to the high flow capacity of SCC, it is more vulnerable to suffer stability problems compared to conventional vibrated concrete. *Segregation resistance is defined as the ability of a concrete mixture to maintain a uniform distribution of its constituents, during casting (dynamic segregation), as well as after placement (static segregation)* [1]. A segregated concrete has a lower compressive, tensile and flexural strength. In addition, it can cause a weaker interface between the aggregate and the cement paste and can adversely affect the bond behavior between steel and concrete [2-4]. Since SCC mixtures have high content of fines, it is more susceptible to develop shrinkage cracking in

comparison to conventional concrete. Cracking due to instability can reduce the concrete's resistance to the ingress of humidity and ions and, if exposed to freeze-thaw temperatures or chlorides ions, can further stimulate the increase of permeation and compromise the long-term durability performance [2].

## **1.2. SIGNIFICANCE OF DYNAMIC SEGREGATION**

Segregation is defined as the ability of the coarse aggregate particles to settle in the mortar matrix during production, transport and placement. It is a common problem observed in SCC as a consequence of its high flowing ability. Stability problems, such as dynamic and static segregation, may lead to a lower compressive, tensile and flexural strength. In addition, it may cause higher cracking risk and a weaker interface between the aggregate and the cement paste, which can adversely affect the bond behavior between steel and concrete. Cracking due to segregation increases the risk of reducing the concrete's resistance to freezing-thawing cycles as well as an increase in permeability, both compromising the structures' integrity. Dynamic segregation is controlled by the rheological properties of the mortar; aggregates properties, such as density, size and volume fraction; the flowing velocity of concrete, and boundary conditions.

## **1.3. SCOPE OF WORK**

Dynamic segregation is one of the least investigated aspects of the workability of SCC. Therefore, very limited test methods have been suggested and none are widely accepted. The only current standard method to assess segregation in general, is the visual stability index described in ASTM C1611/C1611M.

A recent study proposed a new test method: The tilting box test (T-box) to assess dynamic segregation [5], which is used in this project with modifications in dimensions. In this research project, dynamic segregation of SCC was evaluated in the laboratory and in the field using the T-box test method. The SCC mixtures were also characterized by means of rheology. In the laboratory work, 23 SCC mixtures with three different baseline compositions were prepared with alterations in the mix design parameters to investigate their effects on dynamic segregation. In the field work, nine pre-stressed concrete beams were cast, of which three were rectangular with a length of 9 m and three others were 18 m in length. Also, three MoDOT approved “I” beams 9 m in length were investigated to evaluate the consequence of dynamic segregation on in situ performance by means of compressive strength, ultrasonic pulse velocity and bond strength of concrete with pre-stress strands. The SCC mixture variables in this study were delimited to the water-to-cement ratio (w/c), paste volume, sand-to-total aggregate ratio (S/A), superplasticizer, viscosity modifying admixture and air entrainment admixture dosage.

## 2. JUSTIFICATION, HYPOTHESIS AND OBJECTIVES

### 2.1. JUSTIFICATION

With the enhanced development and use of chemical admixtures and supplementary cementitious materials, highly flowable concretes, including SCC, can be produced, providing significant advantages for the pre-cast industry in production, placement, structural quality and work environment compared to conventional vibrated concrete (CVC). The use of SCC in the United States is slowly being implemented in the pre-cast industry due to its sensitivity to small changes in the mix design, characteristics of the constituent materials, and the building process. In addition, SCC is more susceptible to suffer segregation due to the lower values of its rheological properties compared to other concrete types. Segregation resistance means that the concrete must remain homogenous during production, transport and placement. If the distribution of the aggregates in the suspended matrix is disturbed, it can have negative consequences on compressive strength and other hardened properties of SCC.

Dynamic stability is one of the least investigated aspects of SCC and refers to the tendency of the coarse aggregates to separate from the mortar while concrete is flowing. Poor segregation resistance of SCC may lead to a reduction in flowability, induce blockage, high drying shrinkage, non-uniform compressive strength, a weaker interface between the aggregate and the cement paste, and adversely affect the bond behavior between steel and concrete. Therefore, it is necessary to understand dynamic segregation, in order to prevent or limit it. In addition, it is important to identify how dynamic segregation affects the structural performance of SCC.

## 2.2. HYPOTHESIS

Dynamic segregation is an important aspect of SCC that needs to be evaluated and prevented since it has negative effects on mechanical properties and durability of SCC, including bond strength between concrete and pre-stress strands.

## 2.3. OBJECTIVES

**2.3.1. General Objective.** To evaluate the effects of different mix design parameters on dynamic segregation in SCC through rheological measurements, and the consequences on the structural performance of pre-stressed beams in terms of mechanical properties, durability and bond strength of concrete with pre-stressed strands.

**2.3.2. Specific Objectives.** In order to achieve the purpose of this research, the proposed objectives were the following:

- To identify critical mix design parameters influencing dynamic segregation of SCC.
- To evaluate the influence of these mix design parameters by characterizing dynamic segregation, workability and rheological parameters.
- To investigate the consequence of dynamic segregation on the homogeneity of hardened properties of pre-stressed beams.
- To optimize SCC mixtures to improve implementation by guarantying their robustness and homogeneity in pre-stressed beams, evaluated in terms of compressive strength and ultrasonic pulse velocity.
- To develop practical guidelines to assure uniformity of structural elements and enhance the use of SCC in the pre-cast industry.

### 3. BACKGROUND

#### 3.1. SELF-CONSOLIDATING CONCRETE

Self-consolidating concrete (SCC) is a highly flowable concrete that can spread by its own weight, achieve good consolidation, fill the formwork and encapsulate the reinforcement in the absence of mechanical vibration [6]. SCC was proposed in order to satisfy the necessity of producing durable concrete structures that did not depend on the skill of workers. During the 1980's Japan suffered a gradual reduction in the number of skilled workers, which led to the invention of a self-consolidating concrete. SCC can be placed without the need of mechanical vibration and still achieve good consolidation [7]. The first prototype of SCC using materials on the market was developed in Japan in 1988 by professor Okamura from the University of Tokyo [7]. The initial design of SCC was based on increasing the powder content or the proportion of fine aggregates without changing the amount of water relative to the water present in conventional vibrated concrete (CVC), and compensating the water demand using a superplasticizer. In the subsequent years other mix design principles followed including the use of fillers, SCMs and other chemical admixtures (e.g. VMA). The application of SCC technology can result in both economic and technological benefits compared to CVC. Among the benefits are [8]:

- An increase in the rate of placement.
- Provide a higher in-place quality, better consolidation and adherence between the concrete and the steel.
- Improvement of the worker safety and noise reduction.

- Ease of placement through heavily reinforced areas.
- Faster speed of construction and time-savings.
- Labor savings.
- Improve surface finishing.

However, as any technology, SCC also has some limitations. These include:

- Increase in the cost of the concrete due to the high amount of cementitious materials and admixtures.
- Greater need for proper design and control of robust SCC mixtures.
- Increase in cost of the formwork due to the higher pressure exerted for tall structures.
- Difficulties of ensuring robust SCC production.
- Lack of proper test methods for design and control workability.

The main characteristics that define SCC performance are [8, 9]:

- Filling ability is the capacity of the fresh concrete to flow freely under its own weight in to the formwork and fill it without the need of mechanical vibration.
- Passing ability refers to the ability of SCC mixtures to flow through heavily reinforced areas or narrow gaps without blocking.
- Stability refers to the ability of SCC mixtures to maintain a uniform distribution of its constituents during transport and placement (dynamic stability) and after being placed (static stability).

A combination of the above main characteristics is needed to achieve a good SCC design, in addition to other requirements for hardened properties.

The high flowability of SCC is achieved by properly proportioning its constituents, which is usually accomplished by replacing part of the coarse aggregates with fine aggregates and powders. Also, the addition of chemical admixtures, such as high-range water reducer admixtures (HRWRAs) and viscosity-modifying admixtures (VMAs) to enhance stability, makes it possible to achieve the necessary consistency without increasing the water-to-cement ratio (w/c). The required fluidity of SCC is difficult to achieve without decreasing the viscosity or yield stress of the mortar, which increases the tendency of the coarse aggregates to settle [10]. The performance of SCC depends on the sensitive balance between creating more deformability while providing adequate stability, as well as maintaining low risk of blockage [6].

The differences between the mix design principles of SCC compared to conventional vibrated concrete (CVC) are as follows [9, 7]:

- Increase in paste content: by adding SCMs or fillers.
- Lower coarse aggregate content and reduced maximum aggregate size
- Low water-to-cement ratio (w/c)
- Increased high-range water reducer admixture dosage
- Use of viscosity-modifying admixtures (for some cases)

Figure 3.1 shows an example of a typical mixture proportioning of SCC and CVC [11].

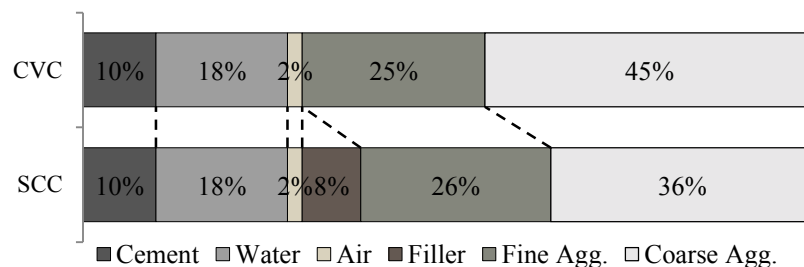


**Figure 3.1 Example of volumetric mixture proportions of CVC and SCC [11].**



One of the general concerns with SCC is the susceptibility to stability problems, which refers to its ability to retain the constituents in suspension: prevent settling and/or excessive bleeding. Severe segregation can have detrimental effects on the structural performance and durability of members and must be avoided before, during, and after placement. Thus, stability is a critical property of fresh SCC.

### 3.2. RHEOLOGY OF CONCRETE

In order to describe the flow properties, including thixotropy, of fresh cement-based suspensions, such as paste, mortar or concrete, it is necessary to study the flow and deformation by means of rheology. The concrete in fresh state can be considered as a fluid, which is composed of a concentrated suspension of aggregates immersed in a cement paste matrix. At the same time, it can be considered as a powder suspension in water [12]. Therefore, the characterization of the rheological properties is complicated due to the wide particle size range that conforms its composition (from  $< 1 \mu\text{m}$  to  $\geq 10 \text{ mm}$ ). Also, time dependent properties due to cement hydration and the development of thixotropy are observed [12, 13]. Rheology has become necessary to understand and predict with precision the behavior of high performance concrete in the fresh state.

Concrete rheology is evaluated using special rheometers that allow the user to relate variations in shear stress to shear rate. SCC is mostly described as a Bingham fluid (Figure 3.2); its equation is a linear relationship between the shear rate and the shear stress in which the shear stress can be expressed as

$$\tau = \tau_0 + \mu_p \cdot \dot{\gamma}$$

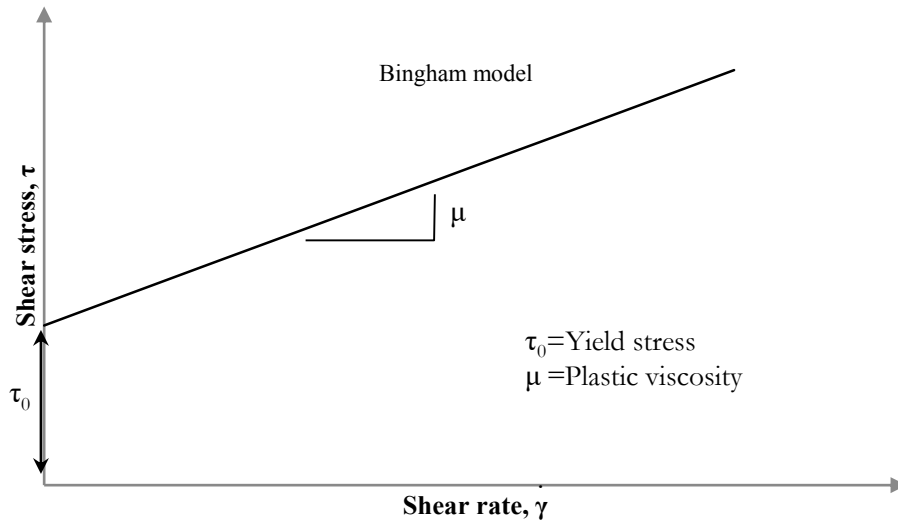


**Figure 3.2 Bingham model.**

This model proposes two constants defining the flow of a material. The yield stress ( $\tau_0$ ), refers to the amount of stress needed to initiate the flow of a material, and the plastic viscosity ( $\mu_p$ ) is defined as the material's internal resistance to flow.

### 3.3. SEGREGATION RESISTANCE

Segregation resistance is the ability of concrete to remain uniform in composition during placement and until setting. Segregation resistance is mainly ruled by gravity, the difference in density between suspending matrix and particles, the distribution and physical properties of the sand and coarse aggregates, their volume fractions, and the rheological behavior of the mortar. Instability of concrete can happen during casting (dynamic segregation) and at rest (static segregation).

When the concrete is at rest, static stability is achieved when the yield stress of the mortar in combination with the buoyancy of the coarse aggregates is sufficiently high in order to maintain the aggregates in suspension [14-16]. Meanwhile, dynamic instability, where the fluid is in movement, the viscosity is expected to have a significant role [17].

During motion, the yield stress is exceeded in specific zones, which may allow aggregates to settle. Therefore, higher viscosities will help drag aggregates along with the flow and also reduce the rate of settlement until the concrete comes to rest [17]. Some concrete mixtures show dynamic segregation and no static segregation. The reason why these two phenomena may not appear simultaneously is due to different governing factors.

### **3.4. DYNAMIC SEGREGATION**

Dynamic segregation occurs when the concrete is flowing, and it refers to the tendency for coarse aggregates to separate from the suspended matrix, usually in a horizontal direction while flowing into the formwork. This phenomenon is controlled by the rheological properties of the paste; aggregates properties, such as density, size, and volume fraction; the initial flow velocity of the concrete, hydraulic pressure head and pump pressure; or the frictional force provided by the flowing surface [18].

It should be noted that since this phenomenon occurs during flow of concrete, it is quite complex to explain its fundamental mechanisms. When SCC is flowing (Figure 3.3), the inclusions (coarse aggregates) are prevented from uniformly migrating with the suspending fluid by shear rates induced inside the suspending matrix (mortar). The separation between the mortar and the coarse aggregates is caused by the difference in velocity developed by the aggregates while the flow continues (Figure 3.4). In the case of an impact, e.g. free-fall, it could be similarly explained that right after the impact the separation or segregation between the mortar and coarse aggregates may happen due to the development of different velocities (mostly due to their density difference and inertia).

Therefore, this difference between velocities of coarse aggregates and mortar is considered the main source of occurrence of dynamic segregation [5].

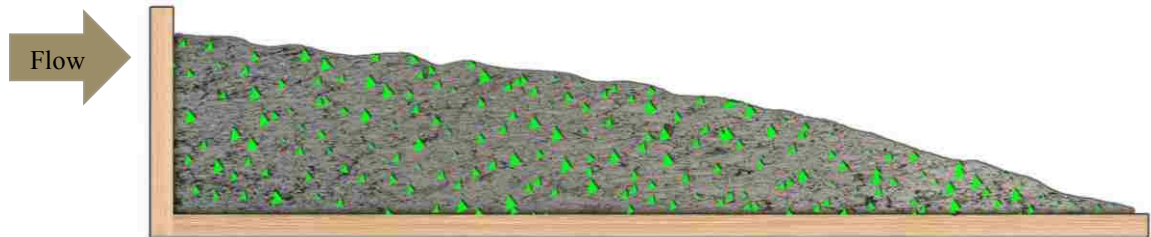


**Figure 3.3 Concrete remains stable during placement.**

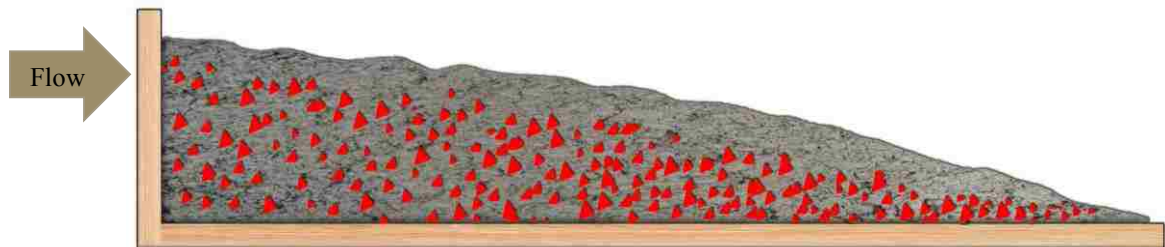


**Figure 3.4 Concrete is segregating during placement.**

### 3.5. FACTORS INFLUENCING DYNAMIC SEGREGATION

It is important to understand the behavior of dynamic segregation as well as the factors that influence this phenomenon, which causes the concrete to be unstable. This can cause a lower compressive strength, poor quality and cracking.

Recent studies have shown the existence of several effects influencing dynamic segregation of SCC, which are described below:

**3.5.1. Effect of Rheology.** Yield stress and viscosity have a significant influence on dynamic stability. Increasing either of these rheological properties can reduce dynamic segregation due to the increased drag force exerted from the mortar on the coarse aggregates during flow [18].

According to Esmailkhanian et al. [18], in order to secure an adequate resistance to dynamic segregation, SCC should have a viscosity greater than 55 Pa s (measured with ConTec Viscometer 5) when the SCC has a relatively low yield stress (lower than 20 Pa). On the other hand, when SCC has a yield stress higher than 20 Pa, the minimum plastic viscosity requirement can be lower than 40 Pa s (Figure 3.5).

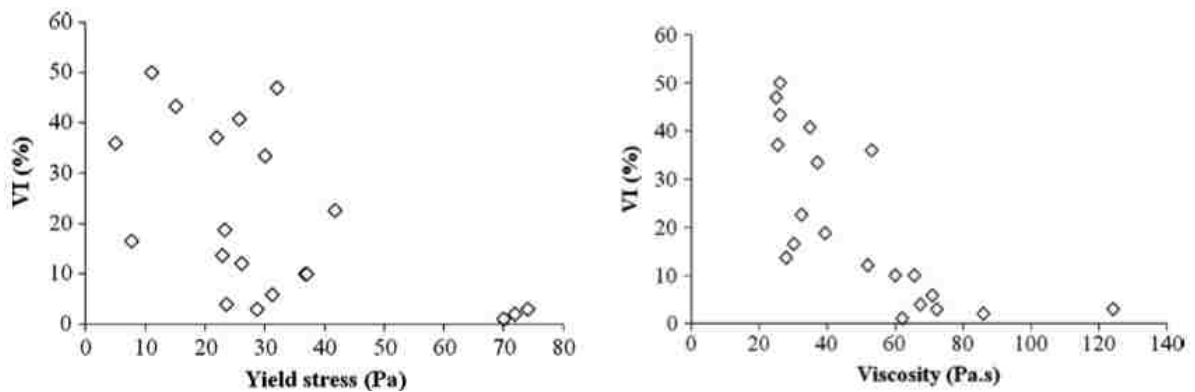


**Figure 3.5 Relationship between rheological properties and dynamic segregation of SCC [18].**

**3.5.2. Effect of Casting Conditions (Flow Distance and Flow Velocity).** There are some effects in segregation induced by the flow distance and flow velocity. First, as flow distance increases, segregation increases, but the segregation rate per unit of distance flown decreases [5]. Second, when reducing flow velocity, first segregation increases until a critical velocity is reached, and then, it starts to either decrease or stay constant for concrete with low stability level [5].

**3.5.3. Effect of Mix Design Parameters.** There are several mix design parameters that have influence on dynamic segregation, such as the paste volume of SCC. An increase in paste volume can increase segregation, as higher paste volume can facilitate the shear-induced aggregate migration in a matrix due to a greater inter-particle

spacing. Also, the difference between density of the aggregates and the mortar has an important effect. If the density of the aggregates and the mortar would be equal, practically no segregation could occur. Another parameter is the variation of the shape of coarse aggregates, crushed vs rounded, while keeping the maximum size aggregates (MSA) and grading constant. However, aggregate shape does not have much influence on dynamic stability. In addition, reducing the water-to-binder ratio (w/b) can considerably decrease segregation. This improvement of stability is attributed to higher yield stress and plastic viscosity for a lower w/b. Moreover, increasing MSA slightly can increase segregation due to decreased aggregate specific surface area-to-mass ratio [18]. Finally having a broader gradation (increasing coarse aggregate distribution) reduce dynamic segregation [19], due to the enhancement of the particle lattice effect.

Table 3.1 shows some factors and their effect on dynamic segregation.

**Table 3.1 Effects of proportioning and casting variables on segregation of SCC [20].**

<b>Factors</b>	<b>Effect on dynamic Segregation</b>
Cementitious Materials	Increases viscosity or yield stress, can reduce dynamic segregation
Coarse aggregate	Higher volume reduces passing ability through restricted sections
Fine aggregate	No effect outside of balancing coarse aggregate volume
Water	Increasing water decreases the viscosity of paste and thereby increases dynamic segregation
Superplasticizer	High dose can create excessive flow resulting in dynamic segregation
VMA	Increasing VMA increases viscosity of the paste resulting in lower dynamic segregation
Air-entrainer	Minimal to none
Fluidity	Greater fluidity results in higher dynamic segregation
Flow Distance	Promotes separation of paste from aggregate
Free Fall	Promotes separation of paste from aggregate
Form dimensions	Narrow form increases wall effects and increases dynamic segregation
Transport no agitation	Vibration can cause dynamic segregation
Pumping	Pressure causes segregation in the pump lines

El-Chabib and Nehdi [10] made a comparison between two methods that can be employed for assessing dynamic segregation and their modified version of the penetration apparatus originally developed by Bui et al [21]. Both methods are described in section 3.6.

In this study, the materials employed to produce the SCC mixtures were CSA type 10 Canadian portland cement (which is equivalent to a Type I cement) with a combination of SCMs including slag, Class C fly ash and silica fume. A polycarboxylate-based HRWRA and a polysaccharide welam gum powder VMA was used as a chemical admixture.

As stated by the cited authors [10], to capture the true nature of segregation of SCC in field applications, two separate values of the Segregation Index (SI) were investigated. First, *SI-STATIC* in which segregation occurs under normal placement conditions and during concrete setting, mainly due to settlement of large aggregate particles under gravity caused by the difference in relative density of the materials and the low viscosity of the mortar. The second is *SI-DYNAMIC* in which transporting, placement, and consolidation have an additional contribution to the global segregation in SCC mixtures, to that caused by static effects. *SI-STATIC* and *SI-DYNAMIC* were determined using the segregation method proposed in their study; therefore, two values of penetration depth (Pd) were established based on the type of segregation. For *SI-STATIC*, the test mold was filled and allowed to rest for 30 minutes before the aggregate content was quantified, whereas for *SI-DYNAMIC* the concrete sample was poured inside the test mold using the V-funnel and finally left undisturbed for 30 minutes. Using the V-funnel as a pre-conditioning method, it was possible to take into account the dynamic effect,

such as the discharge of SCC through a chute of a concrete truck (simulated by the 2:1 slope of the V-funnel sides) and the effect of concrete subjected to free-fall from a height during placement (simulated by placing the test mold at a distance  $d$  below the bottom of the V-funnel), in determining the dynamic segregation index of SCC. The procedure is further described in section 3.6.5.

**3.5.3.1. Effect of cementitious materials content (paste volume).** It is a common practice to increase the content of fine material and reduce the amount of coarse aggregates when designing a SCC mixture to increase the flowability and reduce the risk of blockage and/or segregation. In this study the w/cm, the HRWRA and VMA dosages were kept constant for all mixtures, while the cementitious materials varied between 350 and 550 kg/m<sup>3</sup>. The total aggregate content was adjusted to accommodate changes in cementitious materials and water contents. A constant coarse-to-total aggregate ratio, however was maintained in all mixtures. Figure 3.6 shows an increased segregation tendency of coarse aggregates at constant w/cm of 0.45 when the cementitious materials content (paste volume) increases. This behavior was observed for the sieve stability test using the GTM and SI-DYNAMIC testing protocol. On the other hand, for SCC mixtures subjected to normal placement conditions (SI-STATIC), this effect was less significant. Due to the observation of this behavior, in addition to the original experimental program, El-Chabib and Nehdi [10] included another set of five SCC mixtures to investigate the effect of cementitious materials content on the segregation resistance of SCC having a lower w/cm of 0.4, a constant dosage of VMA of 0.01 % of cementitious materials, a HRWRA dosage varying between 0.22 and 1.13 % of cementitious materials to achieve a similar slump flow of  $615 \pm 15$  mm. Figure 3.7 shows the influence of cementitious



materials content on the segregation resistance of SCC mixtures having lower  $w/cm$  when tested by the authors proposed methods along with the sieve stability test. Results of *SI-DYNAMIC* show that increasing the cementitious materials content slightly reduced segregation in SCC mixtures, while those obtained using the sieve stability test indicate a negligible increase of segregation when cementitious materials content increased.

The sieve stability test (described in section 5.4.4.) is based on measuring the amount of mortar that passes the No. 4 (4.75 mm) sieve of a concrete sample that was held at rest, SCC mixtures with higher mortar fraction are expected to exhibit higher percentage of mortar passing. For the mixtures subjected to the *SI-STATIC* testing protocol, the effect of the variation of cementitious content was negligible, as shown in Figures 3.7.

The effect of the cementitious materials content on segregation illustrated in Figures 3.6 and 3.7 is due to the fact that increasing the cementitious materials content, at a constant  $w/cm$ , increases the water and the paste volume, which could enhance dynamic segregation.

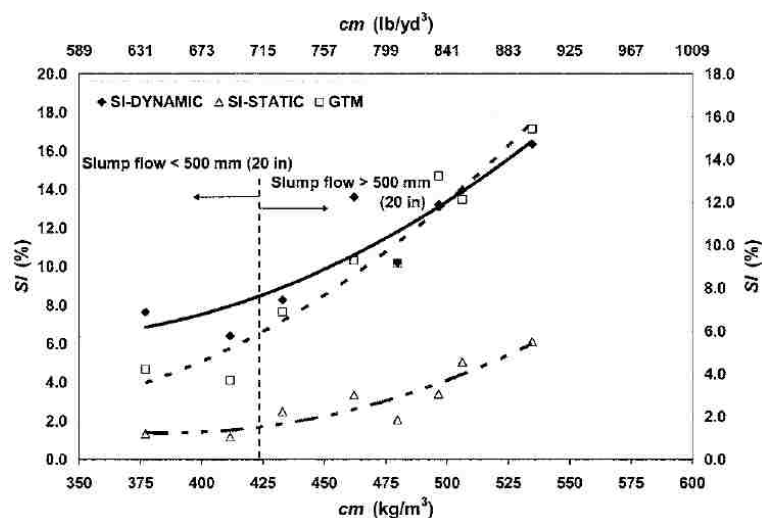


**Figure 3.6 Effect of cementitious materials content on dynamic segregation (black line) of SCC,  $w/cm=0.45$  [10].**

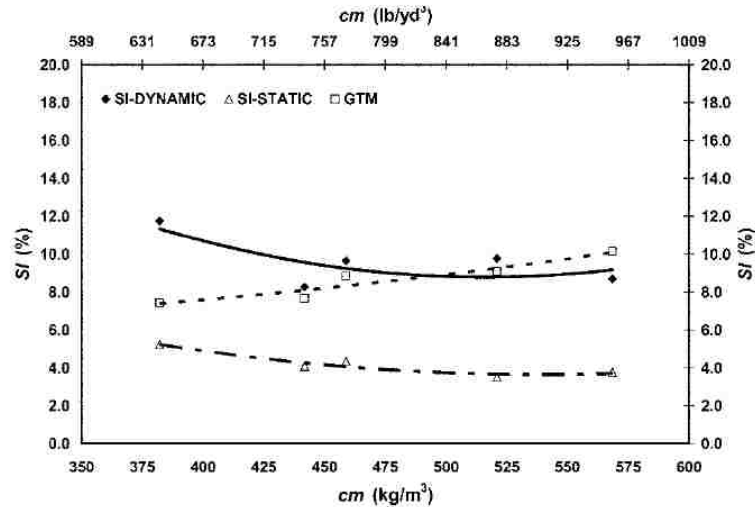


**Figure 3.7 Effect of cementitious materials content on dynamic segregation (black line) of SCC,  $w/cm = 0.40$  [10].**

Results from Esmailkhanian et al. [5], confirm that increasing paste volume, while keeping the  $w/cm$ , HRWRA and VMA content constant destabilizes SCC.

**3.5.3.2. Effect of water to cement ratio.** Increasing the  $w/cm$  can increase significantly the flowability of SCC by reducing the viscosity of the mortar fraction. It also reduces the ability of maintaining a uniform distribution of the coarse aggregates in the mortar matrix. For this set of mixtures, the coarse-to-total aggregate ratio, the HRWRA and VMA dosages were kept constant, while  $w/cm$  was varied between 0.4 and 0.6. Figure 3.8 shows that the results of the sieve stability method (GTM) and the modified penetration apparatus under both testing procedures (*SI-STATIC* and *SI-DYNAMIC*) [10] had a similar tendency when the  $w/cm$  was changed. It was also observed from the *SI-DYNAMIC* test that free-fall increases dynamic segregation. This effect seems more pronounced at  $w/cm$  larger than 0.45. Both testing methods were sufficiently sensitive to detect a significant increase of the segregation index at  $w/cm > 0.45$  for the particular dosages of HRWRA and VMA used.

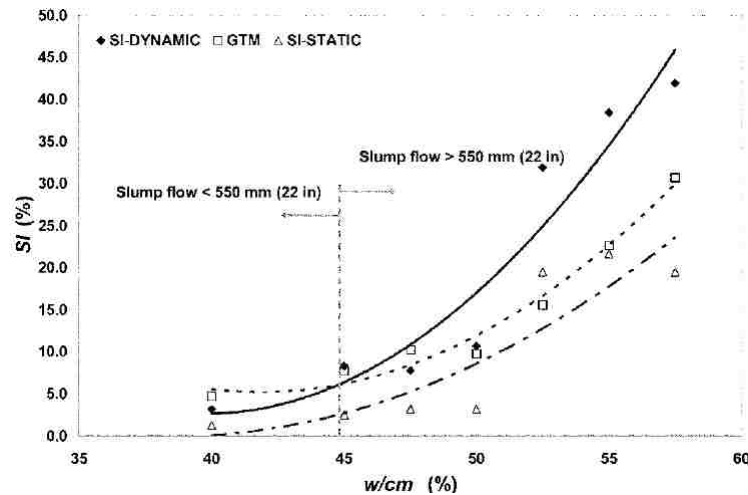


**Figure 3.8 Effect of w/cm on dynamic segregation (black line) of SCC [10].**

**3.5.3.3. Effect of HRWRA and VMA dosages.** Similar to the effect of w/cm, increasing the dosage of HRWRA tends to reduce the stability of SCC. For the first set of mixtures, the HRWRA dosage varied from 0.2 to 0.6% of cementitious materials in order to investigate the effect of HRWRA dosage. While for the second, set the VMA varied from 0.01 to 0.03% of cementitious materials to evaluate its effect on segregation. Figure 3.9 shows that for constant w/cm and VMA content, the ability of SCC mixtures to resist segregation linearly decreased with increasing HRWRA dosage, regardless of the test method used. This was more pronounced in the case where SCC was cast into the test mold using the V-Funnel.

Figure 3.10 shows that for constant w/cm and HRWRA dosage, higher VMA dosages increased the ability of SCC mixtures to resist segregation as expected. However, a nonlinear trend is observed (except for the sieve stability test). It is important to note that the relationships shown in Figure 3.9 and 3.10 reflect the effect of admixtures used in this study, and that other types of admixtures might show a different behavior.

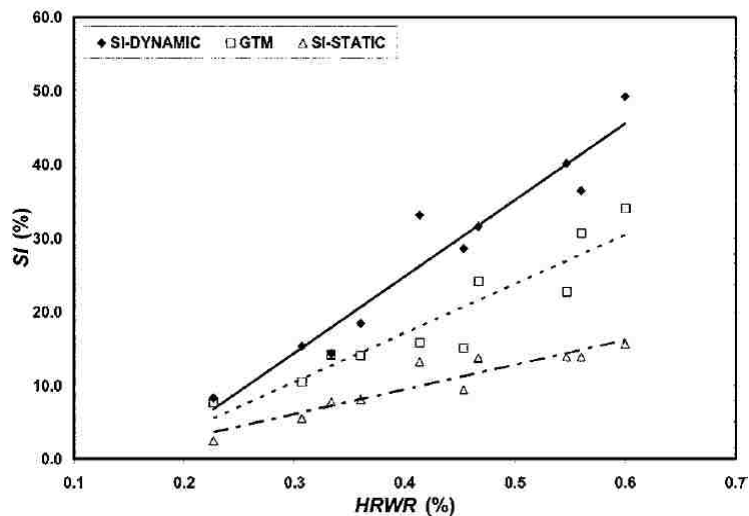


Figure 3.9 Effect of HRWRA on dynamic segregation (black line) of SCC [10].

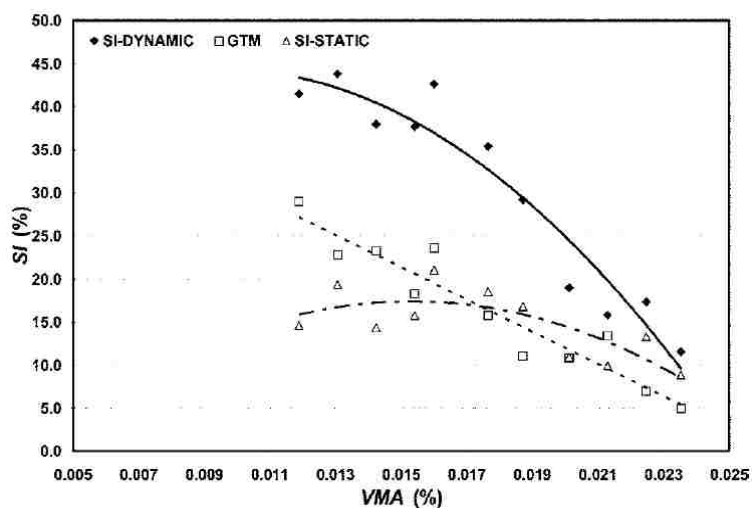
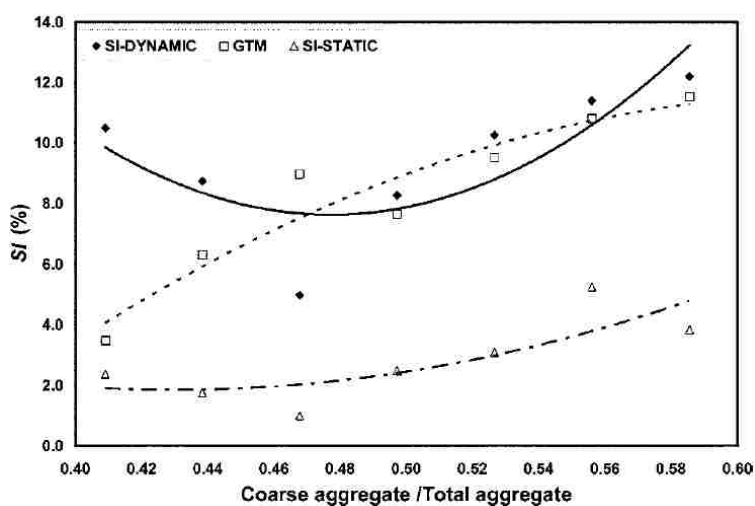


Figure 3.10 Effect of VMA on dynamic segregation (black line) of SCC [10].

**3.5.3.4. Effect of coarse/total aggregate ratio (C/A).** In order to enhance the flowability of SCC, it is typically recommended to limit the C/A to 0.5 to reduce the inter-particle friction between coarse aggregate, thus enhancing the ability of SCC to flow [10]. In these set of mixtures, the C/A was varied from 0.4 to 0.6 to study its effect, while the contents of all other materials were kept constant. Figure 3.11 indicates a slight to negligible increase in SI values obtained from all test methods over the range of

aggregate ratio investigated. The figure also shows that the risk of dynamic segregation in SCC mixtures decreases with increasing the C/A below a threshold value of approximately 0.45, and increased beyond that value. This effect could be attributed to a decrease in the amount of coarse aggregates, leading to a greater inter-particle spacing and a higher potential to segregation. In addition, by increasing C/A beyond 0.5, higher dynamic segregation is observed, which can be caused by a reduction of the particle lattice effect. C/A of approximately 0.45 conforms to current recommendations regarding the coarse aggregate content in SCC mixture design [9]. The sieve stability test exhibited a more uniform increase of SI with higher C/A values.



**Figure 3.11 Effect of coarse/total aggregate on dynamic segregation (black line) of SCC [10].**

### 3.6. CURRENT METHODS TO ASSESS DYNAMIC SEGREGATION

Accurately assessing segregation by testing the fresh concrete is as important as controlling it. This has proven to be difficult, and few accurate and reliable tests are currently available to quantitatively measure it. Several methods are available to assess static segregation but a very limited number of methods are found to be efficient to measure dynamic segregation.

**3.6.1. Visual Stability Index.** The stability of SCC can be assessed by visually evaluating the distribution of coarse aggregate and paste (bleeding) within the concrete mass after the spreading of the concrete has stopped during the slump flow test. Typically, once the slump flow test has been completed, a visual stability index value is assigned to the concrete [22].

This test gives an indication about segregation resistance and it is affected by static and dynamic segregation. Therefore, it is not a suitable method to assess purely dynamic segregation. When there no layer of paste and water on the edge of the concrete is observed, it is considered having a good dynamic segregation resistance. Even though an SCC mixture has a good VSI value, it can show severe dynamic stability problems, especially if the concrete travels over longer distances. VSI does not quantify this property of a concrete mixture, but it is very helpful indicator if there is segregation. Table 3.2 shows the visual stability index rating.

**Table 3.2 Visual stability index rating [22]**

Rating	Criteria
0 = Highly Stable	No evidence of segregation for bleeding.
1 = Stable	No evidence of segregation or slight bleeding observed as seen on the concrete mass.
2 = Unstable	A slight mortar halo < 10 mm and/or aggregate pile in the center of the concrete mass.
3= Highly Unstable	Clearly segregating by evidence of large mortar halo > 10 mm and/or a large aggregate pile in the center of the concrete mass.

**3.6.2. Flow Trough [19].** A flow trough was developed to determine segregation, and shown in Figure 3.12. It was made by assembling 25 mm thick wood boards to form a 150 x 150 x 1800 mm trough inclined with a 230 mm height difference

between the two ends, which is the minimum slope to ensure SCC flow. The test is performed according to the following procedure [19]:

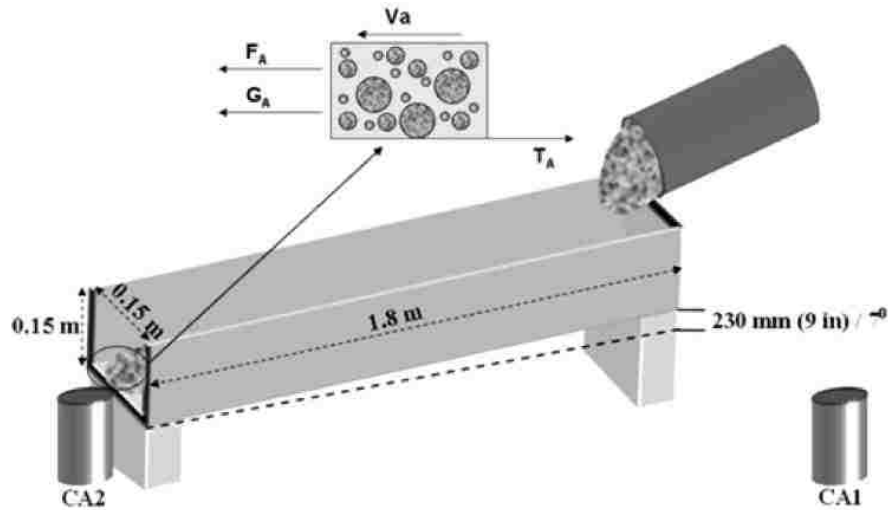


**Figure 3.12 Flow trough for dynamic segregation [19].**

Before the test, the surface of the trough must be wetted with water. In the first step, fresh concrete has to be cast in one 100 x 200 mm cylinder and two 150 x 300 mm cylinders in one lift. Then concrete in one of the 150 x 300 mm cylinders is poured on the higher end of the trough. After the concrete stops flowing, the trough is straightened up vertically for 30 s to let the priming concrete flow off and leave a mortar layer on the trough surface. The trough is then put back into the original position and the other 150 x 300 mm cylinder is poured on the trough from the higher end. The leading portion of concrete flowing through the trough fills another 100 x 200 mm cylinder. Concrete samples in both 100 x 200 mm cylinders are washed over a #4 sieve and coarse aggregates are weighted. The dynamic segregation index (DSI) is calculated using the following equation [19]:

$$DSI = \frac{(CA_2 - CA_1)}{(CA_1)}$$

Where:

$CA_1$  = the mass of coarse aggregates in the SCC mixture (volume measured in a standard 100 x 200 mm cylinder).

$CA_2$  = the mass of coarse aggregates in the SCC (measured in the same volume) that has flowed through the trough.

The limit of DSI for segregation depends on the SCC mix design and flow distance [23].

**3.6.3. Penetration Test [21].** A penetration test was developed to measure dynamic stability, and it is used along with the L-box test. A small set of cylinder molds (type N) with a height of 70 mm and a diameter of 80 mm are used to assess segregation resistance of SCC in a horizontal direction. A simple apparatus, called the penetration apparatus (PA), was also used for rapid testing of segregation. The structure of this apparatus is shown in Figure 3.13 and it consists of a Frame F, Slot E, Reading scale M, Screw D and a penetration head. The penetration head, which has a mass of 54 g, is assembled from a Cylinder C and Rod K. The inner diameter, height and wall thickness of the cylinder are 75, 50 and 1 mm, respectively. The L-box and the penetration apparatus were used together to rapidly test segregation resistance, deformability and blocking behavior of SCC mixtures.

The test procedure starts with gate A of the L-box closed, and place concrete into the vertical leg of the L-box (Figure 3.14) without any consolidation such as rodding or vibration. Level the top of the placed concrete immediately. Before measuring the penetration depth ( $Pd$ ), care must be taken in order to avoid segregation caused by external impacts (such as L-box moving). Also, care must be taken to fill all parts of the



cylinder mold with a representative sample of concrete. After 2 min, place the penetration apparatus (PA) on the top of the vertical leg of the L-box, adjust the penetration cylinder to just touch the upper surface of concrete, and then allow the cylinder to penetrate freely into the concrete for 45 seconds. The penetration depth is recorded from the scale attached. After the gate A is lifted to allow the concrete to flow, when it stops, fresh concrete is taken from the region in front of the reinforcement set and at the end of the horizontal leg of the L-box, and used to fill a pair of small molds (type N) each. Afterwards, the molds are washed out, and the coarse aggregates larger than 9.6 mm are separated and weighed. Concrete has satisfactory segregation resistance when the difference (specified as  $Rh$ ) of average masses of coarse aggregates from in front of the reinforcement set and at the end of the L-box is smaller than 10%. The difference  $Rh$  and  $Pd$  are compared to determine the optimum range of  $Pd$ , which can be used to rapidly evaluate the segregation resistance of SCC in the horizontal direction [21].

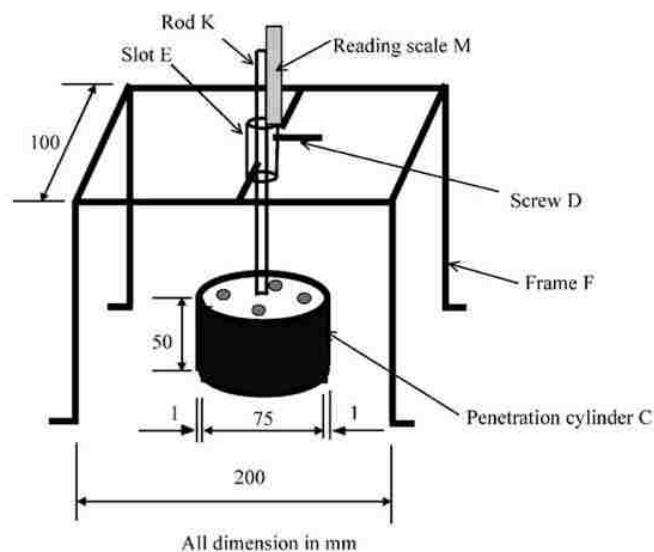


**Figure 3.13 Penetration Apparatus (PA) [21].**

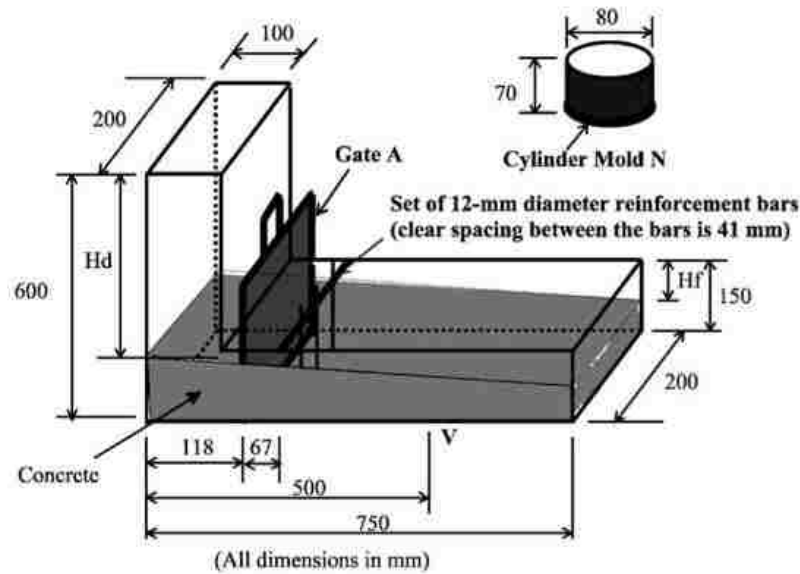


**Figure 3.14** The L box and cylinder mold (type N) [21].

According to the authors, concrete has a satisfactory segregation resistance in a horizontal direction if  $Pd \leq 9$  mm and poor segregation if  $Pd > 9$  mm.

**3.6.4. Tilting Box [24].** The purpose of this test is to evaluate the resistance of flowable concrete and SCC to dynamic segregation occurring due to flow over a certain distance. The T-box consists of a rectangular channel, 1030 mm in length (1000 mm between the inner faces of two extreme walls), 200 mm in width, and 400 mm in height. It is hinged in the middle to a support, as illustrated in Figure 3.15. Such configuration allows the device to freely tilt left-to-right-hand sides. Also, it has a support placed beneath one end of the apparatus to restrict its motion to only one side, which enables the production of the cycles.

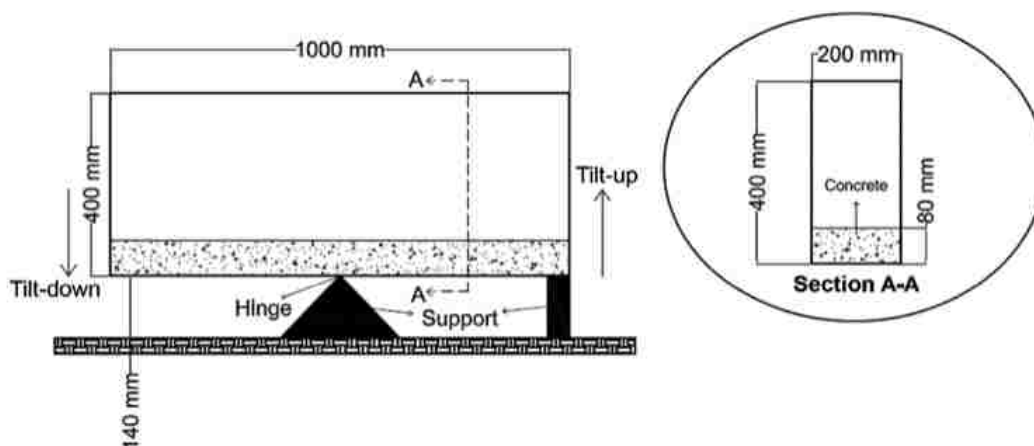


**Figure 3.15 Configuration of the T-box [24].**

The procedure is performed as follows: At the beginning of the test, 16 liters of SCC are introduced into the box. Then, the cycles are performed according to the specific duration and as many as determined based of the given application. A combination of 60 cycles of 2 seconds each was found to be an adequate indicator of segregation [24]. Finally, the box is held horizontal, and the segregation is evaluated using two different techniques.

The easiest assessment technique is the surface penetration test (Figure 3.16). The best indicator of segregation derived using this method, as mentioned, is the penetration depth growth (PDG) on the side that tilts upward (tilt up section). In order to obtain this index, the initial penetration depth on the tilt up ( $D_{pi}$ ) side is measured right after pouring SCC into the box. Likewise, when the test is finished, the penetration depth is recorded on the same side ( $D_{pf}$ ). The difference between these two values presents an indirect indication of segregation. This index is expressed as:

$$PDG(mm) = D_{pf} - D_{pi}$$

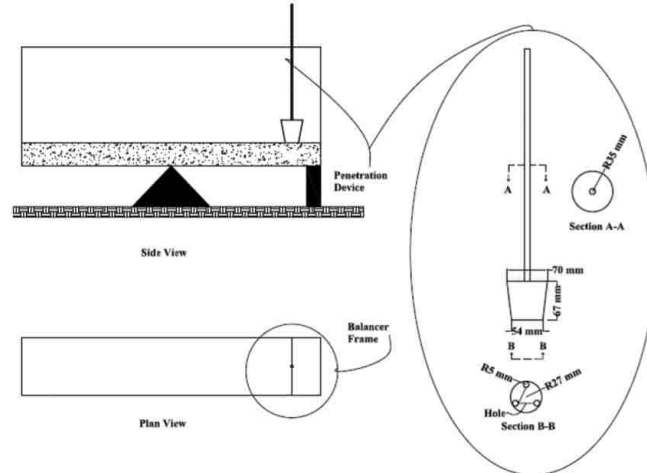


**Figure 3.16 Surface Penetration technique [24].**

The other evaluation method involves taking SCC samples from the two opposite ends of the box (approximate area of 200 by 200 mm). The samples are washed out over a # 4 sieve. The weight of the coarse aggregates retained on the sieve is then determined, and a segregation index is derived from the relative volume of the aggregates of each sample. This index, is calculated with the following equation:

$$VI = \frac{V_{td} - V_{tu}}{\text{Average}(V_{td}, V_{tu})} \times 100$$

where  $V_{td}$  = Relative coarse aggregate volume (the ratio of volume of aggregate > 4.75 mm to the total volume of SCC sample) in the tilt down section and  $V_{tu}$  = relative coarse aggregate volume in the tilt up section.

A volumetric index of  $\leq 13\%$  indicates that the concrete is highly stable. Acceptable segregation is observed when VI is between 13% and 25%, while the segregation zone is defined by  $VI > 25\%$ .

The tilting box test [24] seems the most suitable method to assess dynamic segregation, since it can be used in the laboratory and in the field to evaluate dynamic

segregation of the SCC mixture. In addition, it takes the flow distance of the concrete into account by making the concrete flow through a series of cycles in order to simulate real conditions.

**3.6.5. Modified Penetration Depth Apparatus [10].** Similar to the penetration device, a modified method was proposed to assess dynamic stability of SCC. The developed segregation assessment method is based on studying the profile of the coarse aggregate distribution, particles larger than 9.5 mm, along the height of an SCC sample. The apparatus simply consists of a PVC tube, 300 mm in height and 150 mm in diameter, and a modified version of the penetration apparatus proposed by Bui et al. [21]. The tube is divided into three 150 x 100 mm equal parts using leak free joints that are hinged to a vertical steel rod to assure easy sliding (Figure 3.17). The modified version of the penetration apparatus consists of four penetration heads mounted on a steel frame. Each penetration head is approximately 25 g in mass and 20 mm in diameter with a semi-spherical end (Figure 3.18) [10].



**Figure 3.17** Three compartment hinged cylindrical mold [10].

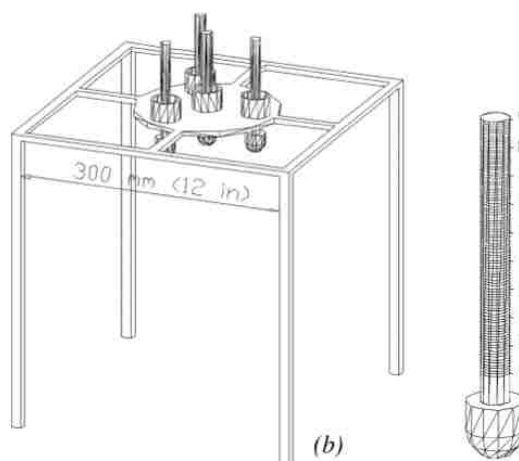


**Figure 3.18** Modified Penetration depth apparatus [10].

First, the average depth of the penetration heads is measured by allowing the heads to penetrate under their self-weight into the concrete just after the cylinder is filled. The three parts of the cylinder are then separated after a rest period of approximately 30 minutes and concrete in each part is washed out over a 9.5 mm sieve. Coarse aggregates larger than 9.5 mm in each part of the cylinder are then retrieved and their mass is determined. The segregation index (SI) is taken as the coefficient of variation (COV) of the coarse aggregate content in all three parts and is calculated using the following equation.

$$SI = \frac{1}{3} \sum_{i=1}^3 \left| \frac{M_i - M_{avg}}{M_{avg}} \right| \times 100$$

Where  $M_{avg} = \frac{1}{3} \sum_{i=1}^3 M_i$  and  $M_i$  equals to the mass of coarse aggregate particles larger than 9.5 mm in each part of the cylinder. Results of SI are then correlated to the corresponding average penetration depth  $Pd$  of the penetration heads.

In the case of evaluating the segregation index for dynamic segregation of SCC mixtures, the concrete sample was prepared using the V-funnel apparatus as a preconditioning method. The dynamic effects were taken into account as the discharge of SCC through the chute of a concrete truck (simulated by the 2:1 slope of the V-funnel sides) and concrete subjected to a free-fall from a height during placement (simulated by placing the test cylinder at a distance  $d$  below the bottom of the V-funnel).

The ability of SCC to resist segregation was evaluated by limiting the COV of the aggregate distribution to 10 %.

As a disadvantage, this test is significantly affected by static stability of the mixture and it does not simulate the flow distance.

**3.6.6. Modified L-box Apparatus [25].** The L-box test apparatus used in this method has a few simple modifications (Figure 3.19). The dimensions of the modified L-box are similar to those of the original L-box, except that the height of the horizontal section is 250 mm instead of 150 mm due to the addition of 100 mm guides. Three metal slides are used to divide the fresh concrete into three portions. First, slide 1 is positioned in front of the smooth bars, while slides 2 and 3 are positioned at equal spacing between the smooth bars and the end of the horizontal section of the L-box.

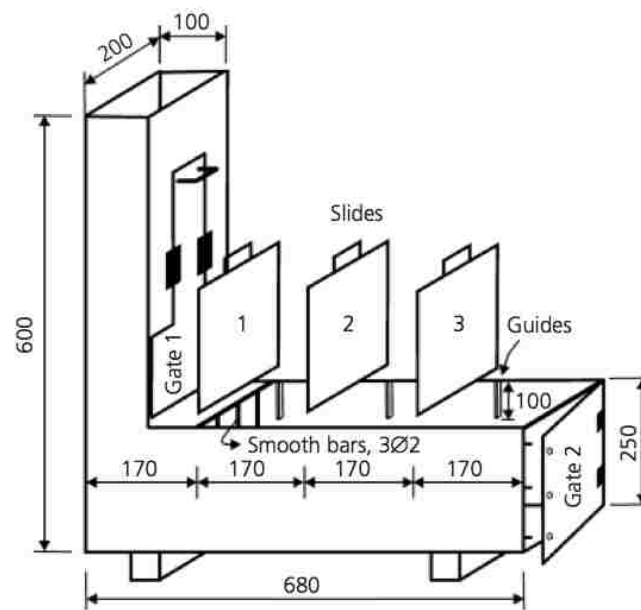


**Figure 3.19 Modified L-box apparatus [25].**

The testing procedure was conducted as follows. First, close gate 1 of the modified L-box and place the concrete into the vertical leg of the L-box without any consolidating such as rodding or vibration. Then, level the top of the placed concrete immediately. Close the sealed gate 2 at the end of the horizontal section of the modified L-box.

After that, wait 60 s and lift gate 1 vertically to allow the concrete to flow between the smooth bars. Next, measure the heights of the concrete in the vertical section ( $H_1$ ) and at the end of the horizontal section ( $H_5$ ) as soon as the flow of concrete into the horizontal

section stops (Figure 3.20). Then, insert metal slides 1, 2 and 3 through the guides into the fresh concrete. Open gate 2 at the end of the horizontal section. Put the concrete from the different partitions into individual trays by removing slides 3 and 2 respectively. Wash the concrete in a #4 sieve, collect the coarse aggregates and immediately determine the coarse aggregate weight in water ( $G_{gsw\ i}$ ) without any treatment. After that, calculate the volume of the aggregates in the different partitions using the following equations based on Archimedes' principle [25].

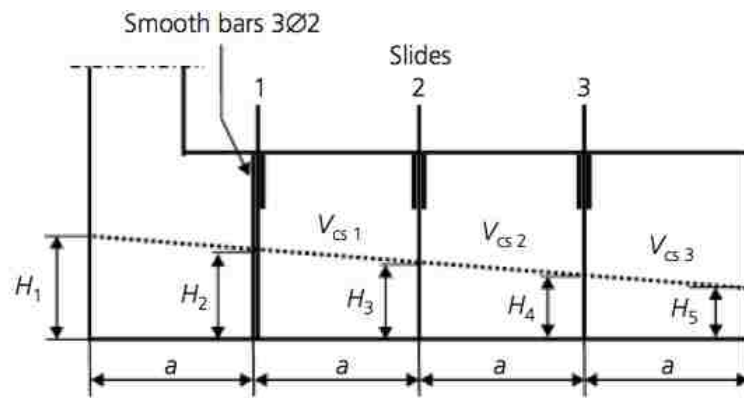


Figure 3.20 General view of the section [25].

$$D_{ssd} = \frac{G_{ssd\ i}}{G_{ssd\ i} - G_{gsw\ i}}$$

$$V_{gs\ i} = \frac{G_{gsw\ i}}{D_{ssd} - 1} \times 10^3$$

Where

$D_{ssd}$  = saturated surface-dry (SSD) density of coarse aggregate. It is known from the mix design. The weight of the coarse aggregate in water in partition  $i$  can be easily found by weighing the coarse aggregate in water.

$G_{gsw\ i}$  = the weight of coarse aggregates in water for partition  $i$  (g).



$G_{ssd\ i}$  = SSD weight of coarse aggregate (g).

$V_{gs\ i}$  = the volume of the coarse aggregate in partition  $i$ .

Find the volume of the concrete by the trapezoid or rectangular shape in partition  $i$  using the geometrical relationship in Figure 3.20.

$$V_{cs\ i} = \frac{1}{8}ab(5H_1 + 3H_5) \quad (i = 1)$$

$$V_{cs\ i} = \frac{1}{8}ab(3H_1 + 5H_5) \quad (i = 2)$$

$$V_{cs\ i} = \frac{1}{8}ab(H_1 + 7H_5) \quad (i = 3)$$

As indicated in Figure 3.21, find the volumetric ratio of the coarse aggregate to the concrete in the sample mixture at partition  $i$  using the following equations.

$$x_{s\ i} = \frac{V_{gs\ i}}{V_{cs\ i}}$$

$$x_o = \frac{V_{go}}{V_{co}}$$

Where:

$V_{cs\ i}$  = Volume of concrete sample at partition  $i$  (mm<sup>3</sup>).

$V_{go}$  = Volume of coarse aggregate in original mixture (mm<sup>3</sup>).

$V_{co}$  = Volume of original mixture (mm<sup>3</sup>).

$x_o$  = Volumetric ratio of coarse aggregate to concrete in original mixture.

$x_{s i}$  = Volumetric ratio of coarse aggregate to concrete in sample mixture at partition  $i$ .

Last, calculate the segregation coefficient ( $SC$ ) by analysis of variance of  $x_{s i}$  and  $x_o$ .

$$SC = \frac{250}{x_o} \sum_{i=1}^3 (x_{s i} - x_o)^2$$

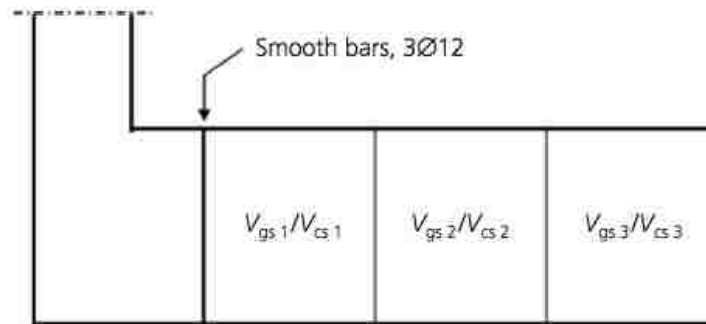
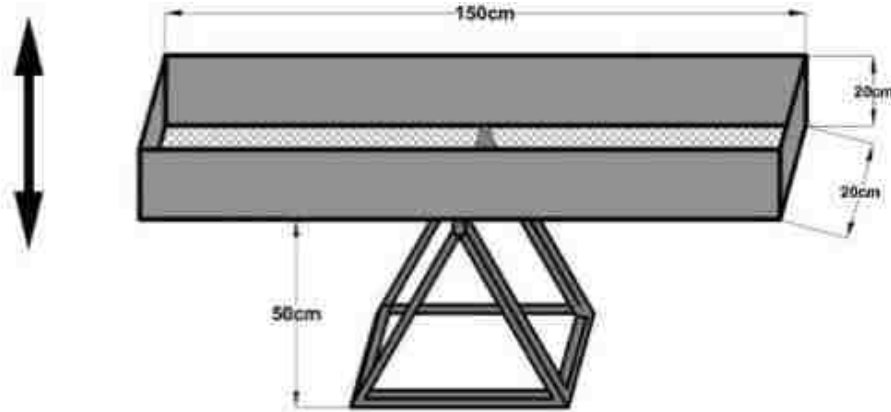


**Figure 3.21 Demonstration of the ratio  $V_{gs i}/V_{cs i}$  from the L-box [25].**

A concrete has good segregation resistance if  $SC \leq 5$  and poor segregation resistance if  $SC > 5$ .

Similar to [21], the segregation measured with this method is more related to the effects of blocking due to the L-box geometry than the segregation assessment.

**3.6.7. Dynamic Sieve Stability Test (DSST) [26].** This test method is proposed to evaluate the dynamic segregation of SCC mixtures and consists of a rectangular steel channel box with a sieve at the bottom having 6 mm sieve opening. This sieve has been selected considering the clustering of the fine aggregates in the fresh mixture. The inner dimensions of the device are shown in Figure 3.22. It is hinged in the middle to a support.



Not to scale

**Figure 3.22 Configurations of the DSST apparatus [26].**

The procedure of this method is as follows. First, the empty box is weighted ( $W_d$ ), and then the box is placed back in the middle of the support stand. After that, a concrete sample weighting 18 kg ( $W_c$ ) is poured into the box from the middle, while the box is horizontal. The box is cycled four times doing an up and down movement of the ends, which is equivalent to a travelling distance of approximately 5.25 m. The duration of each cycle is 15 s to allow the concrete to flow in the box. Then the box is held horizontally on the stand for 10 s. Finally, the box with the remaining concrete is weighted ( $W_f$ ).

The dynamic segregation ratio (DSR) is calculated as the ratio of the mass of material that passes through the sieve ( $W_{ps}$ ) to the total initial mass of concrete sample cast in the channel box ( $W_c$ ). The dynamic segregation ratio is calculated using the following equation.

$$DSR = \left( \frac{W_{ps}}{W_c} \right) \cdot 100 = \left[ \frac{(W_d + W_c - W_f)}{W_c} \right] \cdot 100$$

A maximum DSR value of 30% is recommended for dynamically stable SCC.

This test method has a similar design as the tilting box. Tilting the channel up and down simulates the flow distance but the channel seems too long and heavy to transport to a job site.

### 3.7. INDIRECT INDICATORS OF DYNAMIC SEGREGATION

According to Khayat et al. [27], besides the methods used to directly evaluate dynamic segregation, some current test methods are suggested, such as J-ring, L-box, U-box, V-funnel and the pressure bleed test. These tests can be indirect indicators of the existence of dynamic segregation in self-consolidating concrete. The aim of the presented study was to find field-oriented test methods assessing stability of SCC. Based on their observation, the final conclusions are mentioned below [27]:

1. The slump flow test is suitable to evaluate deformability of SCC. Even though the visual observation does not offer sufficient information regarding segregation, it can provide some basic information for the stability evaluation as it gives some indication of water or paste separation and segregation of coarse aggregate in dynamic and static conditions. The VSI rating is recommended to be coupled with other tests for visual assessment of SCC stability.
2. The J-Ring, L-box, and U-box tests are suitable for evaluating the passing ability of SCC through closely spaced reinforcing obstacles. These tests can be well correlated and can be easily conducted at the job site, and their outcome could give general information about the stability level of the concrete if the relationship between passing ability and dynamic segregation could be established.
3. The L-box test can be considered for field evaluation of the passing ability of SCC. There

could be a relationship between passing ability and dynamic segregation, which means that the results of L-box blocking ratio could provide a basic idea of dynamic stability. The L-box and the slump flow tests are recommended for field-oriented quality control testing of the restricted and non-restricted deformability of SCC.

4. Similar to the slump flow/L-box tests. The slump flow/J-Ring tests can evaluate both the deformability and passing ability characteristics. The L-box is preferable; however, because it can reflect the viscosity of the mixture given the flow time value.
5. The  $T_{50}$  and the flow times evaluated from the V-funnel, L-box, and U-box tests can be used to assess relative viscosity. For a given deformation capacity, the longer the flow time, the higher the viscosity of the mixture. Hence, if the relationship between viscosity and dynamic segregation is known, such results could be used to evaluate dynamic stability.
6. The pressure bleed test can be used to evaluate the ability of the paste to retain free water in suspension and is conducted over a 10 min period. It can then be suitable for frequent quality control and quantitative evaluation of SCC stability in the field.

### **3.8. ASSESSMENT OF UNIFORMITY OF SELF-CONSOLIDATING CONCRETE BY HARDENED CONCRETE TESTING**

The most reported hardened properties of SCC that can be affected by segregation are the compressive strength, elastic modulus, durability, and bond between the concrete and steel reinforcement. In order to assess the in situ uniformity, three test methods were selected in this research project. Ultrasonic pulse velocity (UPV), bond strength and in situ compressive strength on concrete cores drilled from the beams. The tests are further described below.

**3.8.1. Ultrasonic Pulse Velocity Test.** This method consists of sending an ultrasonic pulse through a hardened concrete element. The wave propagation speed reflects elastic properties, concrete composition, and porosity [28].

There are some factors that affect UPV results, which are related to SCC uniformity: segregation, w/cm (strength), density related to the distribution of the constituents and air content, mortar quality, and the interface quality related to the presence of excess water and porosity [29, 30]. The ability to simultaneously account for these factors makes the UPV test method very useful for assessing the effects of possible segregation and for detecting changes in concrete quality at different locations within a concrete element [31].

Cussigh, F. [32] used UPV testing to study the effects of segregation on SCC performance. In this research, walls with dimensions approximately 2.80 m in height by 2.50 m in length and 0.25 m in width were cast using three SCC mix designs. Two mixtures were used without VMA and a third one with an incorporation of a VMA. All mixtures had a controlled variation of water content between 10 to 20 l/m<sup>3</sup>. In situ segregation was evaluated first by sampling concrete from the top of the walls and secondly on hardened concrete by core drilling and pulse velocity measurements. The same walls were also produced using conventional concrete varying degrees of applied consolidation, thus making it possible to compare varying levels of stability in SCC to levels of consolidation in conventional concrete.

UPV measurements were determined along the height of the walls and were compared with core samples to study segregation. SCC that showed segregation in the fresh state proved to have less uniform velocities over the height of the wall than stable

SCC, but all measured velocities through SCC proved to be as uniform as satisfactorily vibrated conventional concrete.

Keske et al. [33] also evaluated the effects of stability on the in place uniformity of SCC mixtures using UPV. Four walls with heights of 2.39, 1.83, 1.37 and 0.91 m were cast with nine different mixtures varying in stability and filling ability, as well as two CVC mixtures which were all designed to achieve the properties required for the construction of precast, pre-stressed members. The in-place effects of segregation were tested using UPV and pull-out of rebars on the hardened specimens.

UPV was measured along the height of the walls. The results showed that the measured velocities tend to decrease with increasing height, but the fastest and slowest velocity were not always measured at the very top of each wall. Although the UPV measurements in a wall may not be consistent over the wall's height, the maximum and minimum velocities likely indicate the level of non-uniformity within the wall.

**3.8.2. Compressive Strength on Cores.** Several researchers have attempted to directly study the effect of segregation on strength uniformity. Elements were cast using SCCs with varying segregation values, and the uniformity of strength was determined by taking cores along their height and length and testing them for compressive strength. Some researchers found that strength variation was statistically insignificant in SCC showing questionable stability [34,35], while others concluded that strength variation is directly affected by segregation [36].

**3.8.3. Pullout Test.** In this test method, the bond strength between the concrete and the prestress strand is evaluated. Since the bond strength is affected by the aggregate settlement, air migration, and bleeding, it is important to investigate the influence of dynamic segregation.

Long et al. [37] evaluated the influence of stability on the uniformity of bond strength between prestress strands and concrete. Six wall elements measuring 1540 mm × 2150 mm × 200 mm were cast using five SCC mixtures and one reference high-performance concrete (HPC) with normal consistency. The results showed that walls with stable SCC mixtures exhibited more homogenous pull-out bond strength along the height compared to walls cast with unstable SCC.

Khayat et al. [38] also investigated the uniformity of bond strength and in situ mechanical properties of SCC. Four SCC mixtures and two CVC mixtures suitable for prestress and precast applications were evaluated. The mixtures incorporated 20% fly ash replacement and were used to cast wall elements measuring 1.54 m in height, 1.1 m in length, and 0.2 m in width. Two types of viscosity-modifying admixtures (VMA) and two high-range water reducers were employed. Results showed a uniform distribution of in-place compressive strength and adequate bond to the prestress strands were obtained with relatively small experimental variations along the wall elements. Also, the strand bond is not compromised in stable SCC.

Bond between a strand and concrete is affected by the position of the embedded reinforcement and quality of the cast concrete. Bond to pre-stressed tendons can be influenced by the flow properties of the SCC, grading of the aggregate and content of fines in the matrix [39].

In comparison to the vertically embedded reinforcement, the horizontal reinforcing bars have larger area under which bleed water could accumulate and adversely affect and weaken the interfacial bond properties (Figure 3.23).



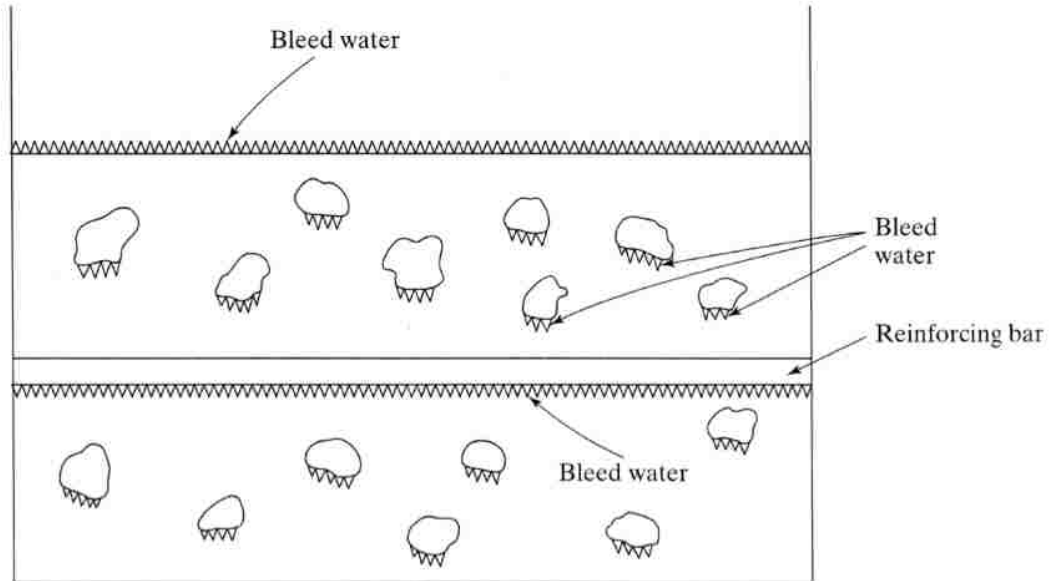


**Figure 3.23 Internal and external bleeding [28].**

Surface settlement, caused by a lower static stability of concrete after being placed, can also have higher influence on bond with horizontal rebars than vertical ones. Therefore, the top-bar effect is usually more prominent in horizontal reinforcements than in the vertical bars, for convectional vibrated concrete, as reported in Figure 3.24 [40]. However, to study the effect of dynamic segregation on bond strength of strands with SCC, vertical strands may be beneficial as the influence of static segregation is less prominently present.

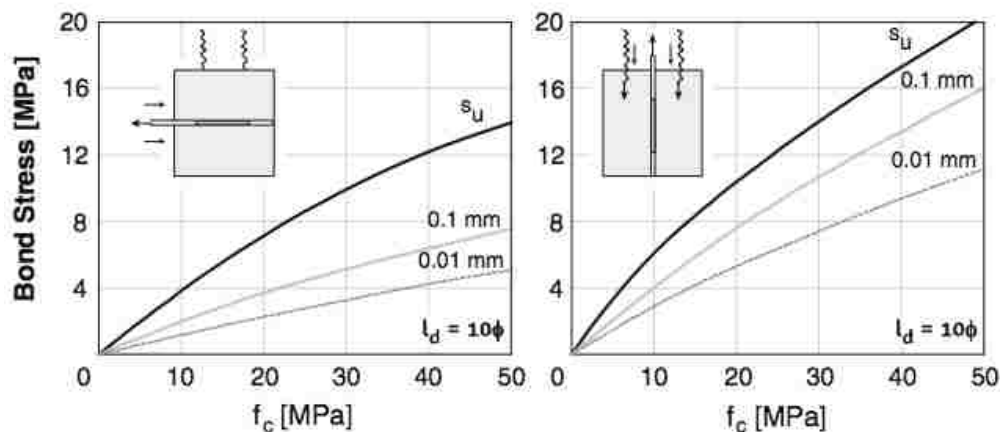


**Figure 3.24 Effect of rebar direction on bond strength [40].**

## 4. MATERIAL

### 4.1. MATERIALS CHARACTERIZATION

This section summarizes the various materials used in the laboratory and field experiments. The material characterization focused on the physical properties to achieve an appropriate mix design for SCC.

**4.1.1. Portland Cement.** Commercially available Types I/II and III ordinary Portland cements were used. Both cements meet ASTM C150-16 [41] requirements. The physical properties of the two cements, according to the manufactures, are presented in Table 4.1.

**Table 4.1 Physical properties of cement.**

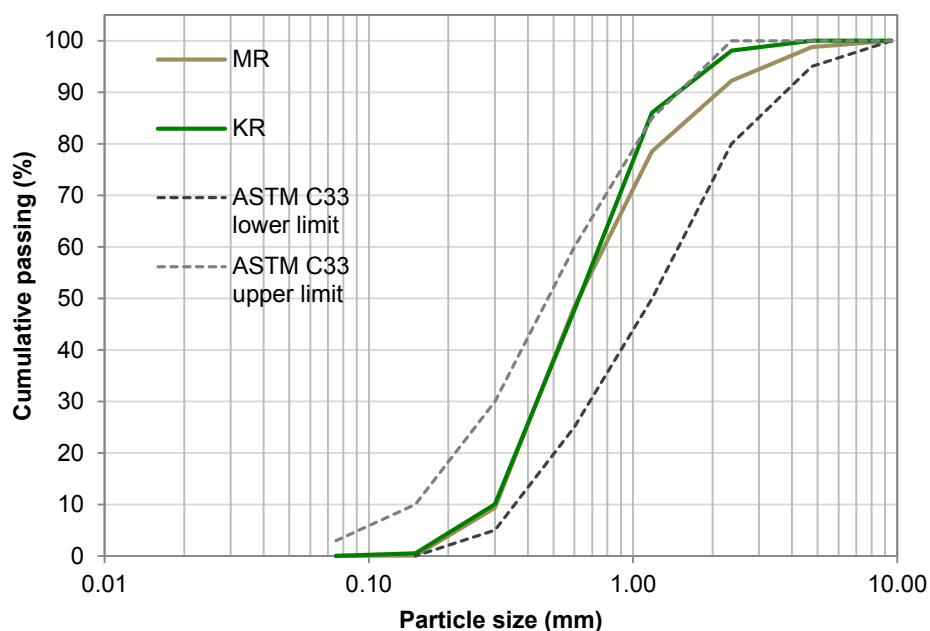
Type	Specific gravity (g/cm <sup>3</sup> )	Blaine specific surface (m <sup>2</sup> /kg)
I/II	3.11	386
III	3.15	-

**4.1.2. Fly Ash.** In order to modify the properties of SCC mixtures, a commercially available Class F fly ash was used. The addition of fly ash was carried out at 20% of replacement by weight of cement. The specific gravity of the fly ash was 2.38.

**4.1.3. Fine Aggregate.** Two types of fine aggregates from different sources were used in this study. Table 4.2 shows the physical properties of the Missouri River (MR) and the Kansas River (KR) sand. The density and absorption results were determined according to ASTM C128-15 [42]. The grading curves of the two types of sand are illustrated in Figure 4.1. Both sands are conforming to ASTM C33-16 [43] gradation requirements. The gradation was carried out according to ASTM C136-14 [44].

**Table 4.2 Physical properties of the fine aggregates.**

Source	Specific gravity (g/cm <sup>3</sup> )	Absorption (%)	Fineness modulus
MR	2.61	0.4	2.72
KR	2.62	0.4	2.53

**Figure 4.1 Gradation curve of fine aggregates from the Missouri and Kansas Rivers.**

**4.1.4. Coarse Aggregate.** The laboratory and field experiments were performed using coarse aggregates from different sources. Table 4.3 shows the physical properties of the three crushed limestones (CL1, CL2, CL3) and pea gravel (PG). The gradation was carried out according to ASTM C136-14 [44]. The density and absorption test were done following the procedure from ASTM C127-15 [45]. Figures 4.3 to 4.5 illustrate the grading curves for the coarse aggregates. Figure 4.2 shows that the crushed limestone (CL1) is non-compliant with the ASTM C33-16 for the sieve number 8 limits for the 9.5 and 4.75 mm sieve size. Also, Figure 4.3 demonstrates that the crushed limestone (CL2) is below the lower limit at the 12.5 mm sieve size, while Figure 4.4 illustrates the

combined gradation of CL1 and PG, which is slightly out of the sieve number 89 limits for the 9.5 mm sieve size. CL3 meets the standard requirements for the sieve number 8 limits.

**Table 4.3. Properties of the different coarse aggregates.**

Aggregate	Maximum nominal size (mm)	Specific gravity (g/cm <sup>3</sup> )	Absorption (%)
CL1	9.5	2.55	3.6
PG	4.75*	2.40	3.6
CL2	12.5	2.67	1.4
CL3	9.5	2.67	1.6

\*PG and CL3 are defined as fine aggregates. It is included as a coarse aggregate when it is combined with a size number 8 material to create a size number 89 [43].

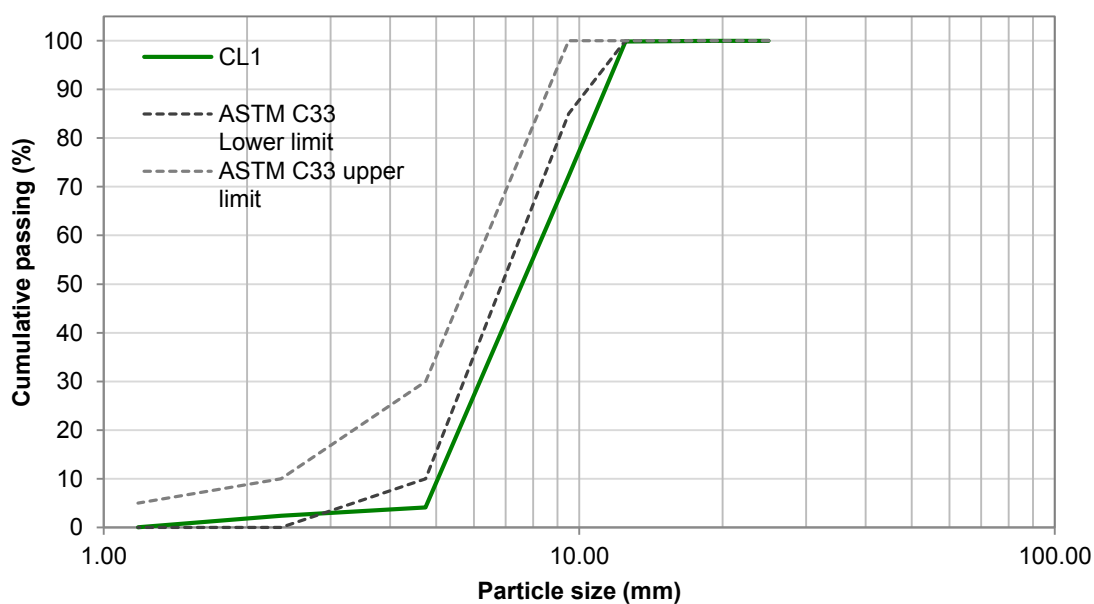


**Figure 4.2 Gradation curve of 9.5 to 2.36 mm crushed limestone (CL1).**

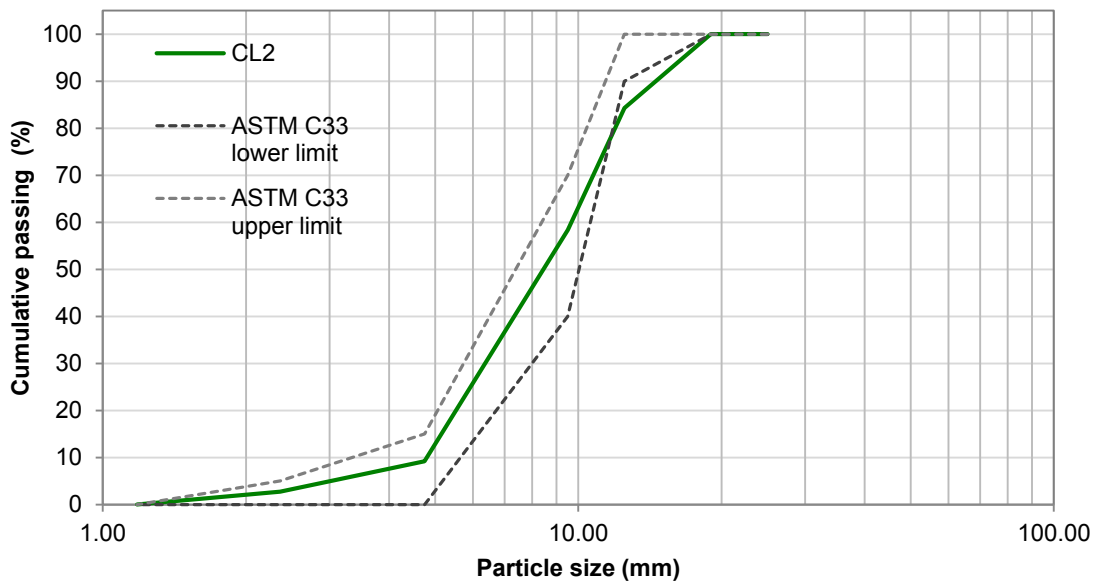


Figure 4.3 Gradation curve of 12.5 to 4.75 mm crushed limestone (CL2).

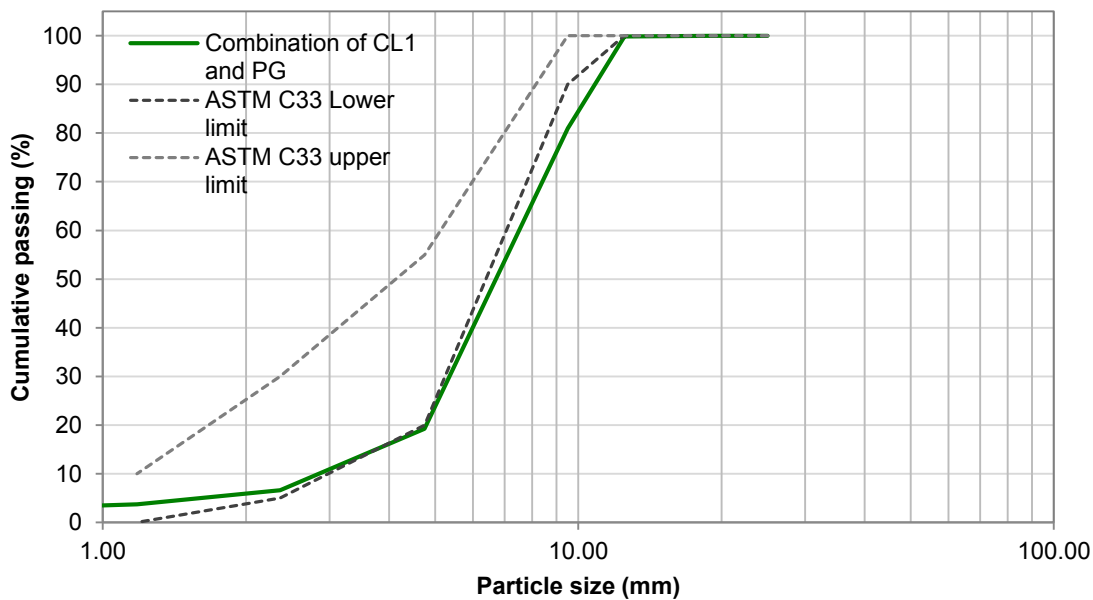
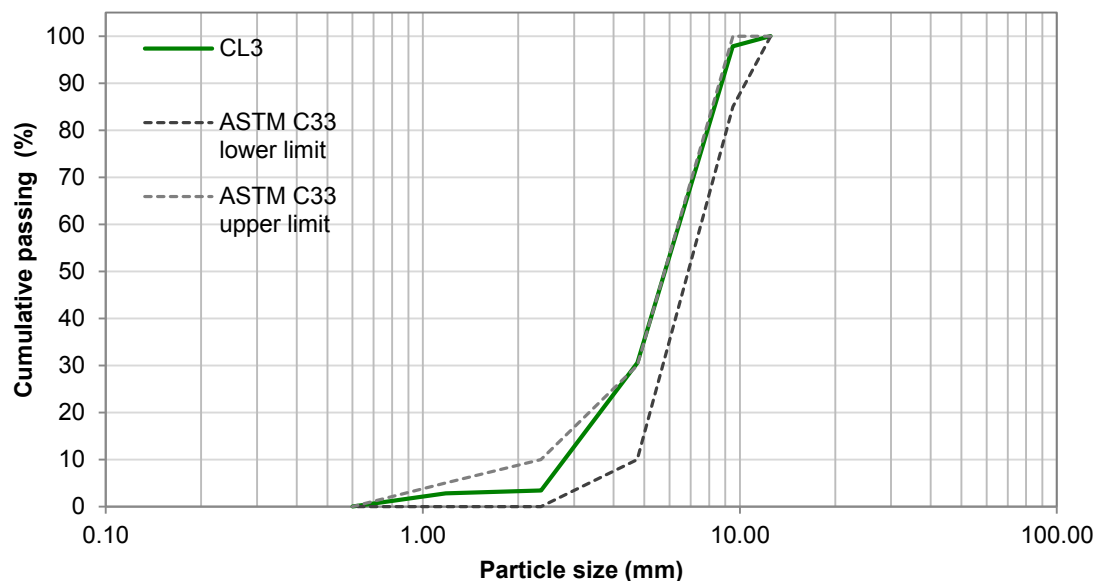


Figure 4.4 Gradation curve for the combination of CL1 and PG (9.5 to 1.18 mm).



**Figure 4.5 Gradation curve of 9.5 to 1.18 mm crushed limestone (CL3).**

**4.1.5. Chemical Admixtures.** To achieve SCC consistency, two commercially available polycarboxyl-ether based superplasticizers (SPs) were used to achieve sufficient flowability. One of the SP was selected to guarantee sufficiently long workability retention to carry out all tests in the laboratory. In addition, a welan gum based viscosity-modifying agent (VMA) was used to enhance the stability of SCC. SP2 is a commercial chemical admixture, which contains both SP and VMA. For a selected series of mixtures, an air-entraining agent (AEA) was added to improve freeze-thaw-resistance in an attempt to replicate the mix design used at Coreslab Structures. All admixtures are conforming ASTM C494-15 [46]. Table 4.4 shows the properties of the admixtures used in this research project.

**Table 4.4. Properties of different chemical admixtures.**

Admixture	Specific gravity (g/ml)	Solid content (%)
SP1	1.085	39
VMA	1.207	44
SP2	-	-
AEA	-	-

## 5. EXPERIMENTAL WORK

### 5.1. INTRODUCTION

This section discusses in detail the mixing and testing procedures employed in this project and the test methods used to characterize the fresh and hardened properties of the mixtures. In addition, the mix designs and materials utilized in different tasks are provided. Existing standard and non-standard methods were applied to study the properties of SCC. The tilting box, a new test equipment developed by Esmailkhanian et al. [24] was used to assess dynamic segregation, but it was modified in order to evaluate the effect of the formwork dimensions.

This research project was divided in three main tasks. Figure 5.1 shows the sequence of the tasks performed to achieve the objectives of this project. The first task was performed in the laboratory and focuses on finding the link between mix design, fresh properties and dynamic segregation of SCC mixtures. Also, the design parameters critical for dynamic segregation are determined. Finally, the modification of a typical SCC mixture used in the precast industry in order to guarantee the robustness and homogeneity of the element to achieve good structural performance is discussed. The second task was executed in the field and investigated the consequences of dynamic segregation on pre-stressed beams by means of ultrasonic pulse velocity, compressive strength and bond strength. The third task consists of the development of practical guidelines and validation in the field.

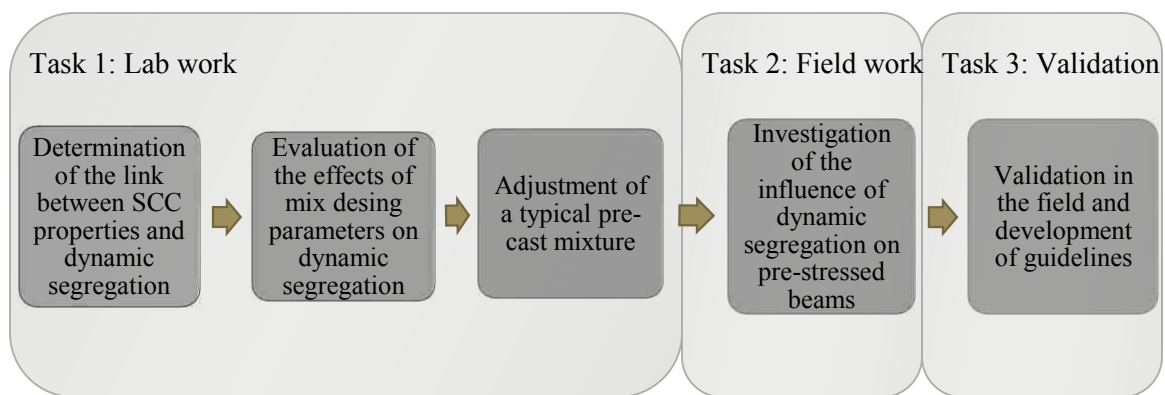


**Figure 5.1 Sequence of executed tasks.**

## 5.2. TASK 1: LABORATORY WORK

**5.2.1. Mix Design.** In this task, three mix designs were evaluated. The SCC reference mix design was made according to the recommendations by EFNARC [9] and ACI 237 [6] shown in Table 5.1. In addition, the SCC was designed to have a  $w/cm$  of 0.40 and to reach a slump flow of  $700 \pm 20$  mm. It was established following the recommendations as shown in Table 5.2. Coreslab Structures provided Mix designs 2 and 3, which are proprietary. Therefore, the detailed mix proportions cannot be shown. Table 5.3 shows the materials used in each mix design in this research project.

**Table 5.1 Constituents comparison between EFNARC and ACI 237 recommended values with reference mixture.**

Constituents	Reference mixture	Recommended values	
		ACI 237	EFNARC
$w/cm$	0.40	0.32-0.45	
$V_w/V_p$	0.90		0.85-1.10
Powder ( $kg/m^3$ )	480		380-600
Water ( $L/m^3$ )	190		150-210
Paste ( $\%/m^3$ )	38.2	34-40	30-38
Mortar ( $\%/m^3$ )	72.2	68-72	
Fine Aggregate (% of total aggregate weight)	55		48-55
Coarse aggregate ( $\%/m^3$ )	27.8	28-32	27-36



**Table 5.2 Reference mix design.**

Material	Mix design 1 (kg/m <sup>3</sup> )
Water	190
Cement	384
Fly ash	96
SP <sup>A</sup>	2.08
VMA <sup>B</sup>	0.24
Coarse Aggregate	709
Fine aggregate	887
Air (2.5%)	-

<sup>A</sup> Dosage: 400 ml/100 kg of cementitious materials

<sup>B</sup> Dosage: 50 ml/100 kg of cementitious materials

**Table 5.3 Materials and parameters used for each mix design.**

	Mix design		
	1	2	3
Water			
Cement	Type I/II	Type I/II	Type III
Fly ash	Type F	-	-
SP	SP1	SP1	SP2
VMA	VMA	VMA	in SP2
AEA	-	-	AEA
Coarse Aggregate	CL1	CL1 and PG	CL2 and CL3
Fine aggregate	MR	MR	KR
Paste Volume (L/m <sup>3</sup> )	380	395	380
w/cm	0.40	0.40	0.36
S/A	0.56	0.51	0.51

**5.2.2. Variations in Mix Design Parameters.** In task 1, 23 SCC mixtures were developed to evaluate the effects of mix design parameters on dynamic segregation. The investigated parameters included the water-to-cement ratio (w/cm), paste volume, SP content, sand-to-aggregate ratio (S/A), air content (through changes in AEA content) and VMA content. The variations in the mix design parameters were induced in a different fashion for each mix design, they are shown in Figure 5.2. In addition, the reference mixture was different for mix design 1, 2 and 3. In all mix designs, the total amount of SP was adjusted to reach the targeted slump flow ( $700 \pm 20$  mm), except for the variations in

the SP content, which were adjusted to reduce or increase the yield stress of the mixture. The variations in the SP content in each mix design were the consequence of designing for a different initial slump flow of the SCC mixture.

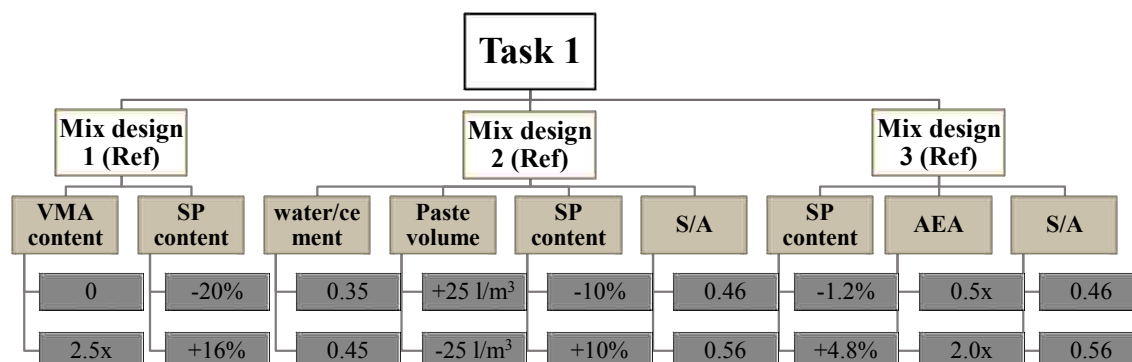


**Figure 5.2 Induced variations on the mixture.**

**5.2.3. Mixing Procedure.** In the laboratory work, all SCC mixtures were prepared in 100 L batches in a drum mixer with capacity of 150 L. During the investigation of mix design 3, an intensive mixer with a capacity of 150 L was used. The mixing sequence consisted of a total of 9 min and is shown in Table 5.4.

**Table 5.4 Mixing sequence for the SCC tested mixtures.**

Task	Time	
	Partial (mm:ss)	Cumulative (mm:ss)
Introducing the sand into the mixer and mixing	01:00	--:--
Correction of the moisture content	--:--	--:--
Adding coarse aggregate to the mixer with half of the water and mixing	00:30	--:--
Introducing cementitious materials along with the remaining water	01:00	01:00
While mixing, the chemical admixture diluted in 1L of water was added	02:00	03:00
Rest period	03:00	07:00
Mixing	02:00	09:00
Visual examination to check whether the mixture meet the expected requirements	--:--	--:--
If necessary, adjust the admixture content	--:--	--:--

### 5.3. TASK 2: FIELD WORK

**5.3.1. Mix Design.** In this task, mix design 3, with specific variations in the parameters, was used to produce nine pre-stressed concrete beams. Beams 1 to 5 and 9 were rectangular beams with a width of 457.2 mm and a height of 915 mm (Figure 5.3). Beams 2, 4 and 9 had a total length of 18 m, while beams 1, 3 and 5 were 9 m long. Beams 6 to 8 were MoDOT approved I-beams (Figure 5.4), each 9 m long, with a bottom flange width of 457 mm, a top flange width of 356 mm and a height of 1143 mm. All beams were pre-stressed with six 12.5 mm diameter prestressing strands at the bottom and two at the top. Minimum shear reinforcement, using #4 steel bars, was installed, spaced 457 mm in the main section of the beams. All beams were cast while keeping the casting point near one end of the beam (Figure 5.5).

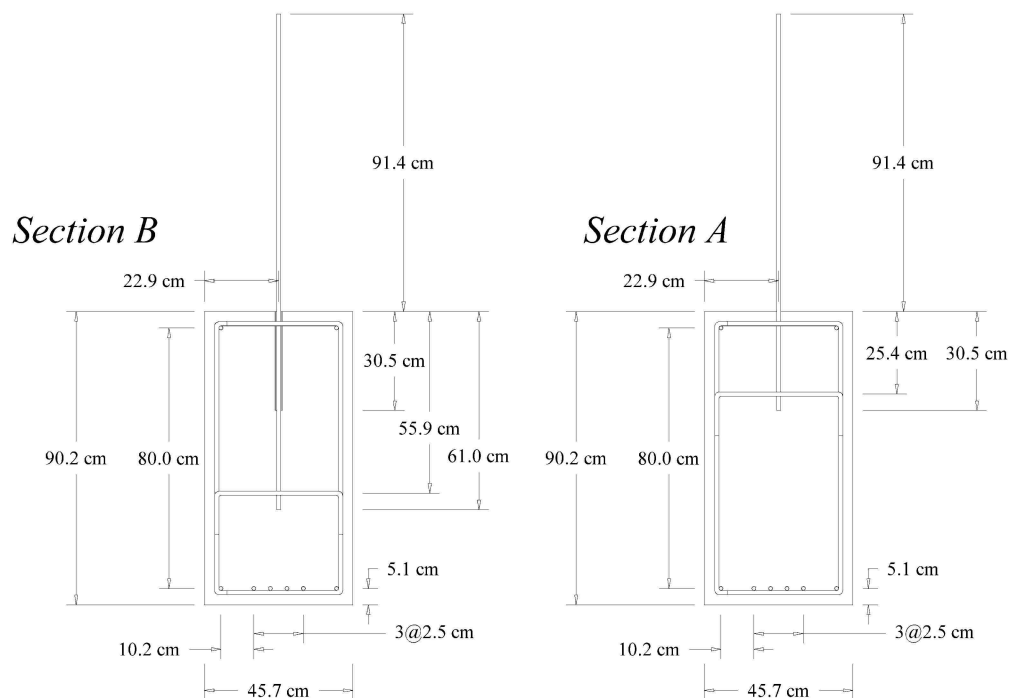


**Figure 5.3 Configuration of the rectangular beams.**

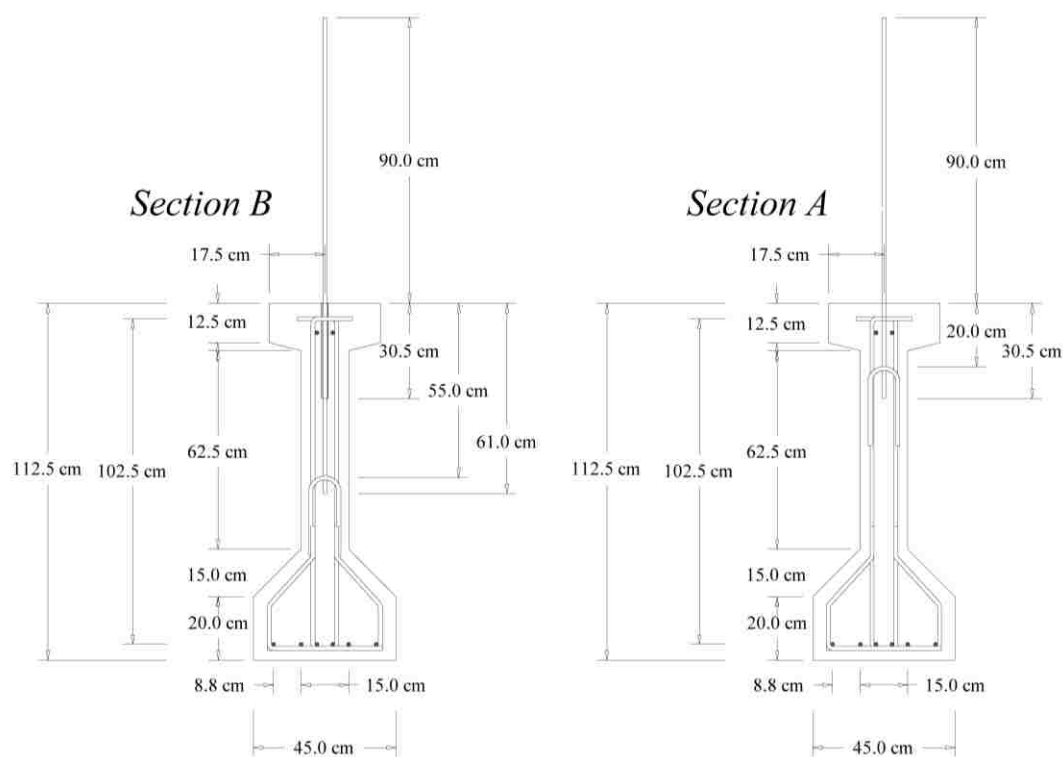
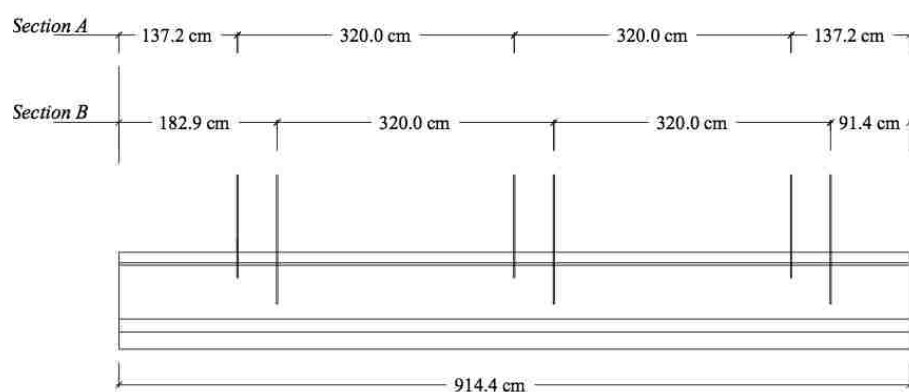


Figure 5.4 Configuration of the “I” beams.



Figure 5.5 Left: Reinforcement of the rectangular beams. Right: Casting beam.

In the 9 m beams, six 12.5 mm diameter pre-stress strands were connected vertically to the shear reinforcement: two near the casting point, two near the end and two in the middle (Figure 5.6 and Figure 5.7). All strands were placed in the middle of the width of the beams. One of the strands in each pair was imbedded in the first 305 mm of concrete, measured from the top, the other was installed from 305 to 610 mm from the top, while the top portion (305 mm) was covered with a plastic sleeve to avoid bond between this concrete and the strand. The strands will be referred to as installed in the top and in the middle section, respectively. For the 18 m long beams, six sets of two strands were equally installed, spaced  $\pm 3$  m apart.



**Figure 5.6 Configurations and strand positions in the 9 m long beams.**



**Figure 5.7 Beam 5 with the three sets of pre-stressed strands. The arrows indicate the direction of casting.**

**5.3.2. Induced Variations in the Mix Design.** In this task, a total of nine beams were cast with different SCC mixtures to evaluate the consequences of dynamic segregation on the performance of pre-stressed beams. Figure 5.8 shows the variations in the mix design parameters that were induced in each beam. These modifications are paste volume, water-to-cement ratio and S/A. In addition, the dimensions and the shape of the beam were also varied. The variations were chosen within the limits of the materials available at Coreslab Structures. In all mix designs, the total amount of SP was modified to reach the targeted slump flow ( $700 \pm 50$  mm).

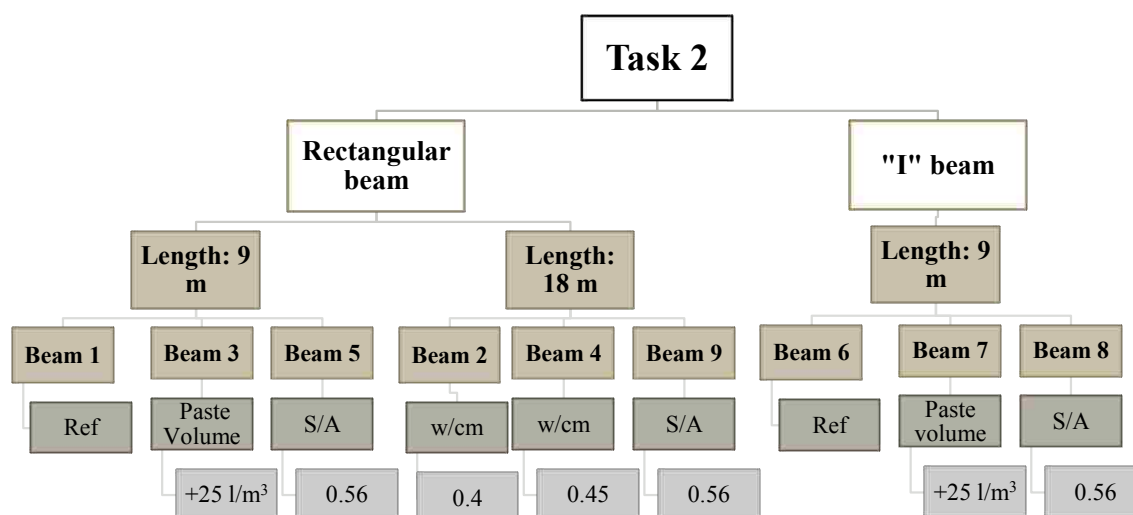


**Figure 5.8 Induced variations in each beam.**

**5.3.3. Mixing Procedure.** Each beam was cast with SCC mixtures that had a volume of approximately  $4.6 \text{ m}^3$  for 9 m, and  $8.4 \text{ m}^3$  for 18 m long beams. The mixtures were prepared in the mixing plant and transported to the casting site in a concrete truck. The mixing sequence was done in accordance to the usual procedure of the company. To verify the targeted workability, the slump flow test was performed. After the slump flow test, each concrete mixture was tested following the procedure shown in Figure 5.9 and was placed simultaneously into the formwork.

## 5.4. TEST METHODS

Since the rheological properties are time-dependent, all tests were performed immediately after the mixing procedure was completed. The slump flow was the main test used to accept the flowability of the SCC. Once the result of this test were on target (i.e.  $700 \pm 20$  mm or  $\pm 50$  for task 2), the other tests were carried out. Table 5.5 shows the tests used in this research project.

**Table 5.5 Test methods used to characterize the fresh properties of SCC.**

Property	Test
Filling ability, yield stress, viscosity	Slump flow and $T_{50}$
Flowability, viscosity	V-Funnel
Segregation resistance	VSI, Sieve stability (GTM) and T-box
Yield stress and viscosity	Contec concrete viscometer or ICAR

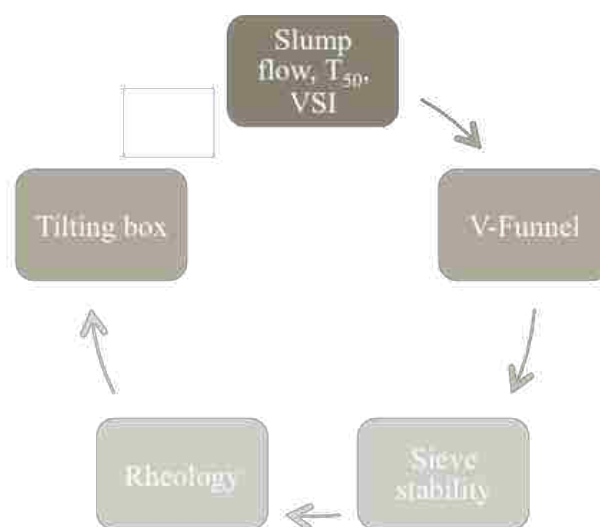


**Figure 5.9 Testing sequence.**

### 5.4.1. Slump Flow, $T_{50}$ and VSI.

This test method is based on ASTM C1611-14 [22] and consists of placing the Abram's cone onto a flat, level and nonabsorbent surface and holding it firmly. Immediately after, start filling the mold with SCC, then vertically raise the mold in  $3 \pm 1$  s and measure two times the diameter of the

resulting circular spread and finally, calculate the average (Figure 5.10). The slump flow test evaluates the ability of SCC to flow under its own weight in unconfined conditions and it is simple to carry out in the laboratory or in the field. According to Roussel and Coussot (2005) [47], this test can also be employed to calculate/estimate the yield stress of the mixture.



**Figure 5.10 Slump flow.**





In addition to the spread,  $T_{50}$  time can be identified to provide an indication of the mixture's viscosity measuring the speed of flow. During the slump flow test, the time is measured from the instant the cone is lifted till the mass of concrete spreads from the initial diameter of 200 to 500 mm. Therefore, a longer  $T_{50}$  time indicates a higher viscosity.

Another important parameter, the visual stability index (VSI), can be observed during the slump flow test. It consists of making a visual examination of the spread and assigning a value in accordance to the criteria shown in Table 5.6. This criterion evaluates the stability qualitatively between SCC mixtures. A VSI value of 0 or 1



indicates that the mixture is acceptable and can be used, while a VSI value of 2 or 3 indicates an unstable mixture with segregation potential and that the mix design should be adjusted to ensure stability. Since the VSI is determined by a visual inspection, it can be subjective. Therefore, the VSI is an excellent initial selection tool for producing SCC, as it can give an indication of segregation, but it should not be used to reject or accept a mixture [6].

**Table 5.6 Visual stability index criteria [48].**

Criteria	Illustration
<p>VSI 0 Highly stable No evidence of segregation or bleeding.</p>	
<p>VSI 1 Stable No evidence of segregation and slight bleeding observed as seen on the concrete mass.</p>	
<p>VSI 2 Unstable A slight mortar halo (<math>\leq 10</math> mm) and/ or aggregate pile in the center of the concrete mass.</p>	
<p>VSI 3 Highly unstable Clearly segregated by evidence of a larger mortar halo (<math>\geq 10</math> mm) and/ or a larger aggregate pile in the center of the concrete mass.</p>	

**5.4.2. V-funnel Time.** This test measures the rate of flow of concrete and consists of filling a V-shaped container completely with approximately 12 liters of concrete. Before starting the stopwatch, the excess concrete is removed and upper surface is leveled with a trowel. The gate should be opened within 10 seconds after filling the container. The concrete is allowed to flow out of the container under gravity. The stopwatch is stopped at the moment light can be seen through the opening from the top of the V-funnel. The flow time obtained with this test does not measure viscosity, but it is well correlated to it [49]. Table 5.7 shows the recommendations provided by EFNARC, which classifies the V-funnel time of the SCC mixtures in two classes.

**Table 5.7 Conformity criteria for V-funnel flow time [9].**

Class	Description	V-funnel time (s)
VF1	Good filling ability, it is capable of self-leveling and generally has the best surface finish.	$\leq 8$
VF2	Increasing flow time it is more likely to exhibit thixotropic effects. Negative effects may be experienced regarding the surface finish (blow holes).	9 to 25

**5.4.3. Air Content (Pressure Method).** The procedure used to determine the air content was performed according to ASTM C231/C231M-14 [50], without consolidating.

**5.4.4. Sieve Stability.** This method was followed according to the procedure described by EFNARC 2005 [9] excluding the prescribed 15 min waiting time before the test. This test was used to assess static stability. The procedure was performed by pouring  $5 \pm 0.2$  kg ( $11 \pm 0.44$  lbs) of fresh concrete on a #4 sieve, with a pan below. The drop height should remain constant at approximately 0.5 m. After 2 minutes of rest, the weight of material which has passed through the sieve, was recorded. The segregation ratio is then calculated as the proportion of the sample passing through the sieve relative to the

mass of concrete poured on the sieve. The suggested values by EFNARC are shown in Table 5.8, which specifies the classes according to the use of the SCC mixture. SR1 is generally used for thin slabs and vertical applications with a flow distance of less than 5 meters and a confinement gap greater than 80 mm. SR2 is preferred if the flow is more than 5 meters. For the purpose of this study, a segregation resistance of SR2 was applied as an acceptance criterion for all the SCC mixtures since a SR lower than 10 % seems to be too strict to be able to measure some segregation in the SCC mixtures.

**Table 5.8 Conformity criteria for static segregation of SCC [9].**

Class	Segregation resistance (%)
SR1	$\leq 20$
SR2	$\leq 15$
SR3	$\leq 10$

**5.4.5. Tilting Box Test.** The purpose of this test is to evaluate dynamic segregation occurring in SCC during flow over long distances. A modified version of the tilting box (T-box) developed by Esmailkhanian et al. [24] was used in this research project. The T-box (Figure 5.11) consists of a rectangular channel of 1 m long, which can tilt from a horizontal to an inclined position. The tilting height of the box is 140 mm. The box width was 400 mm, instead of 200 mm of the original [24]; it can be divided into one section with a width of 100 mm, and one with 200 mm width. These modifications were made to evaluate the effect of different formwork dimensions on dynamic segregation.

Before testing, fresh concrete is placed in the box, reaching a height of 80 mm in the tested sections, while the box was maintained in horizontal position. The box is then tilted during 1 second, and brought back to the horizontal position during another second. Cycle time can be varied during the test, but in this testing program, the cycle time is kept constant at 2 seconds. The 100 and 200 mm channel widths were used in this work.

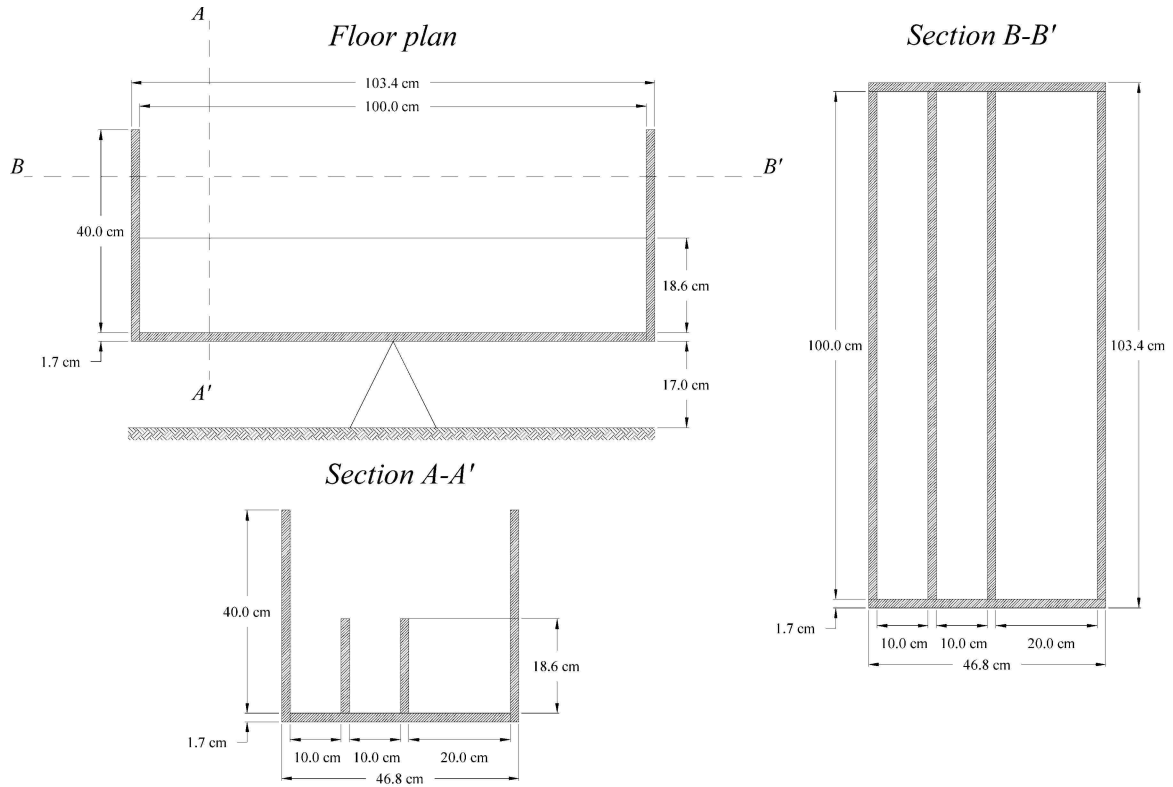


**Figure 5.11 Configuration of the T-box test.**

At the end of the 120 cycles, which corresponds theoretically to a flow distance of 9 m according to Esmailkhanian et al. [24], a sieve-washing technique was used. Samples were taken from the tilt-up and tilt-down sections, from both the 100 and 200 mm width channels. Standard 100 x 200 mm cylinders were filled with concrete, washed over a #4 sieve (4.75 mm opening), and the coarse aggregates were oven-dried to measure their volume in each of the sample sections. The volume of aggregate in each section is used to evaluate dynamic segregation. The Volumetric Index (VI) is defined according to equation below, where  $V_{td}$  is the relative coarse aggregate volume in the tilt-down section, and  $V_{tu}$  is the relative coarse aggregate volume in the tilt-up section.

$$VI(\%) = 100 \frac{V_{td} - V_{tu}}{\text{average}(V_{td}, V_{tu})}$$

**5.4.6. Concrete Rheology.** In this investigation, the dynamic yield stress and plastic viscosity of SCC were evaluated by using rheometers. In the laboratory, a Contec viscometer 5 was used, while the ICAR rheometer was employed during fieldwork. The data acquisition was done in different ways for each rheometer, which is explained in the subsequent sections. The data analysis and plug flow correction were made in the same way for both equipments.

**5.4.6.1. ConTec viscometer.** The Contec viscometer 5 (Figure 5.12) is based on the principle of wide gap coaxial cylinders in which the inner cylinder is static and the outer cylinder rotates at imposed rotational velocities. Its configuration consists of an inner radius ( $R_i$ ) of 100 mm and a container with an outer cylinder radius ( $R_o$ ) of 145 mm. The height of the inner cylinder, which is immersed in the concrete, is measured after each test. In order to prevent wall slip between the concrete and the cylinder surfaces both the inner and outer cylinders have vertical ribs.



Figure 5.12 Contec viscometer 5.

- Testing procedure. Immediately after mixing, approximately 15 liters of concrete are placed into the container and inserted into the rheometer chamber to determine the rheological properties. Before starting the test, a pre-shear period is imposed in order to break down the internal structure of the concrete to avoid errors on the rheological measurements [51]. The pre-shear phase was executed at a rotational velocity of 0.40 rps during 25 seconds, followed by a stepwise decreasing rotational velocity profile, from 0.40 to 0.025 rps in 10 steps of 5 s each, as given in Figure 5.13.

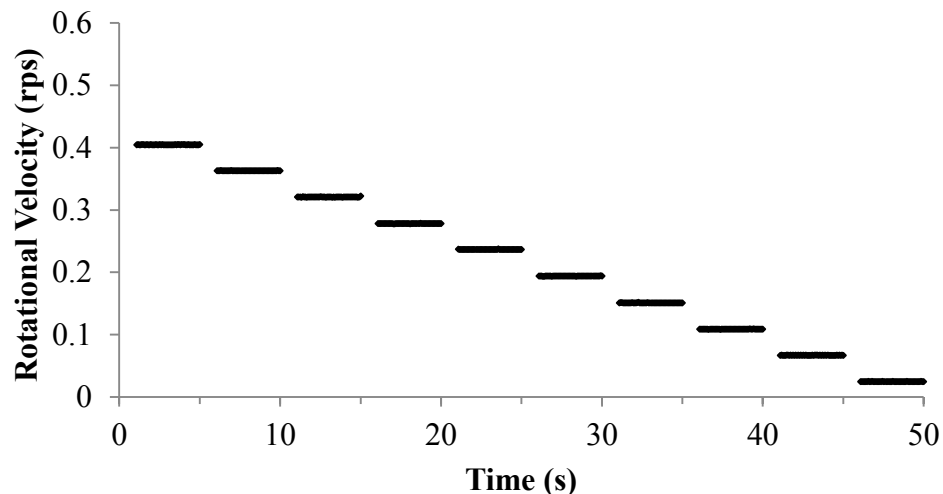


**Figure 5.13** The applied rotational velocity profile performed in Contec Rheometer.

**5.4.6.2. RHM-3000 ICAR rheometer.** The ICAR rheometer (Figure 5.14) is a four-bladed vane rheometer from Germann Instruments, which configuration corresponds to a vane with a radius ( $R_i$ ) of 62.5 mm and a height ( $h$ ) of 127 mm. The container in which the concrete mixture is placed is equipped with vertical ribs and has an outer radius ( $R_o$ ) of 143 mm. In the case of this rheometer, the data obtained was not fully trusted, which can be associated with a problem in the equipment calibration. Therefore, the yield stress was calculated from the slump flow value using the equation in

Roussel and Coussot (2005) [47]. In this way, the viscosity was calculated with a plug flow correction based on the yield stress derived from the slump flow values.



**Figure 5.14 ICAR rheometer.**

- Testing procedure. After the concrete was transported to the casting site in a concrete truck; the concrete was poured into two wheelbarrows. The rheometer container was filled and the impeller was inserted in the container to determine the rheological properties. Before starting the test, a pre-shear period was imposed for 20 seconds at a rotational velocity of 0.50 rps. During this period the torque started to gradually decrease till it reached equilibrium. This reflects the internal structure break down of the concrete. After the initial 20 seconds, a stepwise decreasing rotational velocity profile from 0.50 to 0.025 rps is recorded, in 10 steps of 5 s each, as shown in Figure 5.15.

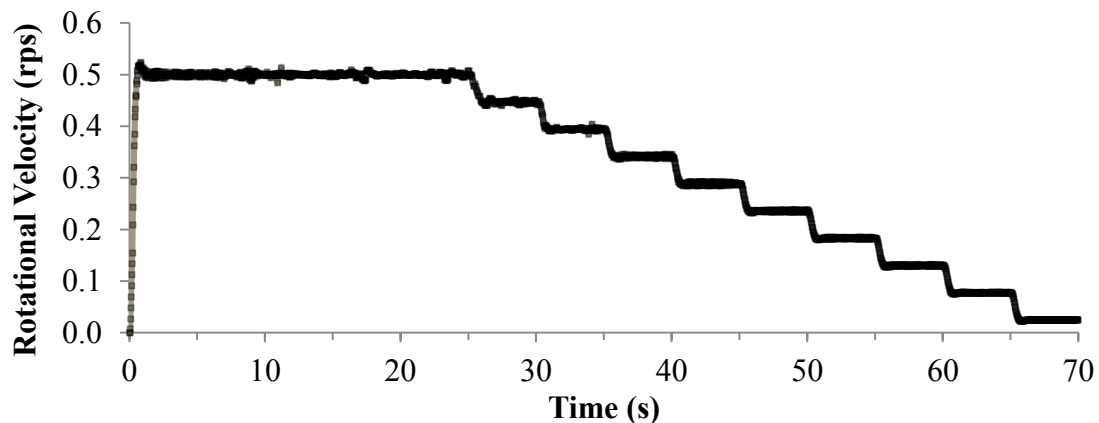


**Figure 5.15 The applied rotational velocity profile performed in ICAR rheometer.**

**5.4.6.3. Data treatment.** The data was manually treated using the same procedure for both equipments. First, the raw torque and velocity data were plotted and corrected using “empty measurement” data, which consist of the data obtained when the test is executed with an empty container. After that, the collected data during the first second of each step was discarded due to the time of transition between each rotational velocity. If during the remaining 4 seconds, the torque seemed to visually reach equilibrium, for each step, the average torque and velocity is calculated. When the torque data showed excessive scatter, those specific points that are distant from average were eliminated, but if the torque measurement at a constant rotational velocity step was not in equilibrium, it was not considered in the analysis. Once it was assured that all points of the torque-rotational velocity diagram were calculated in a state of equilibrium, then a rheological model was selected to calculate the viscosity and yield stress. Figure 5.16 clearly shows the behavior of the SCC mixtures investigated in this research project. For all mixtures, the torque–rotational velocity diagram was linear. Therefore, the rheological model that can be applied to analyze the data is the Bingham model.

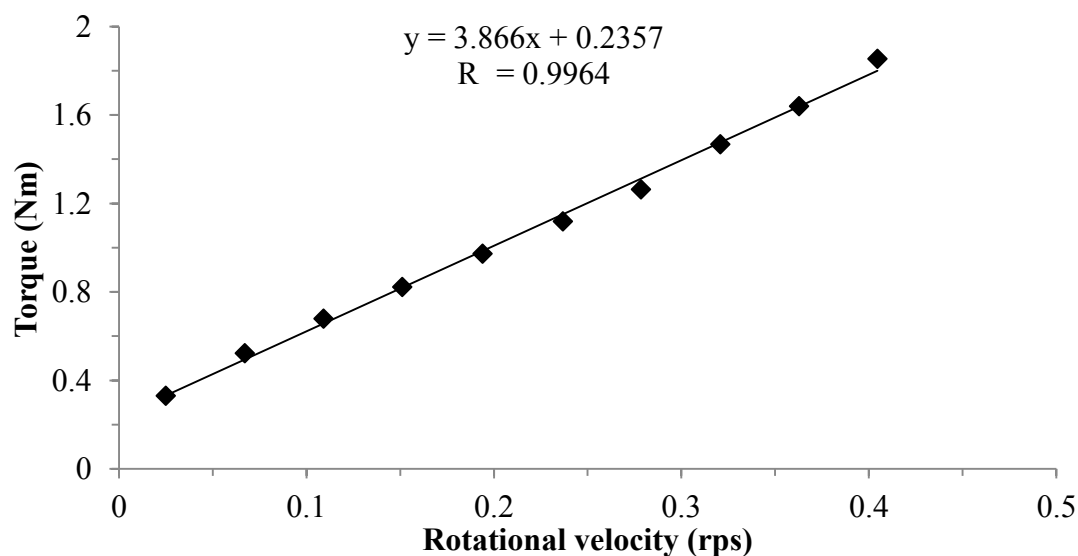


Figure 5.16 Torque vs rotational velocity diagram.



When the torque is in equilibrium at each shear rate step, the rheological properties can be calculated by means of the Reiner-Riwlin equation (see below) [52]. The Reiner-Riwlin equation transforms the parameters G and H into yield stress ( $\tau_0$ ) and plastic viscosity ( $\mu_p$ ), defining a linear relationship between torque (T) and rotational velocity (N), into the Bingham parameters [53].

$$\tau_0 = \frac{G \cdot \left(\frac{1}{R_i^2} - \frac{1}{R_0^2}\right)}{4 \cdot \pi \cdot \ln\left(\frac{R_0}{R_i}\right)}$$

$$\mu_p = \frac{H \cdot \left(\frac{1}{R_i^2} - \frac{1}{R_0^2}\right)}{8 \cdot \pi^2 \cdot h}$$

$$T = G + HN$$

where:  $\tau_0$ = yield stress (Pa)  
 G= intercept of T-N curve (Nm)  
 $R_i$ = radius of inner cylinder (m)  
 $R_0$ = radius of outer cylinder (m)  
 h= height of inner cylinder submerged into the material (m)  
 $\mu_p$ = plastic viscosity (Pa s)  
 H= the slope of T-N curve (Nm s)

**5.4.6.4. Plug flow correction.** After calculating the yield stress and viscosity using the Bingham model, an evaluation of plug flow was done for each mixture. The shear stress at the outer cylinder is compared to the calculated yield stress value. If this value is smaller than the yield stress, then there is a presence of plug flow.

The plug flow correction was done using an iterative procedure in which an initial estimation of yield stress and plastic viscosity is introduced. Afterwards, these values are compared to the yield stress and plastic viscosity derived from the shear stress-shear rate data using the plug radius instead of the outer cylinder radius for the points that have plug flow. The sums of differences between the rheological values at each iteration are minimized to a value smaller than 0.001. The final values are the rheological properties of the mixtures.

**5.4.7. Compressive Strength.** Three standards specimens of 100 by 200 mm were produced for each mixture to determine the compressive strength according to ASTM C31-15 [54]. The specimens were cast into the molds in a single lift; no rodding or consolidation was used. SCC cylinders cast in the laboratory were covered with a plastic membrane to prevent moisture loss and demolded after 24h and cured under water for 28 days. On the other hand, the cylinders made in the field were left adjacent to the beams so that they would be exposed to similar curing conditions until the testing day. Before testing the cylinders were finished using an end-grinder.

According to ASTM C42-13 [55], core samples (Figure 5.17 and Figure 5.18) of 98.43 mm diameter were taken from the pre-stressed beams for uniformity testing. Coring has the advantage of being able to directly analyze the strength and aggregate distribution in certain zones of the beam. Cores were cut with a wet saw to a length of  $152 \text{ mm} \pm 12 \text{ mm}$ , finished with the end-grinder and tested until failure using a Tinius Olsen machine. The compressive strength values were adjusted using a correction factor according to the length-to-diameter ratio. A typical core being tested for compressive strength is shown in Figure 5.19. The locations where the cores were drilled are shown in

Figure 5.20. Three cores were extracted horizontally in each section at top, middle and bottom sections of the beam, and for beams 1, 3, 5, 6, 7 and 8 at 0 m, 3 m, 6 m and 9 m from the casting point. While for beams 2, 4 and 9 the coring locations were at 0 m, 3 m, 6 m, 9 m (not for beam 9), 12 m, 15 m and 18 m from the casting point. It should be noted that the cores extracted at the top were always drilled below the casting line. As a result, they were not all drilled at the same height.



**Figure 5.17 Drilled core in beam.**



**Figure 5.18 Extracting cores from a beam.**



Figure 5.19 Compressive strength test setup of cores.

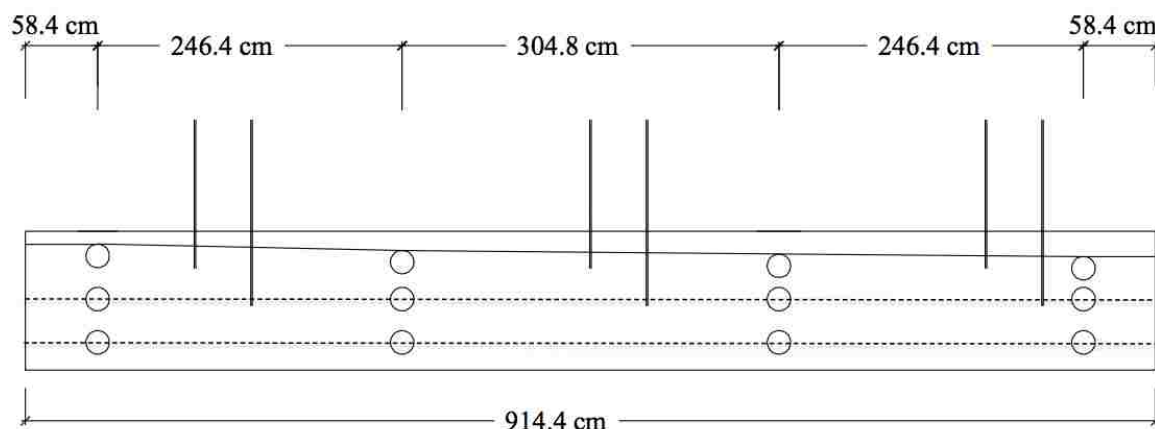


Figure 5.20 Extraction points of concrete cores for 9 m long beam.

**5.4.8. Ultrasonic Pulse Velocity Test.** This method is applicable to assess the quality and uniformity of concrete and to indicate the existence of voids and cracks. The team of Dr. Hartell from Oklahoma State University performed the evaluation of the beams. The ultrasonic pulse velocity test method was conducted following standard procedure ASTM C 597-09 [56] using 54 kHz compressive wave sensors and the direct transmission method. A water-based jelly was used between each sensor and the beam surface; the sensors were placed at opposite points of the beam side surfaces to measure the wave transit times in micro-seconds ( $\mu\text{s}$ ), and to evaluate changes in wave velocity

(m/s) across the beam sections. The change in velocity recorded may be indicative of changes in mixture consistency along the beam. The atmospheric conditions at the time of testing on the beam were recorded: the temperature was between 32°C and 33°C and relative humidity was between 32% and 35%. The moisture content of the beams was considered to be uniform.

An 18 m long beam (Beam 2) and two beams of 9 m in length (Beams 1 and 5) were tested using the UPV method on site (Figure 5.21). The width of all beams was 457 mm. Each beam was divided into different sections, starting from casting point (0 m) up to the end of the beam. Each section was tested at five different points, at a distance of 152 mm from each other and from top surface of the beam as shown in Figure 5.22.



**Figure 5.21 On-site UPV testing on beam.**

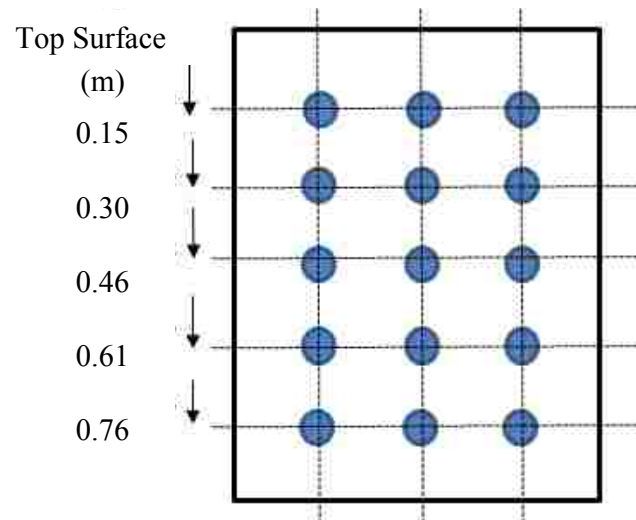


**Figure 5.22 Lay-out of UPV measuring points per section.**

In addition to the beams, cores taken from each beam were tested following the same standard procedure for the ultrasonic pulse velocity method (Figure 5.23). The samples were cut using a wet saw and were subjected to do the UPV measurements before performing compression tests.



**Figure 5.23 Ultrasonic pulse velocity testing equipment.**



**5.4.9. Pullout Test.** The bond strength between the pre-stress strands and the concrete was performed using the pullout test based on the Moustafa method [57, 58]. The test setup is shown in Figure 5.24. For each strand, first, a steel plate was placed over the strand, and then the hydraulic jack was collocated, followed by another steel plate, the 445 kN load cell, another steel plate and a pre-stress chuck. The load was increased manually until a 25 mm slip was measured and the corresponding load was recorded (Figure 5.25).

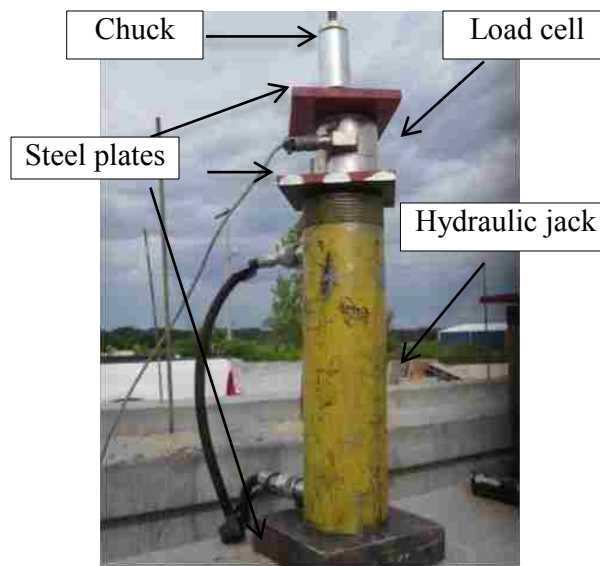


**Figure 5.24 Lay-out of pull-out tests.**



**Figure 5.25 Strands being tested using pull-out test.**

## 6. RESULTS AND DISCUSSION

In this section, the results of the effect of mix design parameters such as: water-to-cement ratio, SP dosage, VMA content, paste volume, and sand-to-aggregate ratio, on dynamic segregation of SCC mixtures and the consequences on the performance of pre-stressed beams are discussed. The rheological properties were obtained using the Contec viscometer 5 and the ICAR rheometer, while the volumetric index values were obtained using the modified T-box described in the previous chapter. Another parameter assessed in this investigation was the effect of a modification in a formwork dimensions, which was done evaluating two widths, 10 cm and 20 cm in the T-box. In addition, bond strength, compressive strength and ultrasonic pulse velocity were also evaluated in order to investigate the effects of dynamic segregation on the performance of pre-cast beams.

### 6.1. PARAMETERS INFLUENCING DYNAMIC SEGREGATION

The summary of the workability and rheological measurements carried out for the 23 SCC mixtures used in task 1 is shown in Table 6.1. For some mixtures, the dynamic segregation properties are not reported since these mixtures were statically unstable (Sieve stability > 15%). Esmailkhanian et al. [5] suggested not to perform the T-box test if the mixtures are statically segregated, as in this case, the results can be compromised. According to Roussel [59], casting in a formwork with a thickness of 10 cm, a flow speed of 1 m/s gives a maximum shear rate of  $10 \text{ s}^{-1}$ . Following this example, a flow speed of 0.25 m/s [24] in a rectangular section with a width of 20 cm results in an approximate shear rate of  $1 \text{ s}^{-1}$ . To obtain the shear stress at  $1 \text{ s}^{-1}$ , the yield stress and the plastic viscosity  $\times 1 \text{ s}^{-1}$  were added, reflecting approximately the shear rate in the tilting box.



**Table 6.1 Workability, dynamic segregation, rheological and mechanical properties for the tested mixtures.**

Mixtures	Workability					Dynamic segregation		Concrete Rheology		Shear stress @ 1s-1 (Pa)	Compressive strength (Mpa)	
	Slump flow (mm)	T 50 (s)	V-Funnel (s)	Air Content (%)	Sieve stability (%)	VI in 100 mm (%)	VI in 200 mm (%)	Yield stress (Pa)	Plastic Viscosity (Pa s)			
<b>Mix design 1</b>												
Ref	710	0.6	4.2	6.5	9.8	20.3	29.9	20.7	17.5	38.2	42.1	
±SP	+16%	760	1.6	2.8	6.8	15.5	-	-	-	-	-	
	-20%	650	1.4	3.8	6.5	8.6	15.1	25.0	24.4	15.6	40.1	43.4
VMA	+2.5x	670	1.4	3.5	4.3	9.9	10.7	21.6	30.2	13.3	43.5	40.8
	0	700	1.1	3.5	5.5	10.0	25.9	34.2	22.3	13.6	35.9	42.7
<b>Mix design 2</b>												
Ref	720	1.5	3.4	6.5	7.0	13.6	21.9	10.1	12.1	22.1	45.5	
w/cm	0.35	690	1.3	11.1	6.5	4.8	1.3	5.4	7.5	33.5	41.0	65.2
	0.45	690	1.1	2.3	2.0	8.9	7.3	17.6	21.0	9.5	30.5	50.6
±SP	-10%	658	0.9	3.8	6.0	7.0	4.4	13.5	14.9	15.4	30.3	50.4
	+10%	740	0.9	3.1	4.5	10.7	12.6	23.2	9.6	12.3	21.8	46.6
Paste Volume	-25 l/m <sup>3</sup>	690	0.8	4.5	7.0	6.2	9.4	13.8	18.0	18.9	36.8	45.8
	+25 l/m <sup>3</sup>	695	0.9	4.5	5.5	10.8	14.1	31.8	11.7	14.6	26.3	49.0
s/a	46%	700	0.9	4.1	6.0	7.6	17.5	23.1	14.7	13.8	28.5	47.5
	56%	695	0.7	3.9	6.5	7.2	23.3	44.1	14.4	17.5	31.9	43.6
<b>Mix design 3</b>												
Ref	683	1.7	8.6	8.5	6.5	0.0	4.2	25.2	22.5	47.7	68.5	
Ref 2	640	1.7	8.3	8.0	8.0	0.0	3.6	34.1	23.1	57.2	67.6	
±SP	+4.8%	775	1.2	4.1	6.8	13.0	36.4	37.7	6.1	14.2	20.2	68.1
	-1.2%	655	2.3	6.9	7.5	6.6	0.0	4.3	35.5	18.7	54.2	73.2
AEA	+AEA	685	1.3	6.4	12.0	9.6	0.0	0.0	31.7	17.2	48.9	41.7
	-AEA	695	1.0	7.4	5.0	11.4	0.0	2.4	24.1	23.3	47.4	80.6
s/a	56%	700	1.5	7.9	9.5	6.4	0.0	0.0	31.1	22.0	53.2	62.8
	46%	710	1.2	4.2	5.5	22.5	-	-	-	-	-	-

**6.1.1. Effect of the Rheological Properties.** In order to evaluate the influence of yield stress and plastic viscosity on dynamic segregation, some variations were induced such as: w/cm, paste volume, S/A, SP content and VMA content. Figures 6.1 and 6.2 illustrate dynamic segregation in relationship with plastic viscosity and yield stress, respectively. Also, no clear correlation between dynamic stability with yield stress and plastic viscosity was found. Although, dynamic segregation appears to decrease with an increase in either the yield stress or viscosity. The shear stress at  $1 \text{ s}^{-1}$  was calculated to evaluate its effect on the segregation of the SCC mixtures. Figure 6.3 shows the relationship between dynamic segregation and the rheological properties of the SCC mixtures as a function of the sand-to-total aggregate ratio tested in this research project. Higher segregation is observed when the SCC mixture has lower shear stress at  $1 \text{ s}^{-1}$ , while when increasing yield stress or plastic viscosity, a reduction of segregation is observed. Plastic viscosity mainly influences the drag force applied by the mortar on the particles. An increase in viscosity leads to an increase in the drag coefficient. As a consequence, the mortar has a higher capacity to maintain aggregates in suspension, which results in lower segregation [5]. Through the casting process, the density difference between the coarse aggregate and the mortar is at the beginning governed by a slow migration of the particles towards the bottom of the formwork if the yield stress is exceeded. This migration is slowed down by the viscosity of the mortar but it is not fully prevented [60]. In the case of yield stress, during casting, only a part of the material is being sheared. There are zones where the stress remains lower than the yield stress and zones where the stress exceeds the yield stress. When the material is not being sheared, it flows as a plug. In this zone the material behaves like it is at rest, thus less gravity-

induced migration shall occur [61]. Therefore, in order to control dynamic segregation, a balance between yield stress and plastic viscosity is needed.

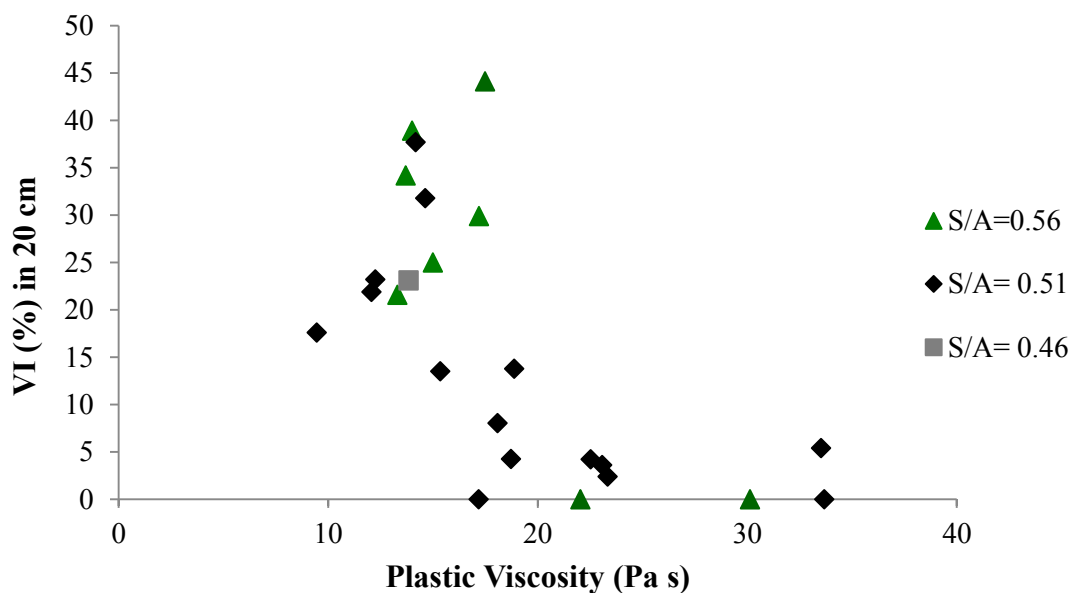


Figure 6.1 Relationship between dynamic segregation and plastic viscosity.

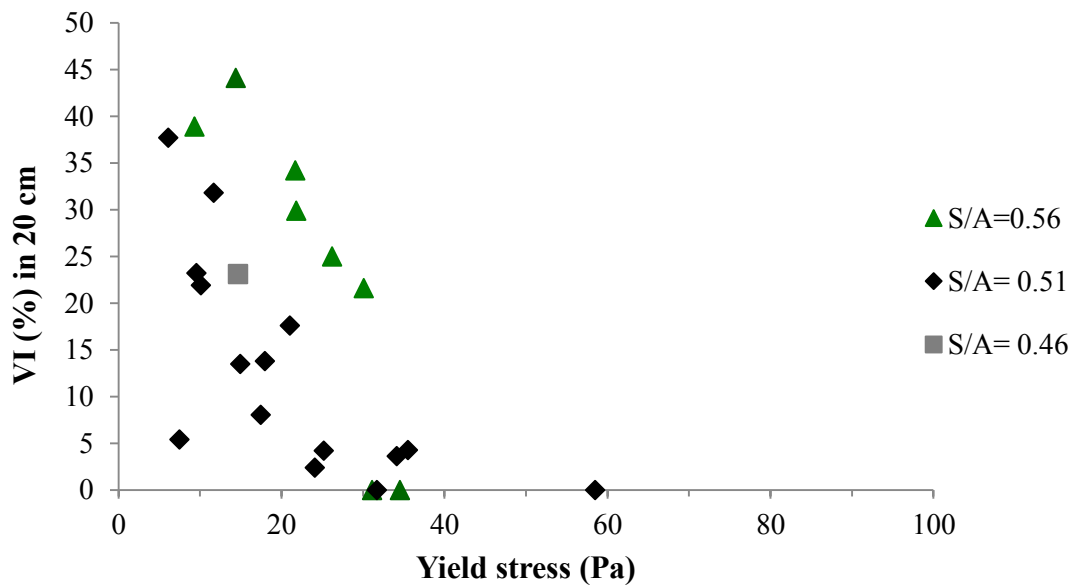
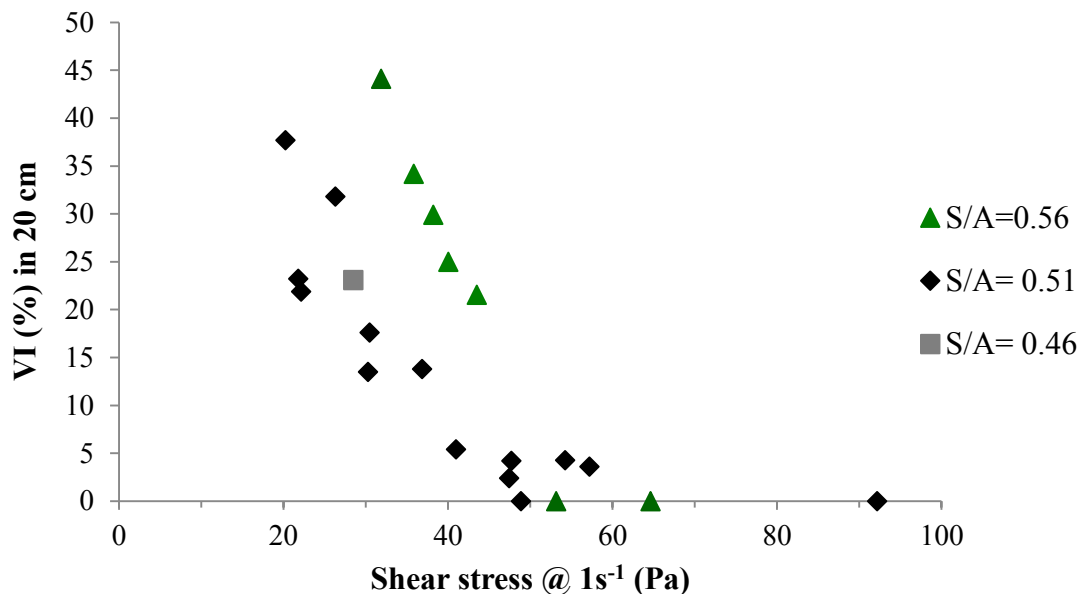
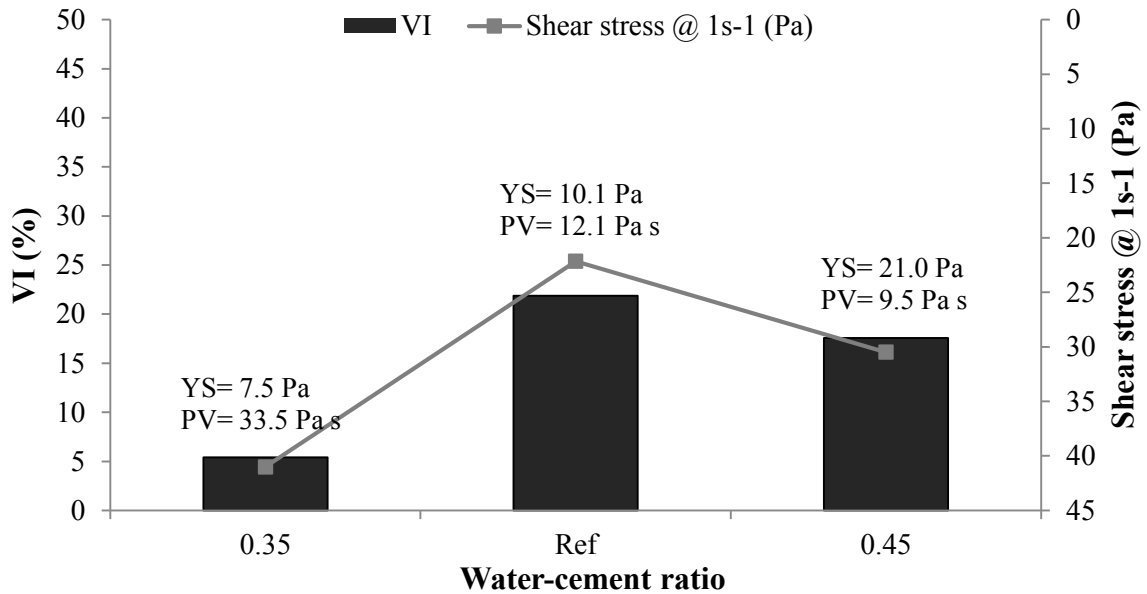


Figure 6.2 Relationship between dynamic segregation and yield stress.



**Figure 6.3 Relationship between dynamic segregation and shear stress @ 1s<sup>-1</sup>.**

**6.1.2. Effect of Water-to-Cement Ratio.** To investigate the effect of the water-to-cement ratio on the dynamic segregation resistance of SCC mixtures, two mixtures derived from reference mix design 2 were prepared, tested, and compared to their reference. The w/cm varied  $\pm 0.05$  to 0.35 and 0.45, where the SP content was adjusted to maintain a slump flow of  $700 \pm 20$  mm. The S/A, paste volume and VMA content were kept constant. Figure 6.4 shows that decreasing w/cm from 0.40 to 0.35 significantly increases plastic viscosity, thus increasing the ability to avoid the aggregate to separate from the suspending matrix. In addition, the water-to-cement ratio of 0.45 has lower segregation compared to the reference mixture; this is due to the presence of a higher yield stress, which was induced by a lower amount of SP needed to achieve the targeted slump flow. When the mixture has a lower plastic viscosity, increasing yield stress can enhance dynamic stability. On the other hand, increasing w/cm results in a slightly higher sieve stability value, making the mixture more susceptible to static segregation. The results are in agreement with the influence of rheology on dynamic segregation.



**Figure 6.4 Influence of water-cement ratio on dynamic segregation in mix design 2.**

**6.1.3. Effect of SP Content.** To investigate the effect of SP content on dynamic segregation of SCC, a total of 9 mixtures were evaluated, using mix designs 1, 2 and 3. Figure 6.3, shows the influence of the SP dosage on the ability of SCC mixtures to maintain a uniform distribution of coarse aggregate during flow. The mixtures were prepared with a constant w/cm of 0.40 for mix design 1 and 2, and 0.36 for mix design 3. The VMA content was kept constant compared to each reference. The SP content was altered by -20% and +16% for mix design 1,  $\pm 10\%$  for mix design 2 and -1.2%, +4.8% for mix design 3, compared to the reference mixture of each mix design. The SP content was increased and decreased in order to achieve a targeted slump flow of around 750 mm and 650 mm respectively. These variations were done to evaluate the influence of yield stress on dynamic segregation. Each mix design had different paste volume or S/A, therefore the trend of the results are different. Figure 6.5 to Figure 6.7 show the relationship between dynamic segregation and SP content for mix design 1, 2 and 3, respectively. A possible reason why mix design 1 is more unstable compared to the other

mix designs might be due to a different gradation, which in this case only contains ½” aggregate and no intermediate aggregates. Mix design 1 also has higher S/A. For mix design 1, the results show that slightly increasing the shear stress at  $1 \text{ s}^{-1}$  reduces the settlement of the coarse aggregate by reducing SP dosage compared to the reference mix. In the case of mix design 2, the results are also in accordance with rheology: lower SP content increases the shear stress at  $1 \text{ s}^{-1}$ , higher SP decreases the shear stress at  $1 \text{ s}^{-1}$ . Dynamic segregation follows also the trend of rheology. For mix design 3, the same tendency is observed. The variation of the SP content significantly affects the segregation resistance. It is well known from the literature that the addition of superplasticizers decreases the yield stress of the mixture. Therefore an increase of the SP content tends to reduce the stability of the SCC mixture. Although, the mix designs were different, the separation of the concrete constituents during casting is more prominent when decreasing yield stress and plastic viscosity [18].

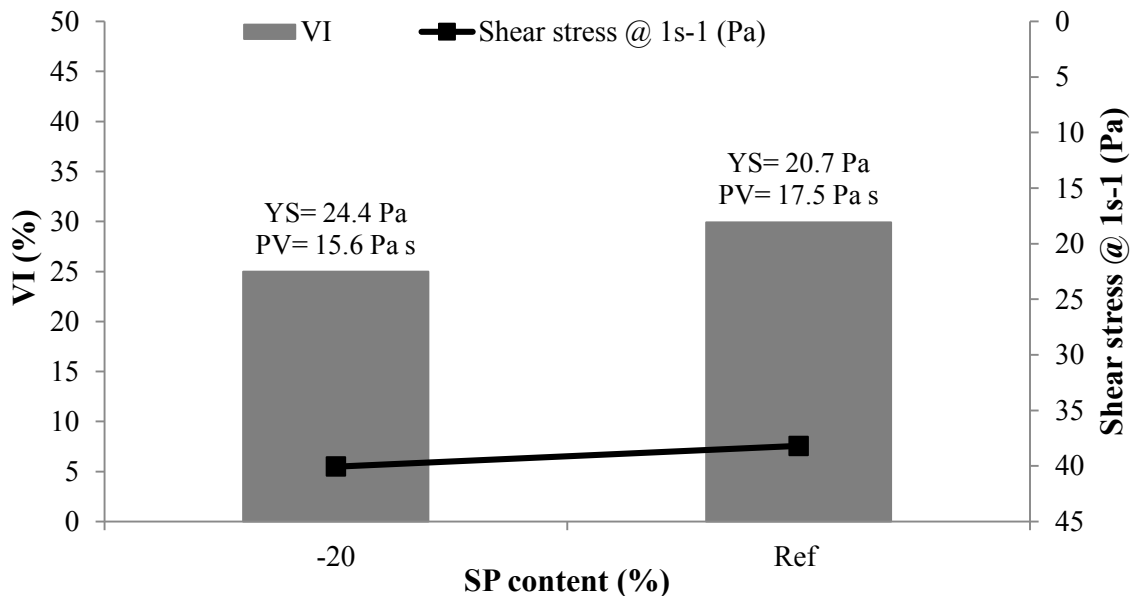


**Figure 6.5 Influence of superplasticizer content on dynamic segregation in mix design 1.**

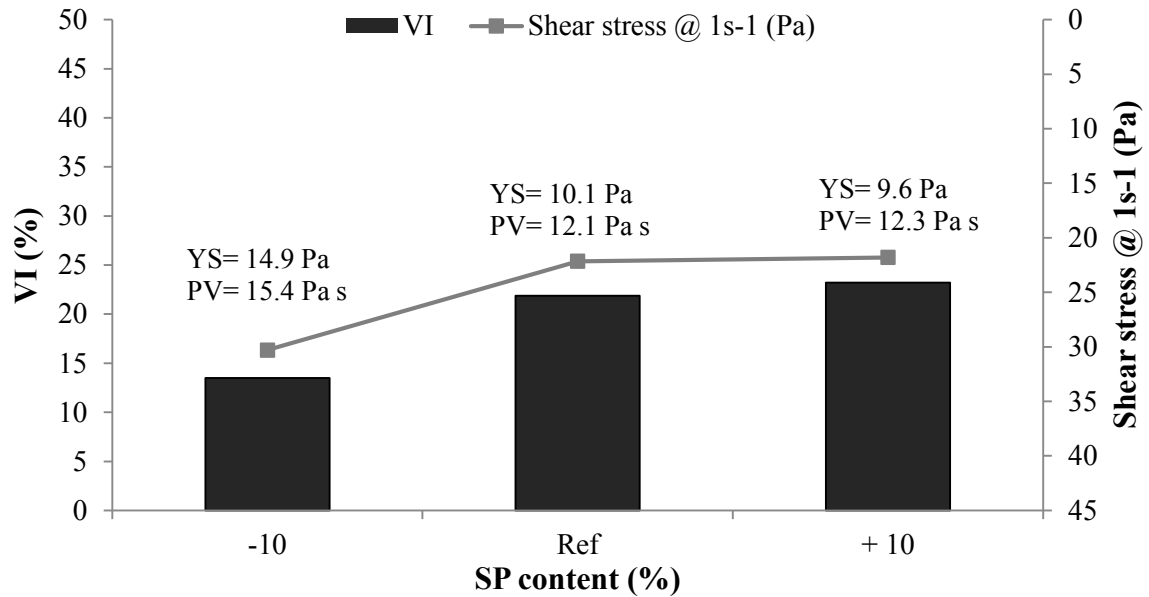


**Figure 6.6 Influence of superplasticizer content on dynamic segregation in mix design 2.**

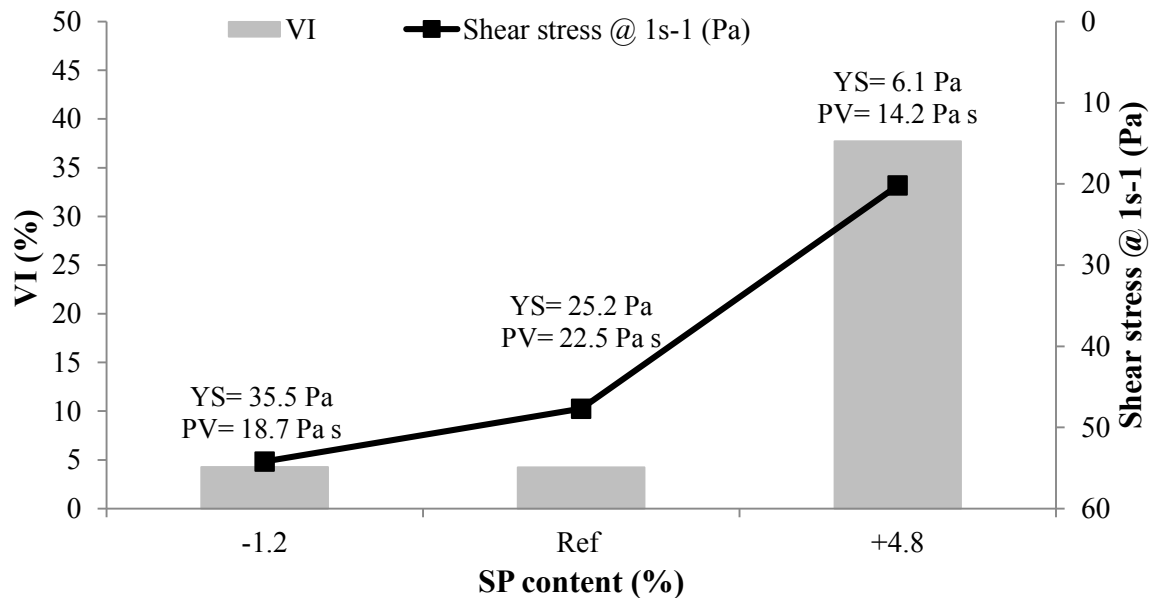


**Figure 6.7 Influence of superplasticizer content on dynamic segregation in mix design 3.**

**6.1.4. Effect of VMA Content.** To evaluate the effect of the VMA content on dynamic segregation of SCC, two mixtures derived from mix design 1 were elaborated with a constant w/cm of 0.40 and sand-to-total aggregate ratio of 0.56. The SP content

was varied in order to achieve a targeted slump flow of  $700 \pm 20$  mm. Higher dosages of VMA increased the ability of SCC to resist segregation. Generally VMAs in concrete are based on cellulose derivatives or polysaccharides of microbial source. These polymers are water-soluble and can imbibe some of the free water in the system and affect the aqueous phase of the cement paste, thus enhance the viscosity and the yield stress [62, 63]. Figure 6.8 clearly shows this behavior. An increase in dynamic segregation is also observed when no VMA is present.

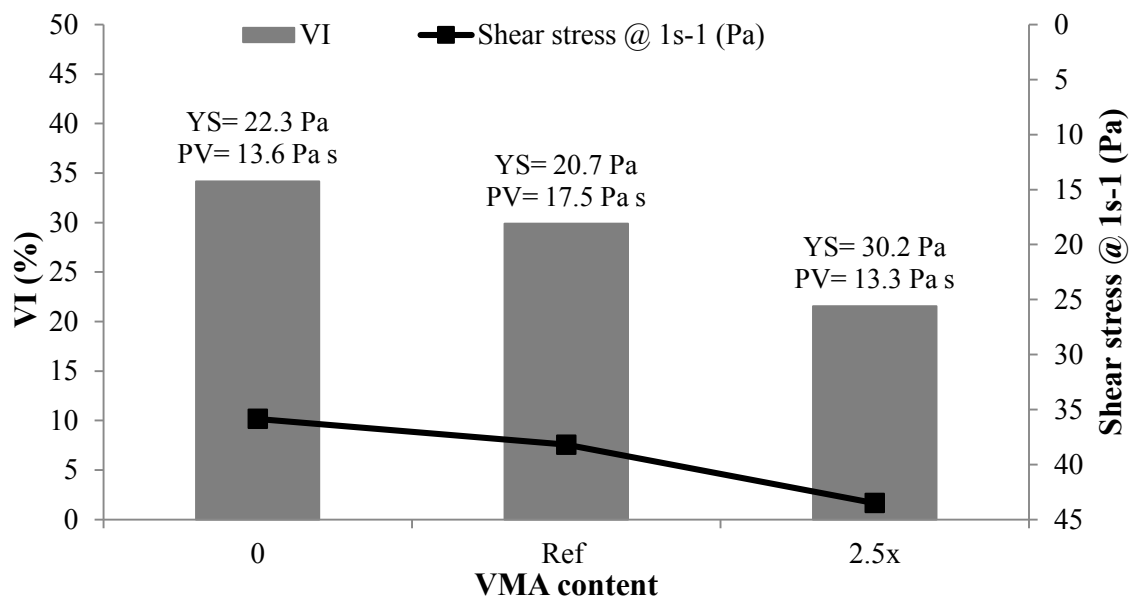


**Figure 6.8 Influence of VMA content on dynamic segregation in mix design 1.**

**6.1.5. Effect of Paste Volume.** Two additional SCC mixtures, using reference mix design 2, were prepared to evaluate the effect of the paste volume on dynamic stability. The variations of the paste volume were  $\pm 25$  l/m<sup>3</sup> from the reference with a constant w/cm of 0.40. Sand/total aggregate and VMA content were also constant while SP content was adjusted to achieve a slump flow of  $700 \pm 20$  mm. Table 6.1 shows that mixtures with higher and lower paste volume have very similar workability properties



such as V-funnel time and slump flow. The same trend was observed for the rheological properties (Figure 6.9). On the other hand, a higher dynamic segregation was observed when increasing the paste volume. Therefore, the paste volume has a marked effect on dynamic segregation in addition to the known effects of plastic viscosity and yield stress. By increasing the paste volume, the amount of aggregates in the concrete decreases, leading to a greater inter-particle spacing and a higher potential for settlement [18]. In Figure 6.10, which is repeated from section 6.1.1, the highlighted points clearly show the trend of the influence of the variations of paste volume. Increasing the rheological properties by reducing the paste volume has a positive effect on dynamic segregation. Increasing paste volume may increase the particle migration from the suspending matrix, despite almost no variation in the shear stress at  $1 \text{ s}^{-1}$ .

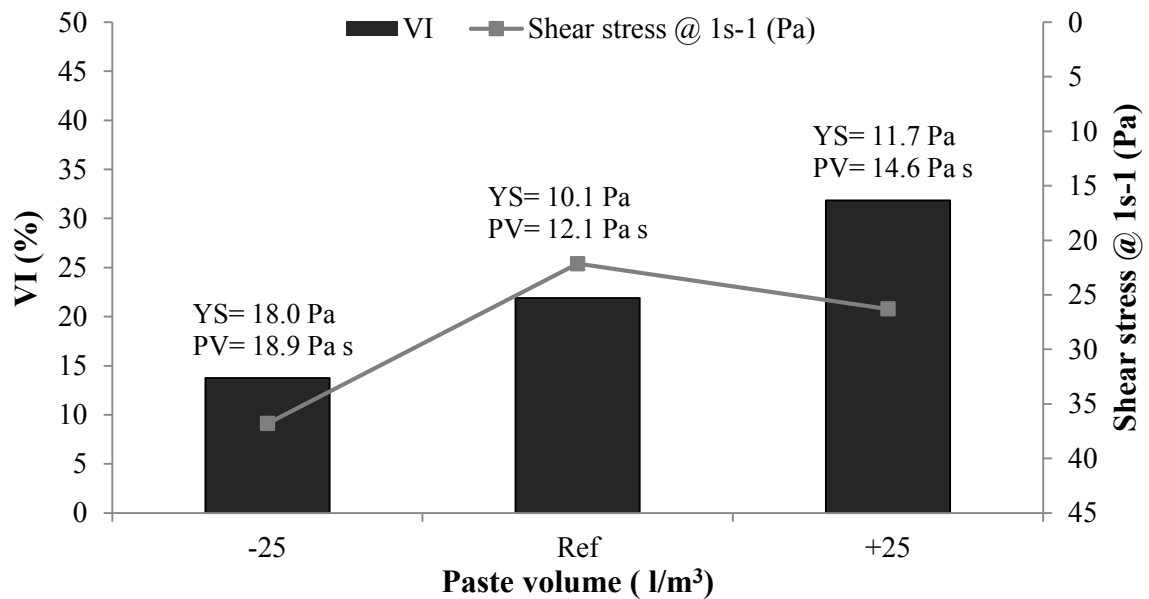
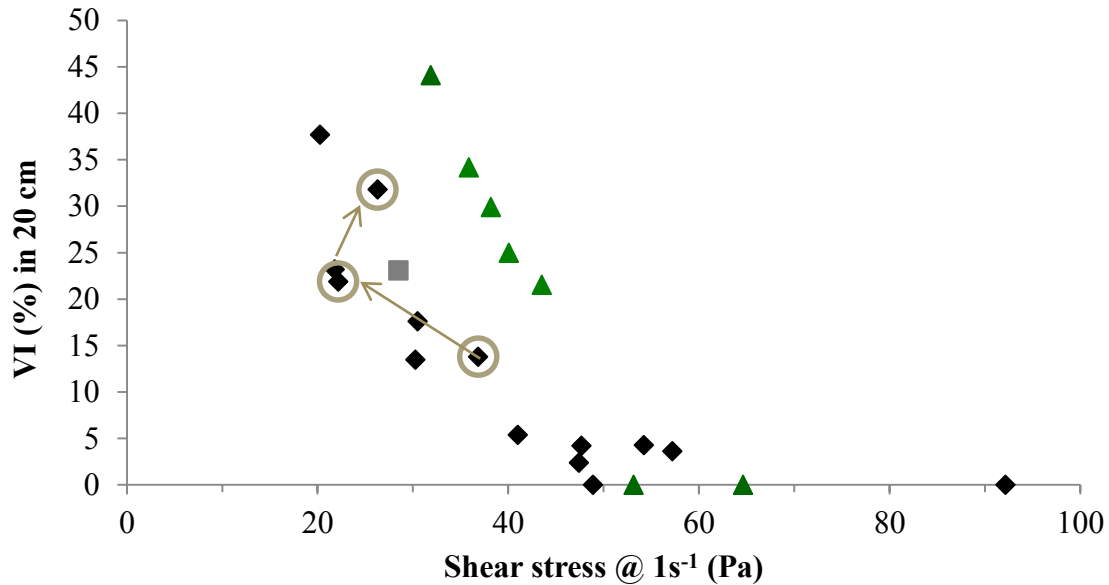


Figure 6.9 Influence of paste volume on dynamic segregation in mix design 2.



**Figure 6.10 Relationship between dynamic segregation and rheological properties @ 1s<sup>-1</sup>. Highlighted points reflect the increase in paste volume.**

**6.1.6. Effect of Sand-to-Total Aggregate Ratio.** The effect of the sand-to-total aggregate ratio (S/A) on segregation of SCC needed to be quantified. For this purpose, two SCC mixtures were prepared and tested with a variation in the sand-to-total aggregate ratio of  $\pm 5\%$  from the reference for mix design 2, with a constant w/cm of 0.40, and w/cm of 0.36 for mix design 3. VMA content and paste volume were kept constant while the SP content was adjusted to achieve a slump flow of  $700 \pm 20$  mm. Results of the volumetric index (VI) for mix design 2 are shown in Figure 6.11. For mix design 2, a high risk of dynamic segregation in the SCC mixtures, which have a relatively low yield stress in combination with a high sand-to-total-aggregate ratio, is observed. While for mix design 3, higher rheological properties are measured, which leads to higher segregation resistance. The effect can be explained in a similar way as an increase in paste volume: an increase in S/A decreases the total amount of coarse aggregates, leaving more space for these to move. When the S/A decreases, the results do not follow the same

tendency, as the VI is approximately equal to the reference mixture. It is important to emphasize that to prevent the coarse aggregate settlement in the mixture, it is necessary to have an appropriate amount of sand, which in the same way needs finer particles to stabilize and so forth [64]. This effect is called the lattice effect and explains why the coarse aggregates stay in suspension in a cement paste. It is expected that a decrease in the S/A caused the mixture to have a reduced lattice effect, explaining why the VI does not decrease with decreasing S/A and with increasing shear stress at  $1s^{-1}$ .

However, for mix design 3, the increase in VI with increase in S/A is not observed as the rheological properties are sufficiently high to prevent dynamic segregation ( $VI < 5\%$ ). Higher amount of sand increases the required amount of water to wet the particle surface adequately, thus the rheological properties increase [65, 66]. This can be a potential explanation of the decreased dynamic segregation in mix design 3 with increasing S/A (Table 6.1).

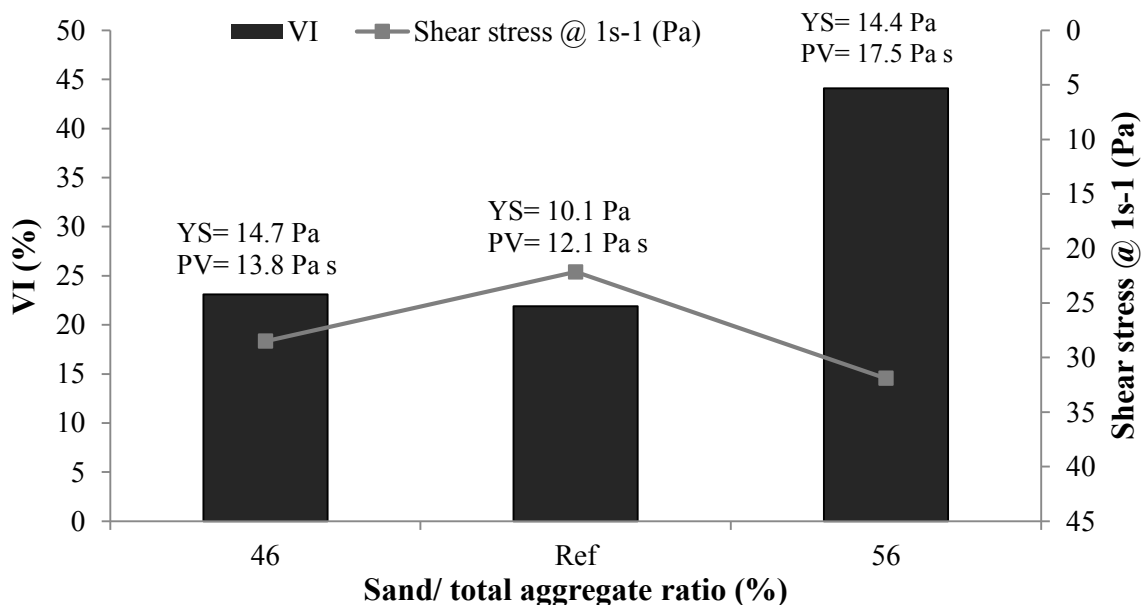


**Figure 6.11 Influence of sand-to-total aggregate ratio on dynamic segregation in mix design 2.**

**6.1.7. Effect of Formwork Dimensions.** The effect of the variations in the formwork width on dynamic segregation was evaluated for all SCC mixtures. Figure 6.12 shows the comparison between the volumetric index in the 100 mm channel to the results in the 200 mm part. The results show that the segregation index in the 100 mm channel is approximately two thirds compared to the 200 mm channel. To achieved equal average velocity in both channels, the peak velocity in the smaller channel is higher. According to Esmailkhanian et al. [5], increasing the flow velocity decreases dynamic segregation. Also, Spangenberg et al. [61] suggest that when increasing the casting rate a reduction of the magnitude of gravity-induced particle migration is observed. Although Daczko, J. [20] stated that in narrow formworks the wall effect increases and increases dynamic segregation, which is opposite to what is found in this project.

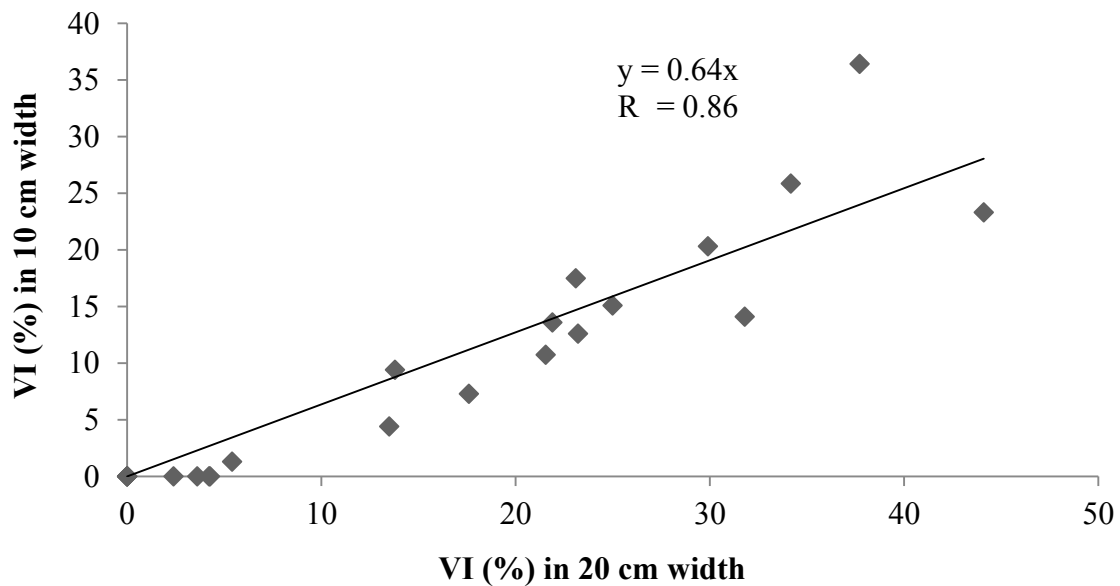


**Figure 6.12 Influence of formwork dimensions on dynamic segregation.**

## 6.2. CONSEQUENCES OF DYNAMIC SEGREGATION ON PERFORMANCE

Table 6.2 summarizes workability and dynamic segregation results for the nine mix designs used in the field study, the volumetric index values range from 10.5 to 68.6% in the 200 mm channel, while for the 100 mm the values are between 5.4 and 48.9%. V-funnel time ranges from 3.1 to 5.4 seconds and air content values vary between 3.0 to 14.0%. Overall, the results show that increasing w/cm from 0.4 to 0.45 has a negligible effect on dynamic segregation, while increasing paste volume may lead to a greater inter-particle spacing and a higher risk for segregation.

**Table 6.2 Workability characteristics, dynamic segregation, rheological and mechanical properties for the SCC tested.**

Beam	Mixtures		Workability					Dynamic segregation		Concrete Rheology		Compressive strength (Mpa)
			Slump flow (mm)	T 50 (s)	V-Funnel (s)	Air Content (%)	Sieve stability (%)	V1 in 100 mm (%)	V1 in 200 mm (%)	Yield stress (Pa)	Plastic Viscosity (Pa s)	
<b>Rectangular Beam</b>												
1	Ref		645	0.8	5.4	14.0	5.8	5.4	16.8	34.8	9.7	42.8
2	w/cm	0.40	725	1.3	4.4	1.5	13.5	9.5	20.1	19.4	8.4	74.2
4	w/cm	0.45	640	0.9	3.1	3.1	9.9	7.4	22.5	36.2	4.9	69.5
3	Paste Volume	+25 l/m <sup>3</sup>	690	0.9	4.3	3.0	5.8	8.3	10.5	24.9	7.9	72.8
5	s/a	56%	675	0.9	2.9	10.0	10.3	11.4	28.1	27.7	10.2	53.3
9	s/a	56%	660	1.6	3.6	8.5	12.9	-	19.7	31.0	15.1	56.9
<b>"I" Beam</b>												
6	Ref		630	1.3	4.0	13.0	16.6	14.8	31.3	39.2	9.1	50.4
7	Paste Volume	+25 l/m <sup>3</sup>	680	0.8	4.3	13.0	24.8	48.9	68.6	26.7	6.1	47.7
8	s/a	56%	680	0.8	3.2	12.0	7.5	6.9	13.0	26.7	7.3	44.5

### 6.2.1. Effect of Dynamic Segregation on Ultrasonic Pulse Velocity. To

evaluate the uniformity of the beams, a non-destructive technique was employed, named ultrasonic pulse velocity, which is described in section 5.4.8. The investigated beams were 3 rectangular beams, beams 1 and 5 (9 m) and beam 2 (18 m long).

At each horizontal point, three readings were taken in a section and an average velocity was calculated. The average velocities were calculated at 5 points at separation distances of 15.2 cm from the top surface towards the bottom in a section, and longitudinally at 0 m, 3 m, 6 m and 9 m from the casting point for beams 1 and 5, while at 0 m, 3 m, 9 m, 12 m, 15 m and 18 m from casting point for beams 2. The results are presented in Figures 6.13 to 6.15.

The UPV results show that the changes in properties in vertical direction are larger at the casting point (where the concrete has an approximate free-fall of 1 m), and the beams are more homogeneous the further the concrete flows. Also, generally, more variation in horizontal direction is observed at the bottom of the beams. It appears thus that a concrete with lower porosity can be found at the bottom of the beam, near the casting point, which could be an indication of a larger content of aggregates, lower w/cm or lower air content. For beam 1, the VI is 16.8%, while for beams 2 and 5, the VI is 20.1% and 28.1% respectively. However, the magnitude of the variations in pulse velocity does not completely match the dynamic segregation index. Figure 6.13 shows higher variations at the casting point for beam 1 compared to beams 2 and 5, which according to the VI measurements beams 2 and 5 appear to be more segregated than beam 1. An additional explanation for the increased variations in pulse velocity may be a difference in local air content. These properties are currently under investigation.

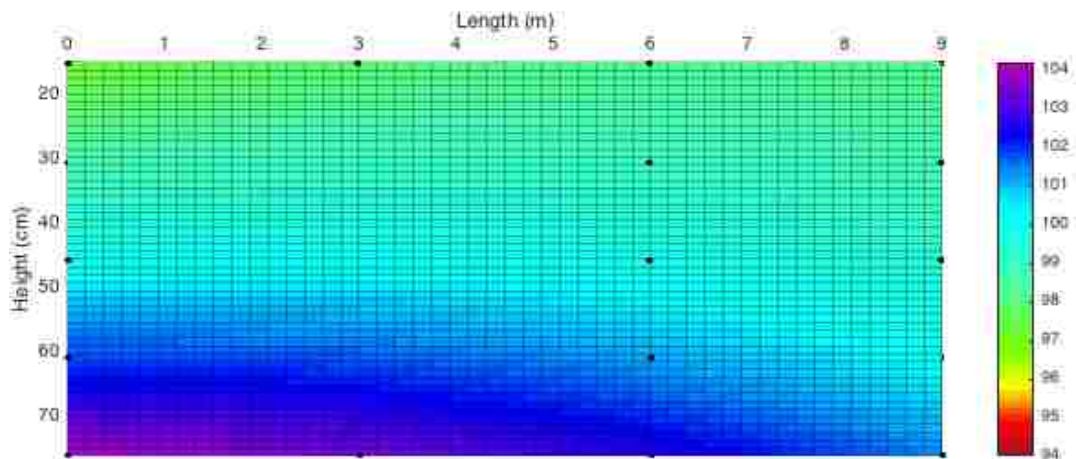


Figure 6.13 UPV results, in % relative to the average value 4130 m/s for beam 1.

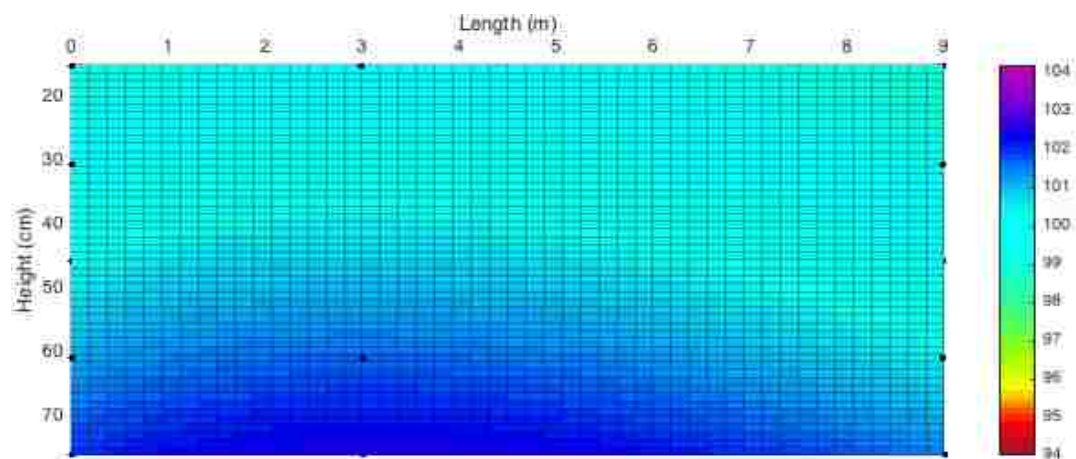


Figure 6.14 UPV results, in % relative to the average value of 4602 m/s for beam 2 for the 9 m closest to the casting point.

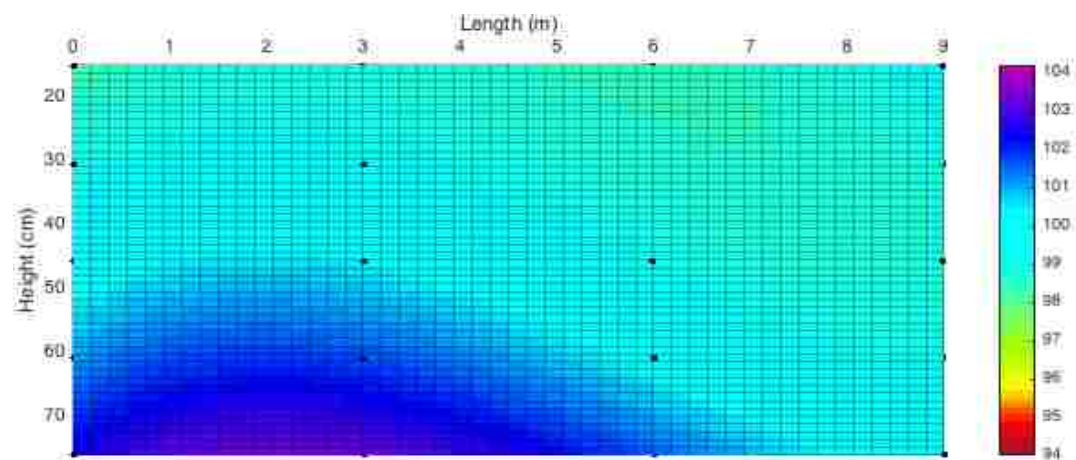
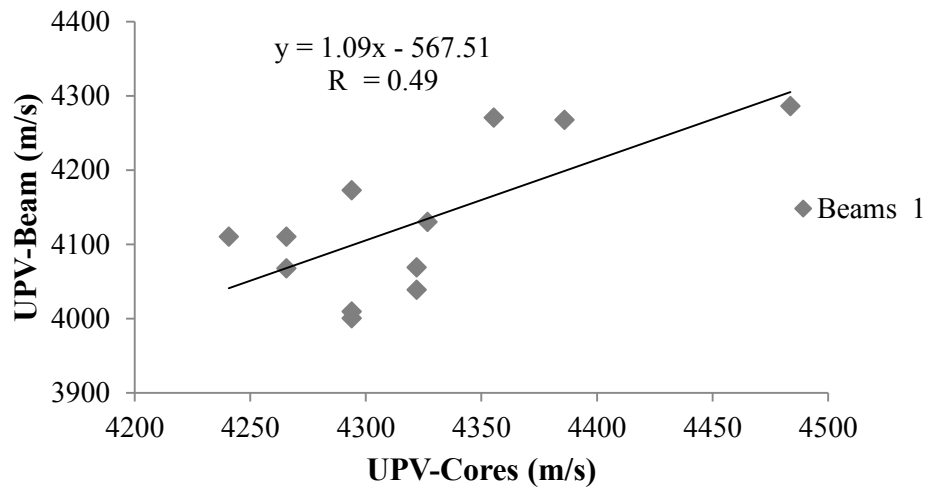


Figure 6.15 UPV results, in % relative to the average value of 4311 m/s for beam 5.

**6.2.2. Ultrasonic Pulse Velocity Measured on Concrete Cores.** the UPV test was also performed to evaluate the uniformity of the cores taken from the beams. All beams were evaluated. Figures 6.16 to 6.18 illustrate the relationship between UPV measurements directly on the beams and the UPV on the concrete cores. The results show that the correlation between UPV on beams and UPV on cores is not so good. The comparison between average UPV measurements and average compressive strength of each beam is shown in Figure 6.19. A good correlation between average UPV on the cores and average compressive strength results can be observed on the overall strength of each beam (Figure 6.19). Although, Figure 6.20 indicates that the correlation in each beam is not good, but the same general trend as in Figure 6.19 can be observed. Detailed results on the UPV measurements on the cores can be found in appendix A.



**Figure 6.16 Correlation between UPV on beam 1 and UPV on cores.**



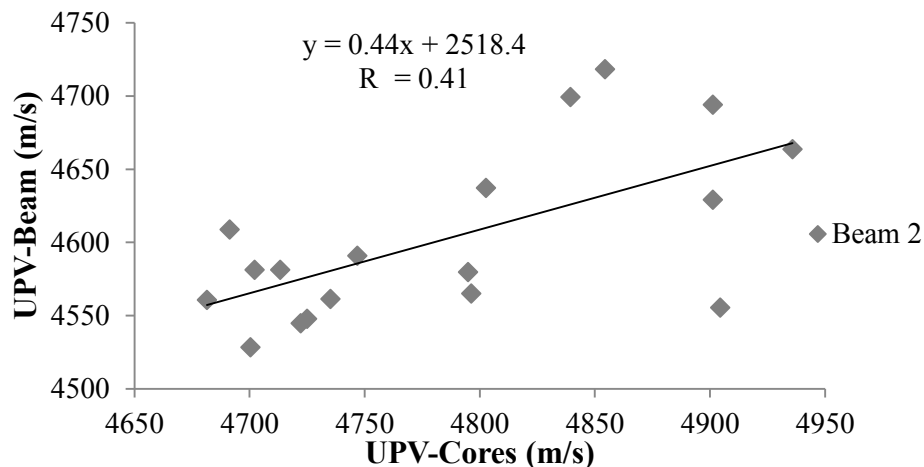


Figure 6.17 Correlation between UPV on beam 2 and UPV on cores.

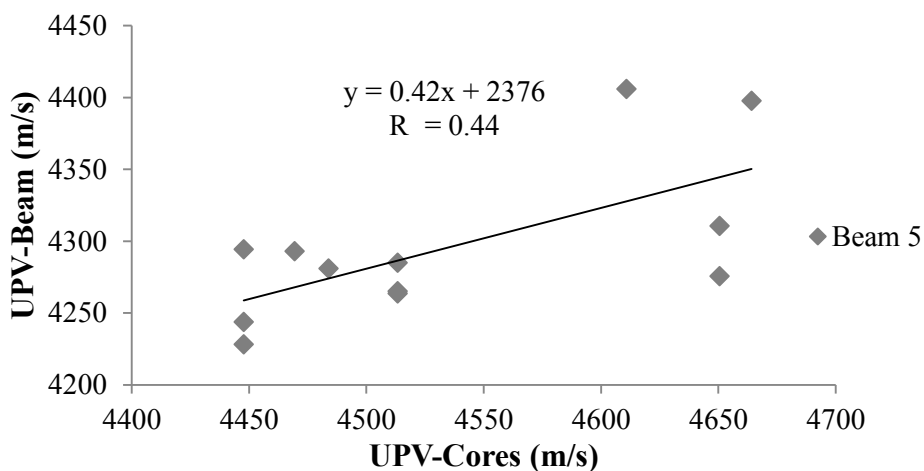


Figure 6.18 Correlation between UPV on beam 5 and UPV on cores.

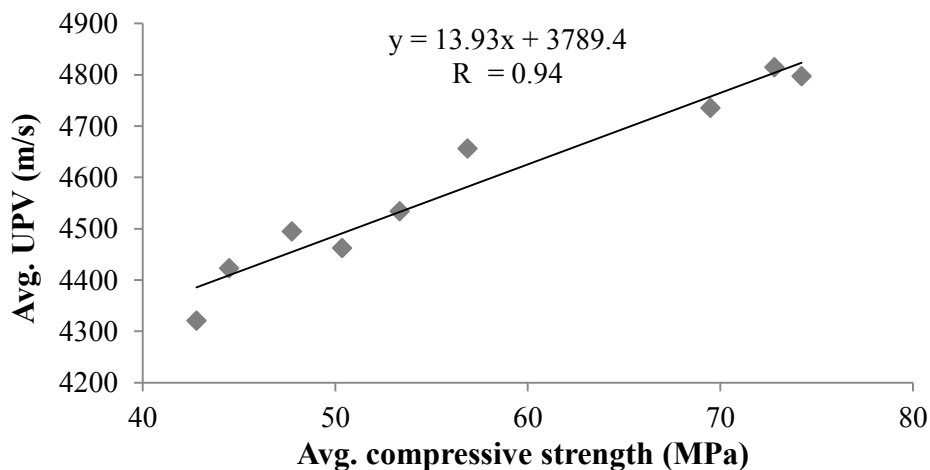
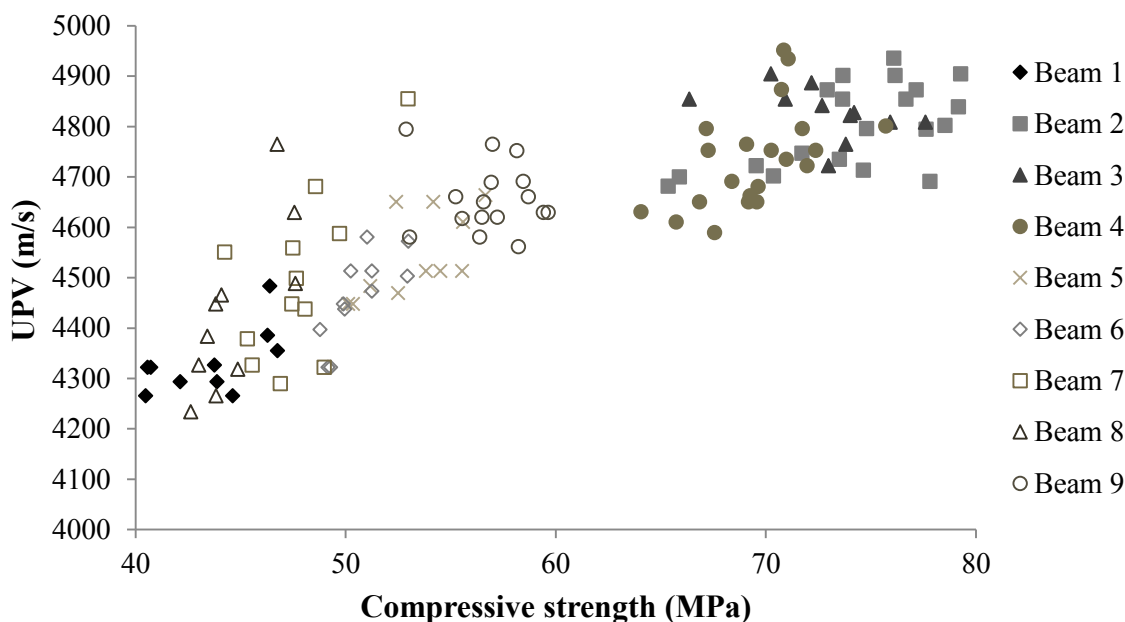


Figure 6.19 Relationship between Average UPV and Average compressive strength of each beam.



**Figure 6.20 Relationship between individual UPV measurements and compressive strength of each core.**

**6.2.3. Effect of Dynamic Segregation on Compressive Strength.** With the purpose of evaluating the influence of dynamic segregation, concrete cores were taken to test compressive strength, which is described in section 5.4.7. All beams were investigated.

At each horizontal point, three cores were taken. The cores were subtracted at the top, middle and bottom from the top surface in a section, and horizontally at 0 m, 3 m, 6 m and 9 m from the casting point for beams 1, 3, 5, 6, 7 and 8. While for beams 2, 4 and 9 cores were extracted at 0 m, 3 m, 6 m, 9 m (not for beam 9), 12 m, 15 m and 18 m. The results are presented in Figures 6.21 to 6.29, which show the deviation of the compressive strength ( $f'_c$ ) results, in absolute values, relative to the average for each beam. For the 18 m long beams only the results in the 9 m closest to the casting point are shown, to enhance visual comparison with the other beams. Figure 6.30, 6.31 and 6.32 show the complete 18 m long beams results.

The compressive strength results show similar trends as the UPV graphs, where the changes in the properties are more visible in the vertical direction at the casting point, where, the concrete has a free-fall of approximately 1 m. The concrete seems to be more homogenous as it is flowing to the end of the formwork. Also, in beams 1, 2, 4, 5, 6, 7 and 8, there are variations in the horizontal direction in the bottom of the beam, close to the casting point. Beams 1 and 4 seem to be the least homogeneous while beams 3 and 9 appear to be most uniform. Matching homogeneity with the VI of each beam does not seem to work for beams 1 and 8. As said in section 6.2.1, the difference of local air content may play a role on these results and further investigation is needed. All detailed results can be found in appendix A.

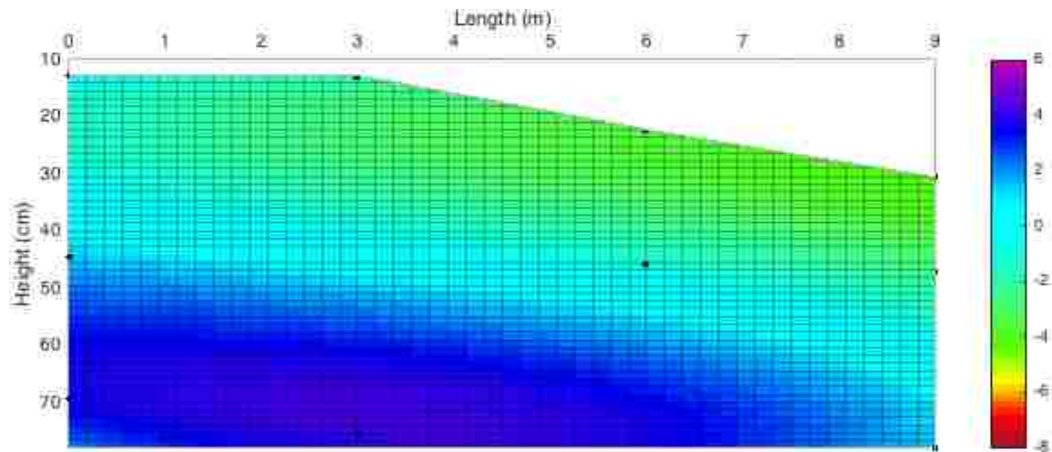


**Figure 6.21. Compressive strength results in absolute values for beam 1 (Avg.  $f'_c = 42.8$  MPa).**

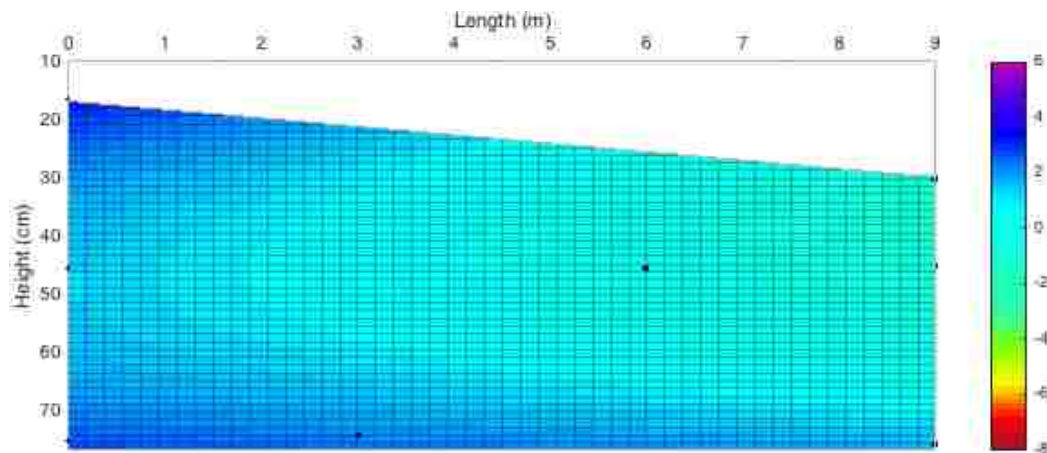


Figure 6.22 Compressive strength results in absolute values for beam 2 (Avg.  $f'c = 74.2$  MPa).

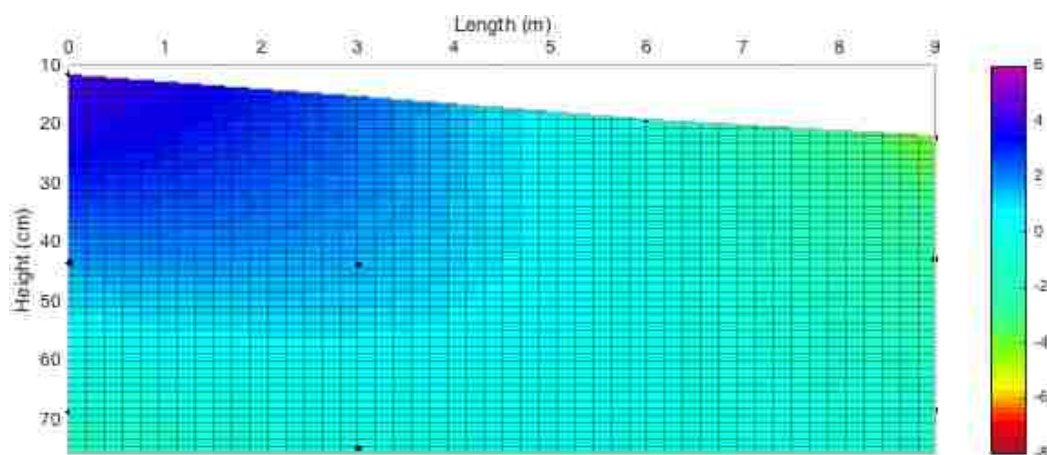


Figure 6.23 Compressive strength results in absolute values for beam 3 (Avg.  $f'c = 72.8$  MPa).

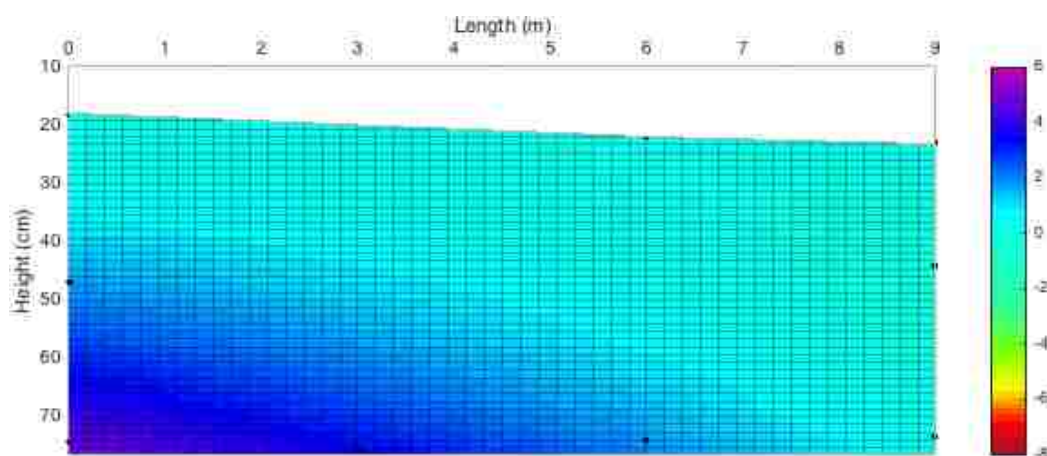


Figure 6.24 Compressive strength results in absolute values for beam 4 (Avg.  $f'c = 69.5$  MPa).



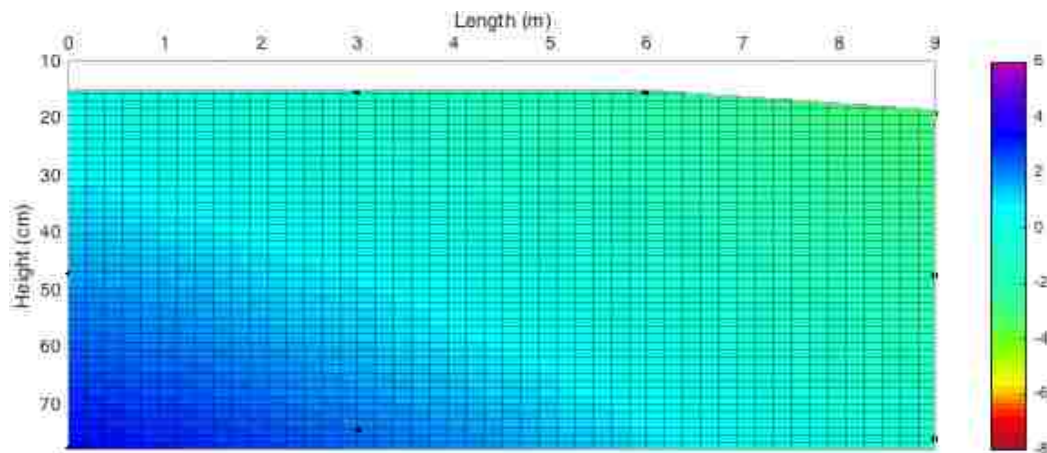


Figure 6.25 Compressive strength results in absolute values for beam 5 (Avg.  $f'c = 53.3$  MPa).

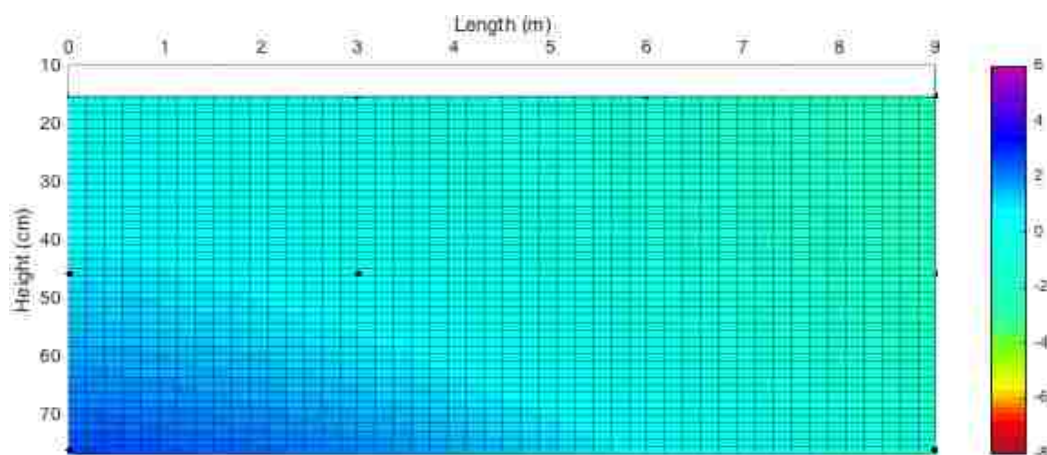


Figure 6.26 Compressive strength results in absolute values for beam 6 (Avg.  $f'c = 50.4$  MPa).

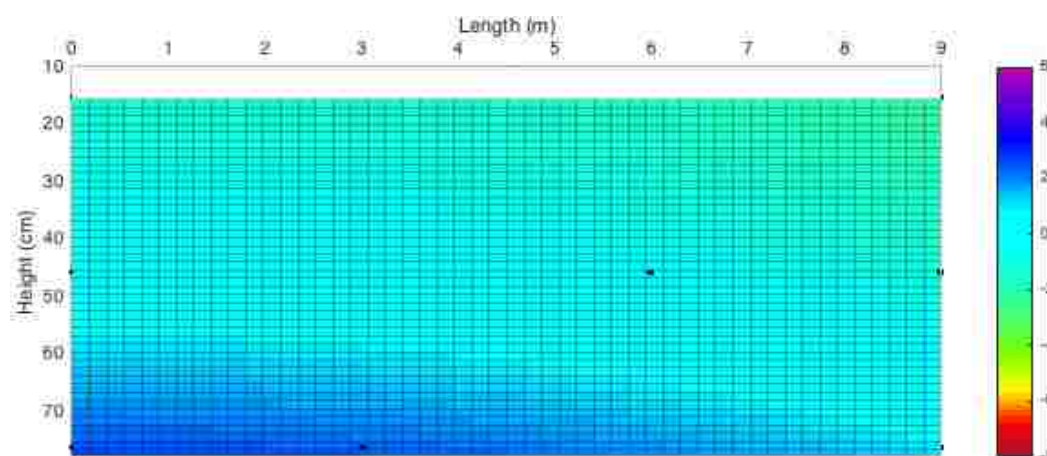


Figure 6.27 Compressive strength results in absolute values for beam 7 (Avg.  $f'c = 47.7$  MPa).

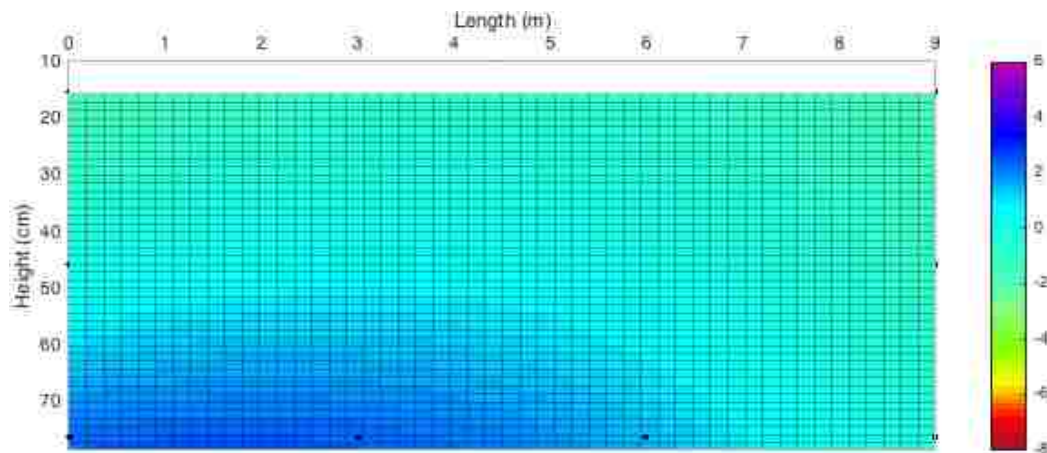


Figure 6.28 Compressive strength results in absolute values for beam 8 (Avg.  $f'c = 44.5$  MPa).

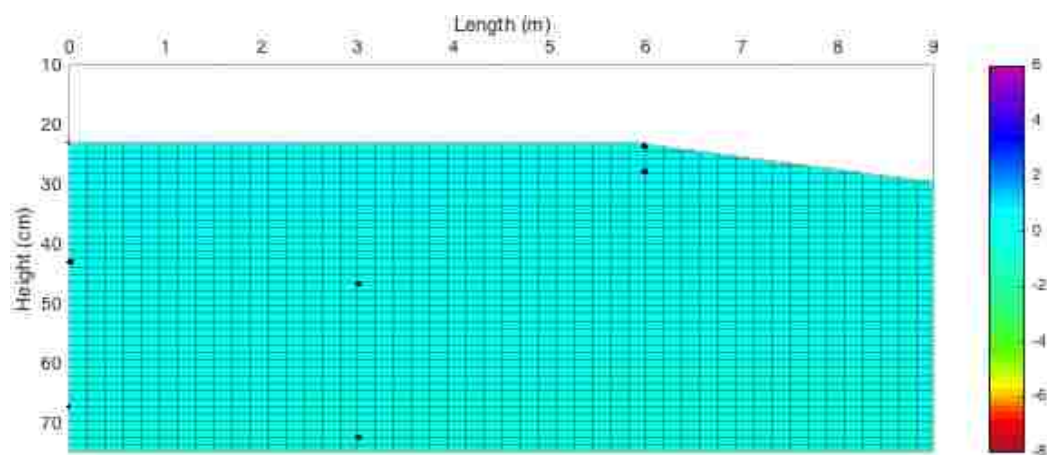


Figure 6.29 Compressive strength results in absolute values for beam 9 (Avg.  $f'c = 56.9$  MPa).

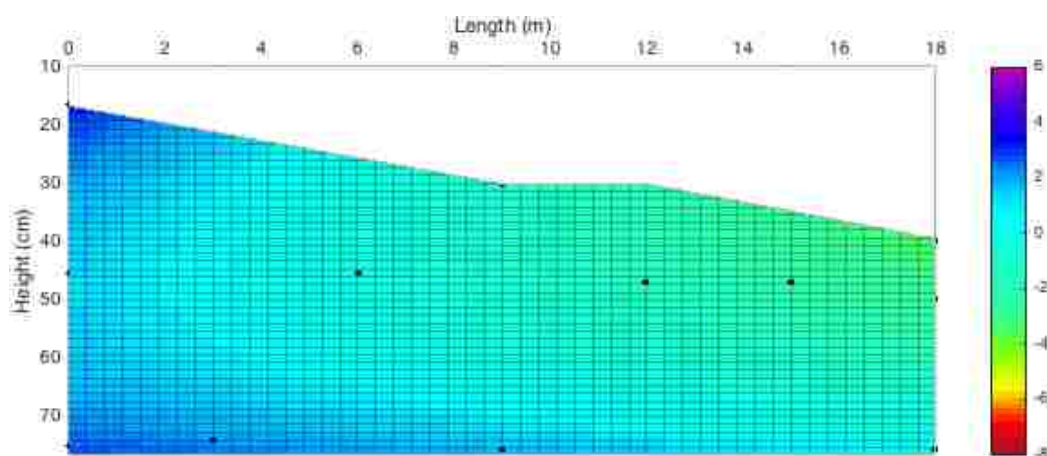
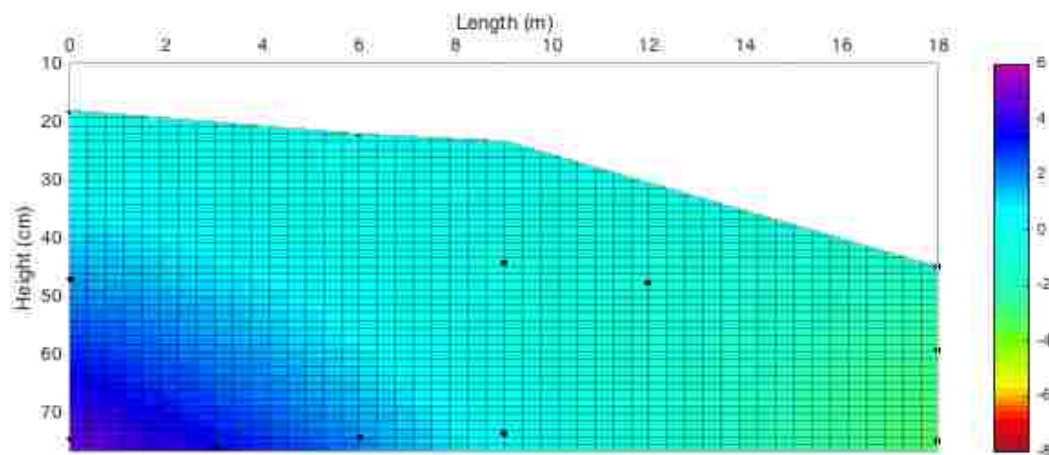
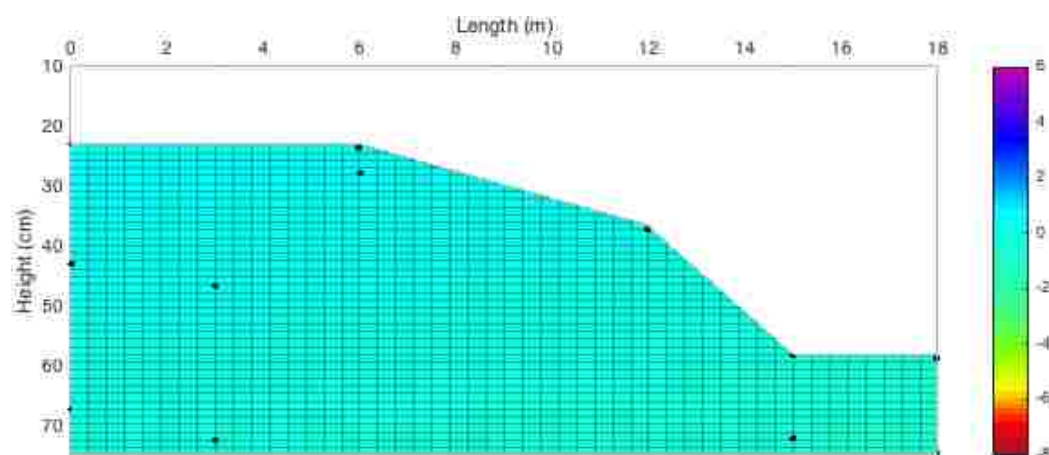


Figure 6.30 Compressive strength results in absolute values for beam 2 (18 m).



**Figure 6.31 Compressive strength results in absolute values for beam 4 (18 m).**



**Figure 6.32 Compressive strength results in absolute values for beam 9 (18 m).**

The effect of entrapped air on the compressive strength of concrete mixtures is well known from the literature. Figure 6.33 shows the relationship between fresh concrete air content and the average compressive strength of each beam. As expected, there is a clear correlation between the air content and the compressive strength. Increasing the air content decreases the  $f'_c$  of the mixture.

Figure 6.34 shows the delta  $f'_c$  and the dynamic segregation of each beam. Delta  $f'_c$  was calculated by subtracting  $f'_c$  in the middle from  $f'_c$  at the bottom at all sections, and taking the average. The top results were not considered in the delta  $f'_c$  analysis since



the cores at the top were at different heights in each beam, due to the location of the casting line. The difference between middle and bottom  $f'c$  shows a good correlation between dynamic segregation and the compressive strength of the beam, except for beams 1 and 8, which are out of the trend. Beam 7, which was the most segregated beam, shows a high variation between the middle and bottom  $f'c$ , while beam 3 has the lowest segregation value and lower variations in  $f'c$ .

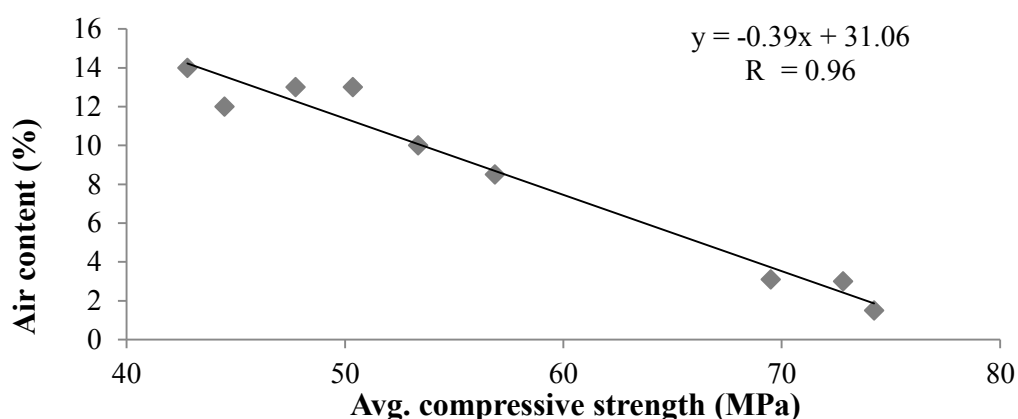


Figure 6.33 Relationship between air content and compressive strength of all beams.

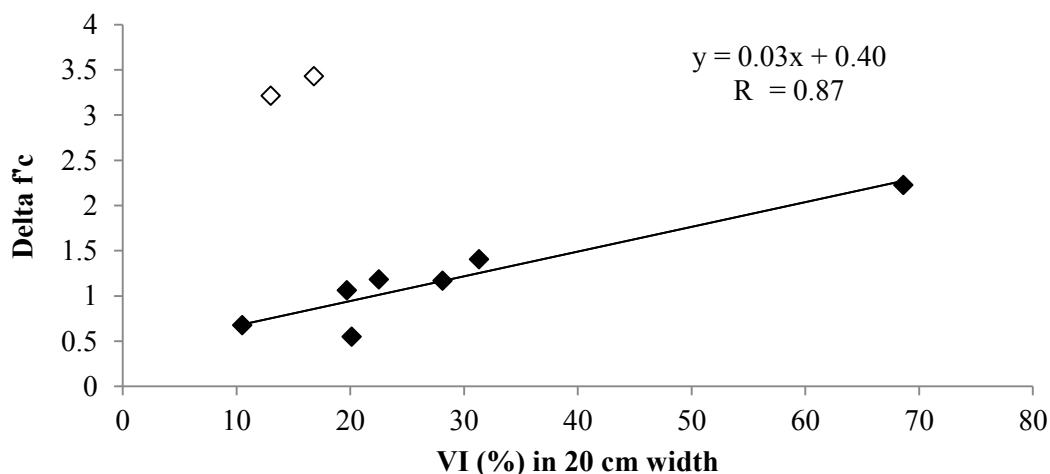


Figure 6.34 Relationship between dynamic segregation and delta  $f'c$  (avg. of bottom – middle) of all beams.

#### 6.2.4. Effect of Dynamic Segregation on Bond Strength. In order to

investigate the influence of dynamic segregation on the adherence between the concrete



and the pre-stress strands, six rectangular and three “I” beams were cast with strands embedded at 305 mm (top) and 610 mm (middle) from the top surface. Figure 6.35 shows the ratio of the average load on all strands embedded in the top portion of the beam, relative to the average load applied to all strands in the middle section of the beams. The results reflect thus some kind of top-bar effect, although the strands were incorporated vertically. In Figure 6.35 it can be observed that with increasing dynamic segregation coefficient, the relative bond strength of the top section decreases.

Beams 3 and 9 have a low VI, leading to bond strengths at the top section of at least 80% of the middle section. Good bond strength is also observed for beams 1, 2 and 4. Beams 5, 6 and 7 showed the higher VI coefficients, which is in agreement with the lower bond strength results in the top section, compared to the middle section. If a minimum relative bond strength of 80% is required, the VI should remain inferior to 20-25%. For beam 8, a relatively low VI is observed, but lower relative bond strengths are obtained. All results for the beams are shown in the appendix B. No clear evolution of bond strength as a function of flow distance can be observed from this results.

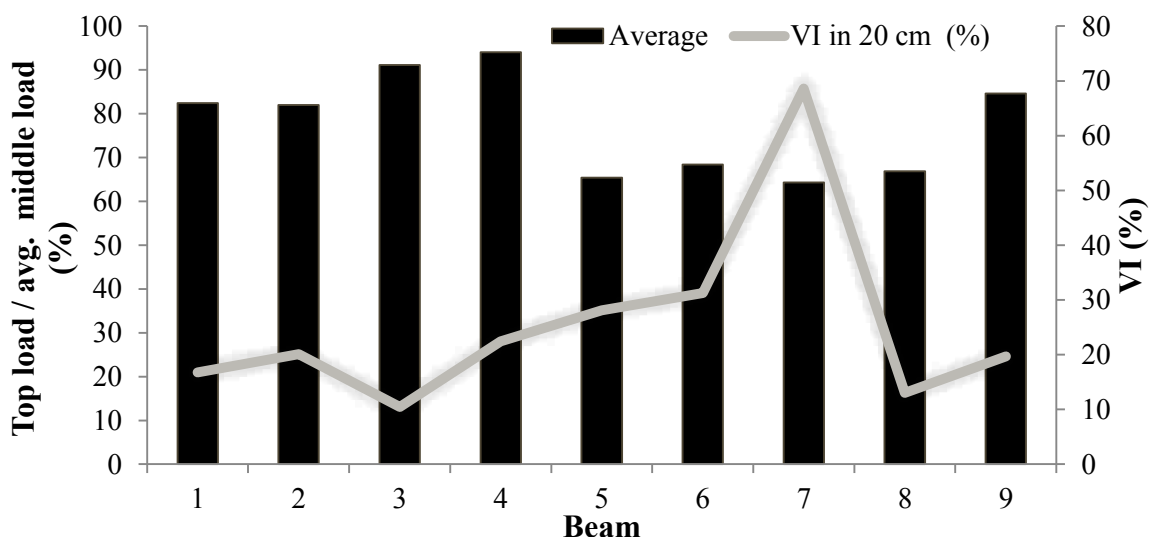


Figure 6.35 Relationship between bond strength and volumetric index of beams.

## 7. CONCLUSIONS, RECOMMENDATIONS AND FUTURE WORK

### 7.1. CONCLUSIONS

A modified T-box was used to evaluate the effects of w/cm, SP content, paste volume, sand-to-total aggregate ratio, workability characteristics and rheological properties on the dynamic segregation of SCC. In addition, nine beams were cast varying their mixture constituents in order to evaluate the effect of dynamic segregation on homogeneity of the beams and bond strength between pre-stress strands and SCC. The following conclusions can be drawn:

1. The tilting box is a suitable method to provide a good indication of dynamic segregation of SCC, as long as the VI assessment method is used.
2. The visual stability index (VSI) cannot provide a suitable measure for dynamic segregation, since dynamic segregation was observed for SCC mixtures with no evidence of segregation according to VSI.
3. There is a clear relationship between dynamic segregation and the rheological properties. Increasing yield stress or plastic viscosity leads to a reduction of segregation. Therefore, to avoid dynamic segregation, yield stress and plastic viscosity must be well balanced.
4. The variations in w/cm, SP and VMA dosage confirm that rheological properties of concrete have a high influence on dynamic segregation.
5. The paste volume has a significant effect on dynamic segregation. An increase in paste volume can ease the shear-induced aggregate movement in the suspension due

- to higher inter-particle spacing, an effect which is additional to the influence of rheology.
6. Varying the sand-to-total-aggregate ratio (S/A) also has an influence on dynamic segregation. A high risk of dynamic segregation in SCC mixtures having a relatively low yield stress in combination with a high S/A, is observed. Also, reducing S/A can destabilize the mixture due to a reduction in lattice effect. If the rheological properties of the SCC are sufficiently high, increasing S/A seems not to affect dynamic segregation.
  7. Reducing the width of the tilting box from 200 mm to 100 mm significantly reduces dynamic segregation due to the increase in peak flow velocity in the narrower channel. It should be further investigated whether an enlargement of the box to 400 mm will have a similar effect.
  8. UPV measurements on the beams indicate higher variations in concrete properties in a vertical direction at the casting point, and in a horizontal direction at the bottom of the beams.
  9. The relationship between dynamic segregation index and UPV measurements does not completely match. Therefore, further investigations are needed.
  10. The comparison between average UPV measurements on cores drilled from the beams and average compressive strength of this cores shows a good correlation.
  11. The relationship between individual UPV and individual compressive strength is not good, especially focusing on each beam separately.
  12. The compressive strength results across the beams show similar trends as the UPV graphs, where the changes in the properties are more visible in the vertical direction

- at the casting point and seems to be more homogenous as it is flowing to the end of the formwork.
13. The difference between middle and bottom  $f'c$  show a good correlation between dynamic segregation and the compressive strength of the beam, except for beam 1 and 8, which are out of the trend.
  14. The results in bond strength on the beams indicate that with increasing dynamic segregation coefficient, the relative bond strength of the top to the middle section decreases.

## 7.2. RECOMMENDATIONS

According to the results found in this research project, the following recommendations to control dynamic segregation of SCC mixtures can be made:

- VSI is a simple method that can be used to have an indication on the stability of SCC mixtures, but it is not good for assessing dynamic segregation. Also, it should not be a decisive method to reject a mixture.
- While using the tilting box, it is important to consider that the surface on which the box is placed is even and is not affected any type of vibration. In addition, it is important to perform the cycles at a constant velocity and by the same operator. This may affect the dynamic segregation results.
- In case of working with a cement developing high early strength or highly thixotropic concrete, an adjustment in the tilting cycles should be made. Otherwise, by the end of the 120 cycles the segregation coefficient will be lower than the real value due to stiffening.

- For the design of an SCC for a particular application, it is highly important to consider the maximum travelling distance of the SCC inside the formwork, as dynamic segregation is directly proportional to the flow distance. However, from this research work, no confirmation of the relationship between the number of cycles and the flow distance has been found.
- For practical applications, to prevent dynamic segregation to occur, a low-cost solution may be to increase the sand-to-total aggregate ratio, which increases the rheological properties, provided that the yield stress is not too low.
- In order to assure adequate dynamic stability the shear stress at  $1\text{s}^{-1}$  should not be less than 30 Pa for  $S/A = 0.51$ . In addition, for a low viscous mixture, a slump flow lower than 700 mm may reduce dynamic segregation.
- In order to ensure adequate bond strength ( $> 80\%$ ) a maximum volumetric index of 20 to 25% should be reached.
- No specific recommendation for VI from  $f'c$  results was obtained, since the results seem to be affected by local air content. Therefore, additional investigations are needed to validate these results.

### 7.3. FUTURE WORK

- Evaluate the local air content and the sorptivity on the concrete cores in order to identify its effects on homogeneity, potentially modifying maximum VI %.
- Evaluation of the air content of the layer created by flow around the reinforcement, and near the formwork of a beam.
- Additional investigation is needed to evaluate the influence of formwork dimensions on dynamic segregation and the influence of obstacles in the formwork.

- Evaluate the effect of the free-fall and its influence of compressive strength and ultrasonic pulse velocity measurements.
- Further investigation is needed to evaluate dynamic segregation in beams by means of the ultrasonic pulse velocity method directly applied on the beams.
- Evaluate the influence of bond strength on dynamic segregation by placing the pre-stress strands in the horizontal position, perpendicular to the flow.
- Evaluation of the tilting box support height in order to investigate its effects on dynamic segregation.

## **APPENDIX A**

### **A. COMPRESSIVE STRENGTH AND UPV DATA OF CONCRETE CORES**

**Table A.1 Compressive strength and UPV measurements for B1.**

Average  $f_c$  42.8 MPa

B1											
Position	Length (m)	#	L/D	Correction factor	Length (m)	Velocity (m/s)	Transmission time ( $\mu$ s)	Velocity Calculated(m/s)	Peak Load (kN)	Compressive Strength (MPa)	Corrected Compressive Strength (MPa)
Top	0	1	1.596	0.968	0.152	4294	35.4	4293.8	310.1	43.5	42.1
Middle	0	2	1.585	0.967	0.151	4327	34.9	4326.6	322.4	45.2	43.7
Bottom	0	3	1.599	0.968	0.152	4386	34.7	4385.9	340.7	47.8	46.3
Top	3	4	1.606	0.969	0.153	4322	35.4	4322.0	298.5	41.9	40.6
Middle	3	5	1.585	0.967	0.151	4266	35.4	4265.5	328.9	46.2	44.6
Bottom	3	6	1.596	0.968	0.152	4355	34.9	4355.3	344.3	48.3	46.7
Top	6	7	1.596	0.968	0.152	4294	35.4	4293.8	288.5	40.5	39.2
Middle	6	8	1.585	0.967	0.151	4266	35.4	4265.5	298.4	41.9	40.5
Bottom	6	9	1.596	0.968	0.152	4484	33.9	4483.8	341.6	47.9	46.4
Top	9	10	1.554	0.964	0.148	4241	34.9	4240.7	285.7	40.1	38.7
Middle	9	11	1.606	0.969	0.153	4322	35.4	4322.0	299.6	42.0	40.7
Bottom	9	12	1.596	0.968	0.152	4294	35.4	4293.8	323.0	45.3	43.9



**Table A.2 Compressive strength and UPV measurements for B2.**

Average  $f_c$  74.2 MPa

B2											
Position	Length (m)	#	L/D	Correction factor	Length (m)	Velocity (m/s)	Transmission time ( $\mu$ s)	Velocity Calculated(m/s)	Peak Load (kN)	Compressive Strength (MPa)	Corrected Compressive Strength (MPa)
Top	0	1	1.617	0.969	0.154	4904	31.4	4904.5	582.7	81.8	79.3
Middle	0	2	1.596	0.968	0.152	4795	31.7	4795.0	571.6	80.2	77.6
Bottom	0	3	1.578	0.966	0.150	4839	30.4	4939.4	583.8	81.9	79.2
Top	3	4									
Middle	3	5	1.617	0.969	0.154	4936	31.2	4935.9	559.4	78.5	76.1
Bottom	3	6	1.575	0.966	0.150	4854	30.9	4854.4	543.3	76.2	73.6
Top	6	7	1.575	0.966	0.150	4854	30.9	4854.4	565.5	79.4	76.7
Middle	6	8	1.606	0.969	0.153	4873	31.4	4872.6	536.5	75.3	72.9
Bottom	6	9	1.606	0.969	0.153	4873	31.4	4872.6	567.6	79.7	77.2
Top	9	10	1.543	0.963	0.147	4682	31.4	4681.5	483.3	67.8	65.3
Middle	9	11	1.606	0.969	0.153	4796	31.9	4796.2	550.2	77.2	74.8
Bottom	9	12	1.564	0.965	0.149	4901	30.4	4901.3	543.9	76.3	73.7
Top	12	13	1.606	0.969	0.153	4722	32.4	4722.2	511.6	71.8	69.5
Middle	12	14	1.564	0.965	0.149	4700	31.7	4700.3	486.4	68.3	65.9
Bottom	12	15	1.533	0.963	0.146	4803	30.4	4802.6	581.2	81.6	78.5
Top	15	16	1.596	0.968	0.152	4735	32.1	4735.2	541.3	76.0	73.5
Middle	15	17	1.575	0.966	0.150	4702	31.9	4702.2	519.1	72.8	70.4
Bottom	15	18	1.564	0.965	0.149	4901	30.4	4901.3	562.3	78.9	76.2
Top	18	19	1.554	0.964	0.148	4713	31.4	4713.4	551.6	77.4	74.6
Middle	18	20	1.596	0.968	0.152	4691	32.4	4691.4	573.0	80.4	77.8
Bottom	18	21	1.564	0.965	0.149	4747	31.4	4746.9	529.5	74.3	71.7

**Table A.3 Compressive strength and UPV measurements for B3.**

Average  $f_c$  72.7 MPa

B3											
Position	Length (m)	#	L/D	Correction factor	Length (m)	Velocity (m/s)	Transmission time ( $\mu$ s)	Velocity Calculated(m/s)	Peak Load (kN)	Compressive Strength (MPa)	Corrected Compressive Strength (MPa)
Top	0	1	1.585	0.967	0.151	4809	31.4	4808.9	571.9	80.3	77.6
Middle	0	2	1.617	0.969	0.154	4828	31.9	4827.6	545.4	76.5	74.2
Bottom	0	3	1.596	0.968	0.152	4842	31.4	4841.8	524.1	73.6	71.2
Top	3	4	1.564	0.965	0.149	4822	30.9	4822.0	544.9	76.5	73.8
Middle	3	5	1.575	0.966	0.150	4854	30.9	4854.4	546.0	76.6	74.0
Bottom	3	6	1.585	0.967	0.151	4887	30.9	4886.7	522.7	73.4	70.9
Top	6	7	1.585	0.967	0.151	4809	31.4	4808.9	531.9	74.6	72.2
Middle	6	8	1.596	0.968	0.152	4691	32.4	4691.4	559.1	78.5	75.9
Bottom	6	9									
Top	9	10	1.575	0.966	0.150	4854	30.9	4854.4	518.1	72.7	70.2
Middle	9	11	1.606	0.969	0.153	4722	32.4	4722.2	488.1	68.5	66.3
Bottom	9	12	1.599	0.968	0.152	4751	32.1	4751.5	537.3	75.4	73.0

**Table A.4 Compressive strength and UPV measurements for B4.**

Average  $f_c$  69.5 MPa

B4											
Position	Length (m)	#	L/D	Correction factor	Length (m)	Velocity (m/s)	Transmission time ( $\mu$ s)	Velocity Calculated(m/s)	Peak Load (kN)	Compressive Strength (MPa)	Corrected Compressive Strength (MPa)
Top	0	1	1.596	0.968	0.152	4735	32.1	4735.2	522.6	73.3	71.0
Middle	0	2	1.617	0.969	0.154	4753	32.4	4753.1	516.5	72.5	70.3
Bottom	0	3	1.603	0.968	0.153	4801	31.8	4801.4	557.1	78.2	75.7
Top	3	4	1.606	0.969	0.153	4650	32.9	4650.5	511.9	71.8	69.6
Middle	3	5	1.585	0.967	0.151	4935	30.6	4934.6	523.8	73.5	71.1
Bottom	3	6	1.606	0.969	0.153	4951	30.9	4951.5	521.2	73.2	70.8
Top	6	7	1.606	0.969	0.153	4796	31.9	4796.2	494.2	69.3	67.2
Middle	6	8	1.617	0.969	0.154	4753	32.4	4753.1	532.0	74.7	72.4
Bottom	6	9	1.617	0.969	0.154	4873	31.6	4873.4	520.0	73.0	70.7
Top	9	10	1.606	0.969	0.153	4650	32.9	4650.5	509.0	71.4	69.2
Middle	9	11	1.617	0.969	0.154	4753	32.4	4753.1	494.3	69.4	67.2
Bottom	9	12	1.596	0.968	0.152	4691	32.4	4691.4	503.6	70.7	68.4
Top	12	13	1.617	0.969	0.154	4681	32.9	4680.9	511.9	71.8	69.6
Middle	12	14	1.585	0.967	0.151	4590	32.9	4589.7	497.9	69.9	67.6
Bottom	12	15	1.606	0.969	0.153	4796	31.9	4796.2	527.8	74.1	71.7
Top	15	16	1.606	0.969	0.153	4722	32.4	4722.2	529.4	74.3	72.0
Middle	15	17	1.596	0.968	0.152	4663	32.6	4662.6	509.9	71.6	69.2
Bottom	15	18	1.596	0.968	0.152	4765	31.9	4764.9	508.7	71.4	69.1
Top	18	19	1.606	0.969	0.153	4650	32.9	4650.5	491.8	69.0	66.8
Middle	18	20	1.617	0.969	0.154	4611	33.4	4610.8	483.2	67.8	65.7
Bottom	18	21	1.599	0.968	0.152	4630	32.9	4630.1	471.6	66.2	64.1

**Table A.5 Compressive strength and UPV measurements for B5 and B6.**

Average  $f_c$  53.3 MPa

B5											
Position	Length (m)	#	L/D	Correction factor	Length (m)	Velocity (m/s)	Transmission time ( $\mu$ s)	Velocity Calculated(m/s)	Peak Load (kN)	Compressive Strength (MPa)	Corrected Compressive Strength (MPa)
Top	0	1									
Middle	0	2	1.606	0.969	0.153	4513	33.9	4513.3	408.6	57.3	55.5
Bottom	0	3	1.603	0.968	0.153	4664	32.7	4664.5	416.9	58.5	56.7
Top	3	4	1.606	0.969	0.153	4650	32.9	4650.5	385.5	54.1	52.4
Middle	3	5	1.606	0.969	0.153	4513	33.9	4513.3	401.0	56.3	54.5
Bottom	3	6	1.606	0.969	0.153	4650	32.9	4650.5	398.6	55.9	54.2
Top	6	7	1.606	0.969	0.153	4448	34.4	4447.7	368.7	51.7	50.1
Middle	6	8	1.606	0.969	0.153	4513	33.9	4513.3	396.0	55.6	53.8
Bottom	6	9	1.617	0.969	0.154	4611	33.4	4610.8	408.6	57.3	55.6
Top	9	10	1.596	0.968	0.152	4484	33.9	4483.8	376.8	52.9	51.2
Middle	9	11	1.606	0.969	0.153	4448	34.4	4447.7	370.4	52.0	50.3
Bottom	9	12	1.606	0.969	0.153	4470	34.2	4469.8	386.2	54.2	52.5

Average  $f_c$  50.4 MPa

B6											
Position	Length (m)	#	L/D	Correction factor	Length (m)	Velocity (m/s)	Transmission time ( $\mu$ s)	Velocity Calculated(m/s)	Peak Load (kN)	Compressive Strength (MPa)	Corrected Compressive Strength (MPa)
Top	0	1	1.606	0.969	0.153	4513	33.9	4513.3	377.0	52.9	51.2
Middle	0	2	1.606	0.969	0.153	4581	33.4	4580.8	375.3	52.7	51.0
Bottom	0	3	1.606	0.969	0.153	4573	33.5	4572.6	389.8	54.7	53.0
Top	3	4	1.617	0.969	0.154	4438	34.7	4438.0	367.2	51.5	49.9
Middle	3	5	1.606	0.969	0.153	4513	33.9	4513.3	369.6	51.9	50.2
Bottom	3	6	1.617	0.969	0.154	4503	34.2	4502.9	389.1	54.6	52.9
Top	6	7	1.606	0.969	0.153	4322	35.4	4322.0	362.5	50.9	49.3
Middle	6	8	1.606	0.969	0.153	4448	34.4	4447.7	367.0	51.5	49.9
Bottom	6	9	1.606	0.969	0.153	4474	34.2	4473.7	377.0	52.9	51.2
Top	9	10	1.617	0.969	0.154	4118	37.4	4117.6	349.7	49.1	47.6
Middle	9	11	1.606	0.969	0.153	4322	35.4	4322.0	361.7	50.8	49.2
Bottom	9	12	1.612	0.969	0.154	4386	35.0	4385.7	358.7	50.3	48.8

**Table A.6 Compressive strength and UPV measurements for B7 and B8.**

Average  $f_c$  47.7 MPa

B7											
Position	Length (m)	#	L/D	Correction factor	Length (m)	Velocity (m/s)	Transmission time ( $\mu$ s)	Velocity Calculated(m/s)	Peak Load (kN)	Compressive Strength (MPa)	Corrected Compressive Strength (MPa)
Top	0	1	1.554	0.964	0.148	4498	32.9	4498.5	352.1	49.4	47.7
Middle	0	2	1.606	0.969	0.153	4448	34.4	4447.7	349.0	49.0	47.4
Bottom	0	3	1.589	0.967	0.151	4587	33.0	4587.1	366.2	51.4	49.7
Top	3	4	1.585	0.967	0.151	4327	34.9	4326.6	335.7	47.1	45.5
Middle	3	5	1.627	0.970	0.155	4379	35.4	4378.5	332.8	46.7	45.3
Bottom	3	6	1.585	0.967	0.151	4855	31.1	4855.3	390.4	54.8	53.0
Top	6	7	1.617	0.969	0.154	4290	35.9	4289.7	344.7	48.4	46.9
Middle	6	8	1.617	0.969	0.154	4438	34.7	4438.0	353.3	49.6	48.1
Bottom	6	9	1.617	0.969	0.154	4681	32.9	4680.9	357.0	50.1	48.6
Top	9	10	1.596	0.968	0.152	4551	33.4	4550.9	325.7	45.7	44.2
Middle	9	11	1.606	0.969	0.153	4322	35.4	4322.0	360.3	50.6	49.0
Bottom	9	12	1.606	0.969	0.153	4681	32.7	4681.6	349.3	49.0	47.5

Average  $f_c$  44.5 MPa

B8											
Position	Length (m)	#	L/D	Correction factor	Length (m)	Velocity (m/s)	Transmission time ( $\mu$ s)	Velocity Calculated(m/s)	Peak Load (kN)	Compressive Strength (MPa)	Corrected Compressive Strength (MPa)
Top	0	1	1.585	0.967	0.151	4266	35.4	4265.5	323.0	45.3	43.8
Middle	0	2	1.585	0.967	0.151	4327	34.9	4326.6	317.0	44.5	43.0
Bottom	0	3	1.591	0.967	0.152	4489	33.8	4488.9	350.7	49.2	47.6
Top	3	4	1.596	0.968	0.152	4234	35.9	4234.0	318.8	44.7	43.3
Middle	3	5	1.606	0.969	0.153	4384	34.9	4384.0	319.4	44.8	43.4
Bottom	3	6	1.575	0.966	0.150	4630	32.4	4629.6	350.8	49.2	47.6
Top	6	7	1.596	0.968	0.152	4318	35.2	4318.2	330.4	46.4	44.9
Middle	6	8	1.606	0.969	0.153	4448	34.4	4447.7	322.4	45.2	43.8
Bottom	6	9	1.596	0.968	0.152	4765	31.9	4764.9	344.2	48.3	46.7
Top	9	10	1.596	0.968	0.152	4234	35.9	4234.0	313.9	44.0	42.6
Middle	9	11	1.585	0.967	0.151	4266	35.4	4265.5	316.2	44.4	42.9
Bottom	9	12	1.601	0.968	0.153	4466	34.1	4466.5	324.5	45.5	44.1

**Table A.7 Compressive strength and UPV measurements for B9.**

Average f'c 56.9 MPa

B9											
Height	Length (m)	#	L/D	Correction factor	Length (m)	Velocity (m/s)	Transmission time (μs)	Velocity Calculated(m/s)	Peak Load (kN)	Compressive Strength (MPa)	Corrected Compressive Strength (MPa)
Top	0	1	1.575	0.966	0.150	4630	32.4	4629.6	438.3	61.5	59.4
Middle	0	2	1.606	0.969	0.153	4650	32.9	4650.5	416.2	58.4	56.6
Bottom	0	3	1.599	0.968	0.152	4752	32.1	4752.1	428.0	60.1	58.1
Top	3	4	1.596	0.968	0.152	4691	32.4	4691.4	430.4	60.4	58.5
Middle	3	5	1.596	0.968	0.152	4765	31.9	4764.9	419.6	58.9	57.0
Bottom	3	6	1.596	0.968	0.152	4795	31.7	4795.0	389.4	54.6	52.9
Top	6	7	1.596	0.968	0.152	4620	32.9	4620.1	421.3	59.1	57.2
Middle	6	8	1.606	0.969	0.153	4581	33.4	4580.8	414.8	58.2	56.4
Bottom	6	9	1.585	0.967	0.151	4689	32.2	4689.4	419.5	58.9	56.9
Top	9	10									
Middle	9	11									
Bottom	9	12									
Top	12	13	1.585	0.967	0.151	4660	32.4	4660.5	407.1	57.1	55.2
Middle	12	14	1.585	0.967	0.151	4660	32.4	4660.5	432.6	60.7	58.7
Bottom	12	15	1.599	0.968	0.152	4561	33.4	4559.9	428.6	60.1	58.2
Top	15	16									
Middle	15	17	1.596	0.968	0.152	4620	32.9	4620.1	416.0	58.4	56.5
Bottom	15	18	1.585	0.967	0.151	4618	32.7	4617.7	409.3	57.4	55.5
Top	18	19									
Middle	18	20	1.606	0.969	0.153	4581	33.4	4580.8	390.3	54.8	53.0
Bottom	18	21	1.575	0.966	0.150	4630	32.4	4629.6	439.9	61.7	59.6

## **APPENDIX B**

### **B. PULL-OUT TEST DATA FOR BEAMS**

Table B.1 Pull-out results for beams 1, 2 and 3.

Beams	#	Position	kN
1	1	M	96.8
	2	T	80.2
	3	M	93.3
	4	T	92.5
	5	M	100.5
	6	T	66.7
		Middle Average	96.9
		Top Average	79.8
		Average	88.3
2	1	T	68.6
	2	M	182.2
	3	T	95.4
	4	M	194.3
	5	T	138.2
	6	M	189.5
	7	T	153.7
	8	M	175.7
	10	M	190.3
	12	M	188.1
		Middle Average	139.1
		Top Average	185.4
	Average	157.6	
3	1	M	188.1
	2	T	155.5
	3	M	184.2
	4	T	176.4
	5	M	187.9
	6	T	178.6
		Middle Average	186.7
		Top Average	170.2
		Average	178.4



Table B.2 Pull-out results for beams 4, 5 and 6.

Beams	#	Position	kN	
4	1	M	163.3	
	2	T	144.2	
	3	M	193.8	
	4	T	181.1	
	5	M	180.3	
	6	T	191.0	
	7	M	187.3	
	8	T	163.9	
	9	M	188.0	
	11	M	171.9	
			Middle Average	180.8
			Top Average	170.1
			Average	176.5
5	1	M	152.0	
	2	T	119.8	
	3	M	167.6	
	4	T	111.7	
	5	M	155.9	
	6	T	79.5	
			Middle Average	158.5
			Top Average	103.7
			Average	131.1
6	1	M	145.3	
	2	T	88.0	
	3	M	135.7	
	4	T	79.9	
	5	M	110.7	
	6	T	100.1	
			Middle Average	130.6
			Top Average	89.3
			Average	109.9

Table B.3 Pull-out results for beams 7, 8 and 9.

Beams	#	Position	kN	
7	1	M	116.6	
	2	T	82.5	
	3	M	133.4	
	4	T	71.5	
	5	M	97.1	
	6	T	69.2	
			Middle Average	115.7
			Top Average	74.4
			Average	95.0
	8	3	M	97.6
4		T	85.8	
5		M	119.4	
6		T	59.2	
			Middle Average	108.5
			Top Average	72.5
			Average	90.5
9	1	T	95.5	
	2	M	179.9	
	3	T	111.2	
	4	M	144.4	
	5	T	122.4	
	6	M	96.9	
	7	T	134.4	
	8	M	106.4	
	10	M	157.4	
			Middle Average	137.0
			Top Average	115.9
			Average	127.6

## REFERENCES

1. ACI 238.1R-08, Report on Measurements of Workability and Rheology of Fresh Concrete, American Concrete Institute, Farmington Hills MI, 2008.
2. Panesar, D. K., & Shindman, B. (2012). The effect of segregation on transport and durability properties of self-consolidating concrete. *Cement and Concrete Research*, 42(2), 252-264.
3. Hoshino, M. (1989). Relation between bleeding, coarse aggregate, and specimen height of concrete. *Materials Journal*, 86(2), 185-190.
4. Khayat, K. H., Manai, K., & Trudel, A. (1997). In situ mechanical properties of wall elements cast using self-consolidating concrete. *ACI Materials Journal*, 94, 491-500.
5. Esmaeilkhanian, B. Dynamic Stability of Self-Consolidating Concrete: Development of Test Methods and Influencing Parameters. M.Sc. Thesis. Sherbrooke, Qc, Canada, Université de Sherbrooke, 2011.
6. ACI Committee 237 (2007). "Self-Consolidating Concrete". ACI 237-07, ACI Manual of Concrete Practice, Detroit, MI, USA.
7. Okamura, H. & Masahiro O. (2003) Self-compacting concrete. *Journal of Advanced Concrete Technology*, 1(1), 5-15.
8. Daczko, J. A. (2012). *Self-consolidating concrete: applying what we know*. CRC Press.
9. Concrete, S. C. (2005). The European Guidelines for Self-Compacting Concrete.
10. El-Chabib, H., & Nehdi, M. (2006). Effect of mixture design parameters on segregation of self-consolidating concrete. *ACI materials journal*, 103(5), 374-383.
11. Kosmatka, S. H., & Panarese, W. C. (2004). Design and control of concrete mixture. *Portland Cement Association*.
12. Ferraris, C. F. (1999). Measurement of the rheological properties of high performance concrete: state of art report. *Journal of research of the national institute of standards and technology*, 104(5), 461.
13. Ferraris, C., De Larrard, F., & Martys, N. (2001). Fresh concrete rheology: recent developments. *Materials Science of Concrete VI, Amer. Cer. Soc. Ed. S. Mindess, J. Skalny*, 215-241.

14. Beris, A. N., Tsamopoulos, J. A., Armstrong, R. C., & Brown, R. A. (1985). Creeping motion of a sphere through a Bingham plastic. *Journal of Fluid Mechanics*, 158, 219-244.
15. Roussel, N. (2006). A theoretical frame to study stability of fresh concrete. *Materials and structures*, 39(1), 81-91.
16. Petrou, M. F., Wan, B., Gadala-Maria, F., Kolli, V. G., & Harries, K. A. (2000). Influence of mortar rheology on aggregate settlement. *ACI Materials Journal*, 97(4), 479-485.
17. Tregger, N., Gregori, A., Ferrara, L., & Shah, S. (2012). Correlating dynamic segregation of self-consolidating concrete to the slump-flow test. *Construction and Building Materials*, 28(1), 499-505.
18. Esmaeilkhanian, B., Khayat, K. H., Yahia, A., & Feys, D. (2014). Effects of Mix Design Parameters and Rheological Properties on Dynamic Stability of Self-Consolidating Concrete. *Cement and Concrete Composites*, 54, 21-28.
19. Shen, L., Struble, L., & Lange, D. (2009). Modeling dynamic segregation of self-consolidating concrete. *ACI Materials Journal*, 106(4), 375-380.
20. Daczko, J. A. (2002). Stability of self-consolidating concrete, assumed or ensured?. *Proceedings of the First North American conference on the design and use of self-consolidating concrete*, Chicago, Illinois, 2002, pp.223-228.
21. Bui, V. K., Montgomery, D., Hinczak, I., & Turner, K. (2002). Rapid testing method for segregation resistance of self-compacting concrete. *Cement and Concrete Research*, 32(9), 1489-1496.
22. ASTM C1611/C1611M-14. (2014). Standard Test Method for Slump Flow of Self-Consolidating Concrete. ASTM international, West Conshohocken, PA.
23. Shen, L., Jovein, H. B., Sun, Z., Wang, Q., & Li, W. (2015). Testing dynamic segregation of self-consolidating concrete. *Construction and Building Materials*, 75, 465-471.
24. Esmaeilkhanian, B., Feys, D., Khayat, K. H., & Yahia, A. (2014). New test method to evaluate dynamic stability of self-consolidating concrete. *ACI Materials Journal*, 111(3), 299-307.
25. Turgut, P., Turk, K., & Bakirci, H. (2012). Segregation control of SCC with a modified L-box apparatus. *Magazine of Concrete Research*, 64(8), 707-716.
26. Alami, M. M. (2014). Development of a new test method to evaluate dynamic stability of self-consolidating concrete. M.Sc. Thesis. Izmir, Turkey, Izmir Institute of technology, 2014.

27. Khayat, K. H., Assaad, J., & Daczko, J. (2004). Comparison of field-oriented test methods to assess dynamic stability of self-consolidating concrete. *ACI Materials Journal*, 101(2), 168-176.
28. Mindess, S., Young, J. F., & Darwin, D. (2003). *Concrete*.
29. Mehta, P. K., & Monteiro, P. J. M. (2006). Microstructure and properties of hardened concrete. *Concrete: Microstructure, properties and materials*.
30. Soshiroda, T., Voraputhaporn, K., & Nozaki, Y. (2006). Early-stage inspection of concrete quality in structures by combined nondestructive method. *Materials and structures*, 39(2), 149-160.
31. Keske, S.D. 2011. Assessment of Stability Test Methods for Self-Consolidating Concrete. M.S. thesis, Auburn University.
32. Cussigh, F. (1999). Self-compacting concrete stability control. In Å. Skarendahl, & Ö. Petersson (Eds.), *First International RILEM Symposium On Self-Compacting Concrete* (pp. 153-167).
33. Keske, S. D., Schindler, A. K., & Barnes, R. W. (2013). Assessment of Stability Test Methods for Self-Consolidating Concrete. *ACI Materials Journal*, 110(4).
34. Soylev, T. A., & François, R. (2003). Quality of steel–concrete interface and corrosion of reinforcing steel. *Cement and Concrete Research*, 33(9), 1407-1415.
35. Zhu, W., Gibbs, J. C., & Bartos, P. J. (2001). Uniformity of in situ properties of self-compacting concrete in full-scale structural elements. *Cement and Concrete Composites*, 23(1), 57-64.
36. Khayat, K. H., Manai, K., & Trudel, A. (1997). In situ mechanical properties of wall elements cast using self-consolidating concrete. *ACI Materials Journal*, 94, 491-500.
37. Long, W. J., Khayat, K. H., Lemieux, G., Hwang, S. D., & Xing, F. (2014). Pull-out strength and bond behavior of prestressing strands in prestressed self-consolidating concrete. *Materials*, 7(10), 6930-6946.
38. Khayat, K. H., Petrov, N., Attiogbe, E. K., & See, H. T. (2003). Uniformity of bond strength of prestressing strands in conventional flowable and self-consolidating concrete mixtures. In O. Wallevik, & I. Nielsson (Eds.), *Self-Compacting Concrete: Proceedings of the Third International RILEM Symposium* (pp. 703-709).
39. Holschemacher, K., & Klug, Y. (2002). A database for the evaluation of hardened properties of SCC. *Lacer*, 7, 123-134.
40. Models TGB (2000) Bond of reinforcement in concrete, CEB-fib, fib Bulletin No. 10, Lausanne, p 427

41. ASTM C150/C150M-16. (2016). Standard Specification for Portland Cement. ASTM international, West Conshohocken, PA.
42. ASTM C128-15. (2015). Standard Test Method for Relative Density (Specific Gravity) and Absorption of Fine Aggregate. ASTM international, West Conshohocken, PA.
43. ASTM C33/C33M-16. (2016). Standard Specification for Concrete Aggregates. ASTM international, West Conshohocken, PA.
44. ASTM C136/C136M-14. (2014). Standard Test Method for Sieve Analysis of Fine and Coarse Aggregates. ASTM international, West Conshohocken, PA.
45. ASTM C127-15. (2015). Standard Test Method for Relative Density (Specific Gravity) and Absorption of Coarse Aggregate. ASTM international, West Conshohocken, PA.
46. ASTM C494/C494M-15a. (2015). Standard Specification for Chemical Admixtures for Concrete. ASTM international, West Conshohocken, PA.
47. Roussel, N., & Coussot, P. (2005). "Fifty-cent rheometer" for yield stress measurements: From slump to spreading flow. *Journal of Rheology (1978-present)*, 49(3), 705-718.
48. RMCAO. (2009). Best Practices Guidelines for Self-Consolidating Concrete. Appendix A. Ontario, Canada.
49. Utsi S., Emborg M., & Carlsward J. (2003). "Relation between workability and rheological parameters". Proc. of the 3<sup>rd</sup> int. RILEM symposium on SCC, Reykjavik, 154-164.
50. ASTM C231/C231M-14. (2014). Standard Test Method for Air Content of Freshly Mixed Concrete by the Pressure Method. ASTM international, West Conshohocken, PA.
51. Wallevik, O. H., Feys, D., Wallevik, J. E., & Khayat, K. H. (2015). Avoiding inaccurate interpretations of rheological measurements for cement-based materials. *Cement and Concrete Research*, 78, 100-109.
52. Wallevik, J. E. (2003). Rheology of particle suspensions. *Fresh concrete, mortar and cement paste with various types of lignosulfonates*, PhD dissertation, The Norwegian University of Science and Technology, Trondheim.
53. Reiner, M. (1949). *Deformation and flow: an elementary introduction to theoretical rheology*. HK Lewis.
54. ASTM C31/C31M-15. (2015). Standard Practice for Making and Curing Concrete Test Specimens in the Field. ASTM international, West Conshohocken, PA.

55. ASTM C42/C42M-13. (2013). Standard Test Method for Obtaining and Testing Drilled Cores and Sawed Beams of Concrete. ASTM international, West Conshohocken, PA.
56. ASTM C597-09. (2009). Standard Test Method for Pulse Velocity Through Concrete. ASTM international, West Conshohocken, PA.
57. Cousins, T. E., Badeaux, M. H., & Moustafa, S. (1992). Proposed test for determining bond characteristics of prestressing strand. *PCI Journal*, 37(1), 66-73.
58. Logan, D. R. (1997). Acceptance criteria for bond quality of strand for pretensioned prestressed concrete applications. *PCI journal*, 42(2), 52-90.
59. Roussel, N. (2006). A thixotropy model for fresh fluid concretes: theory, validation and applications. *Cement and Concrete Research*, 36(10), 1797-1806.
60. Spangenberg, J., Roussel, N., Hattel, J. H., Thorborg, J., Geiker, M. R., Stang, H., & Skocek, J. (2010). Prediction of the impact of flow-induced inhomogeneities in self-compacting concrete (SCC). In Proc. of the 6<sup>th</sup> Int. RILEM and the 4<sup>th</sup> North American conference on *Design, Production and Placement of Self-Consolidating Concrete*, Montreal (pp. 209-215).
61. Spangenberg, J., Roussel, N., Hattel, J. H., Sarmiento, E. V., Zirgulis, G., & Geiker, M. R. (2012). Patterns of gravity induced aggregate migration during casting of fluid concretes. *Cement and Concrete Research*, 42(12), 1571-1578.
62. Khayat, K. H., & Guizani, Z. (1997). Use of viscosity-modifying admixture to enhance stability of fluid concrete. *ACI Materials Journal*, 94(4), 332-340.
63. Khayat, K. H. (1995). Effects of anti-washout admixtures on fresh concrete properties. *Materials Journal*, 92(2), 164-171.
64. Wallevik, O. H. (2003, August). Rheology—a scientific approach to develop self-compacting concrete. In *Proceedings of the 3rd international RILEM Symposium on Self-Compacting Concrete*, Reykjavik (pp. 23-31).
65. Celik, T., & Marar, K. (1996). Effects of crushed stone dust on some properties of concrete. *Cement and Concrete research*, 26(7), 1121-1130.
66. Westerholm, M., Lagerblad, B., Silfwerbrand, J., & Forsberg, E. (2008). Influence of fine aggregate characteristics on the rheological properties of mortars. *Cement and Concrete Composites*, 30(4), 274-282.

## VITA

Aida Margarita Ley Hernandez was born in Culiacan, Sinaloa, Mexico. In the fall of 2009, she started her undergraduate studies at Universidad Autonoma de Sinaloa and graduated in fall 2013. During her time as an undergraduate student, Margarita had the opportunity to contribute in three summer research projects, two were national and the last one was an international stay. In 2011, she participated in the XVI scientific summer DELFIN edition under the advice of Dr. Alejandro Duran Herrera in the Universidad Autonoma de Nuevo Leon. In 2012, she had the opportunity to participate in the XXII scientific summer Academia Mexicana de la Ciencia edition advised by Dr. Prisciliano Felipe de Jesus Cano Barrita in the CIIDIR Oaxaca. In 2013, she participated in the VII international scientific summer edition of the Universidad Autonoma de Sinaloa advised by Dr. Kamal H. Khayat and Dr. Dimitri Feys at the Missouri University of Science and Technology. In spring 2014, she started the Civil Engineering Master's program at the Missouri University of Science and Technology. During her graduate studies she held positions of graduate research assistant and graduate teaching assistant in the Department of Civil, Architectural, and Environmental Engineering. Margarita completed her Masters of Science in Civil Engineering with a Construction Materials emphasis in July 2016.